Western Australian
Geothermal
CENTRE OF EXCELLENCE

Perth Basin Assessment Program

Project 4: PRODUCTIVITY AND SUSTAINABILITY OF LOW-TEMPERATURE GEOTHERMAL RESOURCES

Authors:

L. P. Ricard, M. G. Trefry, L. B. Reid,
S. Corbel, L. Esteban, J.-B. Chanu,
P. G. Wilkes, G. B. Douglas, A. H. Kaksonen,
D. R. Lester, G. P. Metcalfe, L. Pimienta,
S. Gutbrodt, S. Tressler, G. Bloomfield,
C. Evans and K. Regenauer-Lieb

May 2012

CSIRO
Curtin University
The University of Western Australia
Achieving International Excellence
Government of Western Australia

Enquiries should be addressed to:

Dr Ludovic Ricard
CSIRO Earth Science and Resource Engineering

Australian Resources Research Centre
26 Dick Perry Avenue, Kensington WA 6151
ludovic.ricard@csiro.au

ISBN 978-0-643-10909-4

Report 5

Project 4: Productivity and Sustainability of Low-Temperature Geothermal Resources,
L. P. Ricard, M. G. Trefry, L. B. Reid, S. Corbel, L. Esteban, J.-B. Chanu, P. G. Wilkes, G. B. Douglas, A. H. Kaksonen, D. R. Lester, G. P. Metcalfe, L. Pimienta, S. Gutbrodt, S. Tressler, G. Bloomfield, C. Evans and K. Regenauer-Lieb - PRINT

Copyright and Disclaimer

© 2012 WAGCoE To the extent permitted by law, all rights are reserved and no part of this publication covered by copyright may be reproduced or copied in any form or by any means except with the written permission of WAGCoE.

Important Disclaimer

WAGCoE advises that the information contained in this publication comprises general statements based on scientific research. The reader is advised and needs to be aware that such information may be incomplete or unable to be used in any specific situation. No reliance or actions must therefore be made on that information without seeking prior expert professional, scientific and technical advice. To the extent permitted by law, WAGCoE (including its partners, employees and consultants) excludes all liability to any person for any consequences, including but not limited to all losses, damages, costs, expenses and any other compensation, arising directly or indirectly from using this publication (in part or in whole) and any information or material contained in it.

CSIRO

Curtin University

The University of Western Australia
Achieving International Excellence

Government of Western Australia

CONTENTS

EXECUTIVE SUMMARY XI

PREFACE XIII

ACKNOWLEDGEMENTS XIV

1. INTRODUCTION 1

2. RESEARCH BACKGROUND 5

2.1 Hot Sedimentary Aquifer geothermal reservoirs 6

2.1.1 Reservoir Nomenclature 6

2.2 Direct use and aquifer thermal energy storage 7

2.3 Geothermal exploration 8

2.4 Reservoir development 9

2.5 Reservoir management 9

2.6 Geothermal projects in Western Australia 10

2.6.1 Geothermal exploration 10

2.6.2 Perth Basin settings 11

2.6.3 Geothermal projects in the Perth Metropolitan Area 14

2.7 Concluding remarks 15

3. NEW RESERVOIR EXPLORATION METHODS 16

3.1 Noonkanbah, Canning Basin 16

3.1.1 Structural and hydrothermal modelling 16

3.1.2 Reservoir modelling 19

3.1.3 Discussion 22

3.2 Reservoir assessment via stratigraphic forward modelling 22

3.2.1 Reservoir assessment methodology 23

3.2.2 Reservoir assessment for absorption chiller applications 24

3.2.3 Discussion 24

3.3 Conclusions 26

4. THERMAL CHARACTERIZATION OF THE PERTH BASIN 27

4.1 GeoTemp™ 27

4.2 Perth Basin temperature corrections 28

4.2.1 Non-corrected temperatures 29

4.2.2 Corrected temperatures 30

4.2.3 Discussion 35

4.3 Temperature of shallow formations in the PMA 35

4.3.1 Data collection and collation 35

4.3.2 Shallow temperature distribution 36

4.3.3 Thermal regime analysis 37

4.3.4 Discussion 38

4.4 Characterisation of the Gnangara Mound low temperature anomaly 39

4.4.1 Logging campaign 40

4.4.2 Possible fault controls 40

4.5 M345 Aquifer Storage and Recovery 41

4.5.1 Geophysical data collection 43

4.5.2 Time-lapse observations 45

4.5.3 Summary 46

4.6 Thermal conductivity modelling 47

4.6.1 Thermal conductivity estimation 48

4.6.2 Core measurements and results 49

4.7 Deep temperature predictions in the Perth Metropolitan Area 51

4.7.1 Existing Cockburn 1 dataset 51

4.7.2 Wireline temperature analysis 52

4.7.3 Thermal conductivity estimates from temperature logging 53

4.7.4 Thermal conductivity measurements on core samples 53

4.7.5 Temperature predictions 54

4.7.6 Discussion 55

4.8 Conclusions 55

5. SESKA PROJECT 56

5.1 Exploration objectives 56

5.2 Geodetic and geological information 57

5.3 Geophysics 58

5.4 Hydrodynamics and temperatures 58

5.5 Water quality 59

5.5.1 Background salinity 59

5.5.2 Background water saturation 60

5.6 Reservoir targets 61

5.7 Conclusions 61

6. ADVANCES IN RESERVOIR MANAGEMENT 62

6.1 Introduction 62

6.2 Subsurface Stirring 62

6.2.1 Chaotic processes in porous systems 63

6.2.2 Fundamentals of subsurface stirring in porous media 65

6.2.3 Physical phenomena and robustness 70

6.2.4 Example Application – Control of Emplaced Heat Plume 72

6.2.5 Example Application – Homogenization in Heat Rejection 78

6.3 Stochastic spectral characterization of reservoirs 80

6.3.1 Generalized viscoelastic dynamics 81

6.3.2 Effects of spatial correlation in reservoir structure 82

6.3.3 Robustness and invertibility 84

6.4 Biogeochemical assessment for in situ heat rejection 84

6.4.1 Pawsey Centre site characteristics 85

6.4.2 Analytical techniques 88

6.4.3 Results 88

6.4.4 Discussion 92

6.4.5 Summary 96

6.5 Conclusions 97

7. CONCLUDING REMARKS **99**

7.1 Synthesis of research outcomes 99

7.2 Future directions 100

REFERENCES **102**

APPENDIX A: LISTING OF STUDENTS **114**

APPENDIX B: CONFERENCE AND WORKSHOP CONTRIBUTIONS **115**

Conferences and workshops 115

Courses and public outreach 116

Courses and curriculum 116

Local and national outreach 116

Kensington 1 workshops 117

APPENDIX C: SCIENTIFIC PUBLICATIONS **117**

Student theses 117

Peer-reviewed journal articles 118

Conference abstracts 119

WAGCOE TECHNICAL REPORTS **121**

Patents 122

Additional publications 122

EXECUTIVE SUMMARY

Reservoir productivity and sustainability are key factors in the exploration, development and management of geothermal resources.

Through “Program 1, Project 4 - Reservoir Productivity and Sustainability” the Western Australian Geothermal Centre of Excellence (WAGCoE) has developed innovative tools, analyses, workflows and software, which facilitate the study of geothermal resource productivity and sustainability, both in the Western Australian context and for geothermal systems in general.

Two new multi-disciplinary modelling workflows integrating geology, hydrogeology and reservoir engineering have been developed to assist geothermal exploration. These workflows target thermal regimes and geological structure, and were applied to evaluate geothermal potentials for targets within the Canning and the Perth basins in Western Australia. This research highlighted the great geothermal resource potential of these basins for direct-use applications.

WAGCoE has originated and developed the GeoTemp™ software package to assist the processing, interpretation and modelling of temperature measurement datasets. GeoTemp™ has been used in a range of projects that have generated new understandings of the subsurface thermal characteristics of the Perth Basin and how best to exploit them sustainably. The thermal workflow assists the reservoir engineer in characterizing the thermal regime of target formations.

WAGCoE has also helped CSIRO to pursue a major geothermal infrastructure project (SESKA Geothermal) in Perth to stimulate the development of large-scale use of geothermal resources in Western Australia. Together with CSIRO, WAGCoE has pioneered new resource assessment methods for shallow and deep systems, and is leading the development of a major heat rejection technology within the Perth Metropolitan Area. An innovative concept for physical manipulation of thermal fluids in situ was developed and has been submitted for international patent review.

Research conducted in this Project has been widely applied to Western Australia (Canning Basin, Perth Basin, Perth Metropolitan Area, Gnangara Mound, M345 ASR trial site, and the Kensington 1 well site at the Australian Resources Research Centre). The research outcomes of this Project were presented at local, national and international conferences, and have been published in leading international scientific journals. This project also provided training to 13 Honours and MSc students, and 1 PhD student on specific technical skills and techniques that are immediately transferrable to various fields of research associated with geothermal energy and reservoir engineering.

PREFACE

The Western Australian Geothermal Centre of Excellence (WAGCoE) was established in 2009 for an initial three year term with a $2.3M grant from the Western Australian Department of Commerce. WAGCoE operated as an unincorporated joint venture between CSIRO, University of Western Australia, and Curtin University, with CSIRO as the Centre agent. The remit of WAGCoE was to assist the Western Australian Government to provide a foundation for a sustainable geothermal industry by conducting advanced scientific and engineering research into WA's geothermal resources, principally HSA resources in the Perth Basin, and to develop and transfer to industry innovative new technologies for direct heat use.

In order to deliver on this task, WAGCoE was structured into three mutually supportive research Programs:

- Perth Basin Assessments (Program 1)
- Above-Ground Engineering (Program 2)
- Deep Heat and Future Resources (Program 3)

The Perth Basin Assessments Program contained the following four research Projects:

- WAGCoE Data Catalog (Project 1)
- Perth Basin Geomodel (Project 2)
- Hydrothermal Simulations (Project 3)
- Reservoir Productivity and Sustainability (Project 4)

This document is the final research report of Project 4 within Program 1 of WAGCoE. The format of the document is that of a summary report; detailed tabulations of technical data and results are to be found in the supporting research reports, papers and theses cited herein.

ACKNOWLEDGEMENTS

This work was supported by the Western Australian Geothermal Centre of Excellence (WAGCoE) and CSIRO. WAGCoE was funded by the Western Australian government and its three partners: CSIRO, The University of Western Australia and Curtin University of Technology. This document is an output from the CSIRO Petroleum & Geothermal Portfolio.

The authors are grateful to many WAGCoE colleagues and collaborators for assistance and advice in the preparation of this document. Particular thanks are expressed to Chris Botman, Lisa Miotti, Guillaume Pons, Kristina Kazakoff and Libby Colgan for their valuable inputs to this document. Particular thanks to Belinda Godel and Heather Sheldon for reviewing parts of the document.

The research conducted in this report would have not been possible without the support of the following people or entities: Geoscience Australia for loaning the temperature logging equipment and providing training with the gear, Maike Willuweit and Frans Otten from Emerson Process Management for providing the Roxar software TEMPEST MORE, RMS and Enable, Brett Harris from Curtin University of Technology for providing the M345 ASR project dataset, Steve Harvey and Jacqui Cook from the CSIRO SESKA project for the opportunity to work on the SESKA geothermal project, Grant Bolton and Martin Pujol from Rockwater Pty Ltd for access to data and facilities on the St Hilda's Anglican School geothermal project, the Western Australian Department of Water for granting access to Artesian Monitoring bores throughout the Perth Metropolitan area, Sandra McLaren and Ben Harrison from the School of Earth Sciences at the University of Melbourne (Victoria, Australia) for providing access to the Optical Thermal Scanner. The M345 project was funded by the Department of Water administered Premier's Water Foundation grant (Western Australia). The research partners are Water Corporation, CSIRO and Curtin University.

The authors also express their gratitude to Alison Kirkby, Rikki Weber and Tim Jones from Geoscience Australia for assisting in the evaluation of the GeoTemp™ software at an early stage of development.

1. INTRODUCTION

The direct use of heat from reservoirs exhibiting low and intermediate temperatures (< 100 °C) within sedimentary basins was the topic studied by the Western Australian Geothermal Centre of Excellence (WAGCoE). Western Australia has several large sedimentary basins which contain significant resources of heat which, if used efficiently, have the potential to generate and/or offset large amounts of electrical power. WAGCoE's goal was to contribute to the development of geothermal energy in Western Australia and to address a major national energy challenge via demonstrations of sustainable geothermal technology in Western Australia.

Sedimentary basins have vast global coverage and have been widely explored and exploited for resources such as groundwater, oil and gas, and more recently carbon storage. Consequently, the development of geothermal energy resources in sedimentary basins benefits significantly from transfers of knowledge from other areas of the geosciences. However, in addition to the data obtained in connection with these conventional resources, geothermal energy investigations require the collection, processing and interpretation of specific data (e.g. temperature, thermal conductivity, specific heat) and specialized interpretation and modelling studies. In this way, geothermal reservoir engineering can be seen as an extension of classical reservoir engineering, and the specific expertise required depends heavily on the nature of the geothermal resource under consideration. For example, high-temperature geothermal resources may engender complexities regarding flow assurance and fluid phase transitions that are not usually problematic in low- to intermediate-temperature reservoirs where more attention must be paid to potential impacts on potable water supplies and related ecosystems. Low- to intermediate-temperature reservoirs were the main topic of research in WAGCoE.

The direct use of geothermal energy, i.e. the conversion of heat energy to useful work without the generation of electrical power as an intermediate step, has been demonstrated to be efficient for energy conversion. Direct use approaches also widen the application of available geothermal resources by including reservoirs of lower temperature. Direct-use applications are diverse and therefore have a wide range of production requirements. Combination of different direct-use applications, e.g. via cascading of heat, allows the optimisation of energy extraction, use and heat rejection, and is a crucial step towards large scale integrated use of geothermal energy (e.g. through the establishment of geothermally integrated cities and industrial precincts). Optimization of direct-use geothermal energy systems aims to provide a solution to an energy problem, rather than solving a specific electricity problem.

To address the challenge of exploiting geothermal resources, reservoir engineering aims at identifying reservoirs, evaluating the resources, and then developing and managing them sustainably by considering production and resource constraints. In the geothermal industry the definition of a direct-use geothermal reservoir is closely linked to the surface application(s) envisaged. This is at odds with conventional approaches in the oil and gas industry where the viability of a reservoir is solely linked to the presence or the absence of hydrocarbons. Geothermal applications using directly the heat energy at the surface can operate over a large range of working temperatures, from 20 °C

to 200 °C. As a result, the definition of a geothermal reservoir depends on the target geothermal application, thus reservoirs suitable for low-temperature ground source heat pumps are widespread and accessible, while reservoirs suitable for high-temperature electricity generation are much harder to locate and characterize.

Apart from the recovery of energy from the subsurface, the storage of heat in the subsurface is also a useful concept and is embodied in so-called aquifer thermal energy storage (ATES) and ground source heat pump technologies. The implementation of these technologies provides a solution for waste heat storage and the relatively small load of heating and cooling for buildings. Consequently, direct-use geothermal exploration and production requires a match between the need and the available resources.

Consistency and integration of data analysis and risk assessment is needed to develop large-scale hot sedimentary aquifer (HSA) projects. The main challenges faced in characterizing a reservoir are related to data scarcity as existing data are usually sparse and often have low reliability. Furthermore, methodologies employed for reservoir interpretation and modelling are often lacking or are not suitable for geothermal applications. It was the purpose of Project 4 of the Perth Basin Assessments Program of WAGCoE to remedy this situation by developing reservoir engineering techniques that help to reduce risk and uncertainty in geothermal reservoir characterization.

The WAGCoE objectives were to:

- Provide novel tools and methods to assist industry and regulatory organizations
- Investigate Western Australia's geothermal resources
- Engage with industry and local stakeholders on existing projects
- Engage with service providers and software development companies to improve the current software tools

This report summarizes WAGCoE's research on productivity and sustainability of geothermal reservoirs by presenting a compilation of new concepts and techniques and their application to several geothermal projects in Western Australia. The projects are mainly focussed on exploration, development and management of geothermal reservoirs for direct-use applications in the Perth Metropolitan Area. The research results identify new geothermal potential, contribute to the development of a demonstration project, and provide better understanding of existing geothermal projects. This report emphasises the processing and interpretation of temperature data, and the need for fully integrated geothermal assessments.

This report is divided into seven sections; the following six sections are organized as follows:

- **Section 2** surveys the existing knowledge of geothermal reservoir engineering and its application to the Perth Basin.
- **Section 3** investigates two innovative reservoir modelling workflows for direct use geothermal exploration.
- **Section 4** describes the thermal characterization and temperature interpretation considerations which support geothermal reservoir engineering.
- **Section 5** presents the exploration objectives of the large-scale direct use geothermal demonstration project under development in the Perth Metropolitan Area.
- **Section 6** explores new concepts in aquifer thermal energy storage in term of characterization, development and management of the resources applied to a shallow heat rejection project under development in the Perth Metropolitan Area.
- **Section 7** provides an overview of research outcomes and proposes future directions.

2. RESEARCH BACKGROUND

Geothermal energy has been used by humans for millennia. Hot spring water was used for medicinal purposes by the early Chinese dynasties, and has been used in Europe since at least the Greco-Roman period for direct-use applications such as heating and thermal bathing. Electricity was first generated from geothermal energy in 1904 (Cataldi et al., 1999). Electricity power generation has been the main target of geothermal energy conversion for decades, and the development of plants in volcanic areas, such as Iceland and New Zealand, have defined the "conventional" geothermal system. Such systems aim to use geothermal energy for high electricity generation capacity (more than 20 MWe) with working fluids (either in the vapour phase or with both vapour and liquid phases) at high pressure and temperature. As a result, the geographical areas where conventional geothermal systems can be implemented are limited and are usually located along zones of active plate tectonics (especially along the Ring of Fire and the Mid-Atlantic Ridge). In contrast, the direct use of geothermal energy has mostly been developed in sedimentary basins. These direct-use geothermal energy systems are not specifically related to a particular tectonic setting and are widespread across the world.

Direct-use applications are very diverse and notably include district heating, bathing, agricultural drying, and greenhouse heating (see Lund et al. (1998, 2011) for more details). Besides these applications, heat rejection schemes and aquifer thermal energy storage (ATES) schemes also provide solutions for waste heat problems by rejecting or storing the heat in the subsurface (Lee, 2010; Paksoy, 2007). Ground source heat pumps address heating and cooling load for households and small buildings (Lund et al., 2004). In a broad sense, geothermal energy can be viewed as a potentially bidirectional heat exchange between the surface and the subsurface. The efficiency of a geothermal system is linked to the mechanism of energy conversion. Geothermal systems that convert energy to electricity before delivery to the end user necessarily run at lower thermodynamic efficiencies than direct-use systems.

In 2010, the global installed capacity for geothermal electricity generation was approximately 10.7 GWe (Bertani, 2012) whereas the global installed capacity of direct-use projects was estimated at 50 GWth (equivalent to 5 GWe based on a 10% conversion factor, DiPippo (2007)). Geothermal heat pumps represented most of installations (68.3%). The rest represented very diverse activities including bathing and swimming (13.8%), space heating (11.1%), greenhouse heating (3.2%), aquaculture pond heating (1.3%), industrial uses (1.1%), cooling and snow melting (0.8%), and agricultural drying (0.3%). Over the last five years, the global installed electricity and the direct-use capacities increased by 20% and 100%, respectively (Bertani, 2012; Lund et al., 2011). The growth of direct use geothermal is mostly related to the boom in ground source heat pumps which accounted for 70% of the installed direct use capacity in 2010 (Lund et al., 2011). Over the past decade, ground source heat pumps (GSHP) have been very successful in delivering geothermal energy solutions for household applications including space cooling and heating.

2.1 Hot Sedimentary Aquifer geothermal reservoirs

Hot sedimentary aquifer geothermal systems can be defined as existing aquifers within sedimentary systems where the groundwater is at a temperature above the mean surface temperature. Typically, these resources occur at shallow to moderate depth (up to several kilometres or more). In most cases, the water temperature increases with depth, i.e. according to the mean geothermal gradient. In that case, the water is heated by either (i) vertical heat conduction through the crust or (ii) heat advection resulting from the circulation of groundwater through permeable zones within the aquifers. Heat conduction is often the main process of water heating, however in some cases heat advection may be as important as conduction and there is clear evidence of advection in similar settings (Anderson, 2005; Saar, 2011). Deep sedimentary aquifers heated by the mean thermal gradient are found in many continental environments. These systems are water-dominated and usually close to hydrostatic pressure. The range of temperatures associated with sedimentary basins and regional aquifers is estimated as 20 °C to 150 °C (Lund et al., 1998).

2.1.1 Reservoir Nomenclature

In the following, we use the terms geothermal field and geothermal reservoir as defined by Grant and Bixley (2011). The term geothermal field is intended to be purely a convenient geographic description and makes no assumptions about the greater geothermal system that has created and makes the field active. A geothermal reservoir is that part of a geothermal field that is so hot and permeable that it can be economically exploited for the production of fluid or heat. According to this definition, whether a geothermal reservoir exists or not depends in part on the current engineering technology and energy prices.

The geothermal potential is classified by the two collective terms resources and reserves (Muffler and Cataldi, 1978). The term resource refers to the useful accessible identified and undiscovered geothermal energy beneath a specified geographic area. The term reserve refers to the part of the resource that is both identified and economic for a particular geothermal application (e.g. power generation, space heating etc.). The terms resource and reserve are intrinsically linked to the field and reservoir definitions, respectively.

Several methods exist for the quantitative evaluation of resources and reserves. The volumetric method also called “stored heat” or “heat in place” provides an evaluation of the energy contained in a certain volume of rock. More complicated methods involving lumped models (Alkan and Satman, 1990, Sarak et al., 2005, Tureyen and Akyapı, 2011) or three-dimensional numerical modelling (Cacace et al., 2010, Hamm and Bazargan Sabet, 2010, Kiryukhin, 1996, Mottaghy et al., 2011, O'Sullivan et al., 2009) are available. The Australian Geothermal Reporting Code (2010) proposes a detailed breakdown of the definitions depending on the level of confidence in the information used in the calculation and the calculation method itself. Those methods evaluate the resources and reserves but do not consider the possible geothermal applications or their feasibilities.

The recovery of heat at the surface is the aim of geothermal production. For any technology or type of resource, the produced geothermal power can be expressed in terms of the thermal energy

contained in the pumped fluid of specific heat Cp at a flow rate Q, recovered at the temperature Te and re-injected at temperature Ti from the subsurface as follows (Muffler and Cataldi, 1978):

$$\text{Power} = Q * C_p * (T_e - T_i) \qquad (2.1.1)$$

The thermal recovery performance of a geothermal project is then evaluated using the heat recovery factor (Gringarten, 1978) which is the ratio between the extracted heat and the recoverable heat. Reservoir performance is dependent on the development scheme and on the sustainability of the produced power over time. Initial temperature and flow rate are critical parameters for the exploration and development of geothermal projects whereas the temperature and pressure changes over time are key parameters for the management of the geothermal resource.

2.2 Direct use and aquifer thermal energy storage

Geothermal energy uses are commonly divided into two categories, electricity generation and direct use. These different categories require different minimum production temperatures as illustrated in Figure 2.1. Conventional electric power production is nowadays limited to fluid temperatures around 100 °C or hotter.

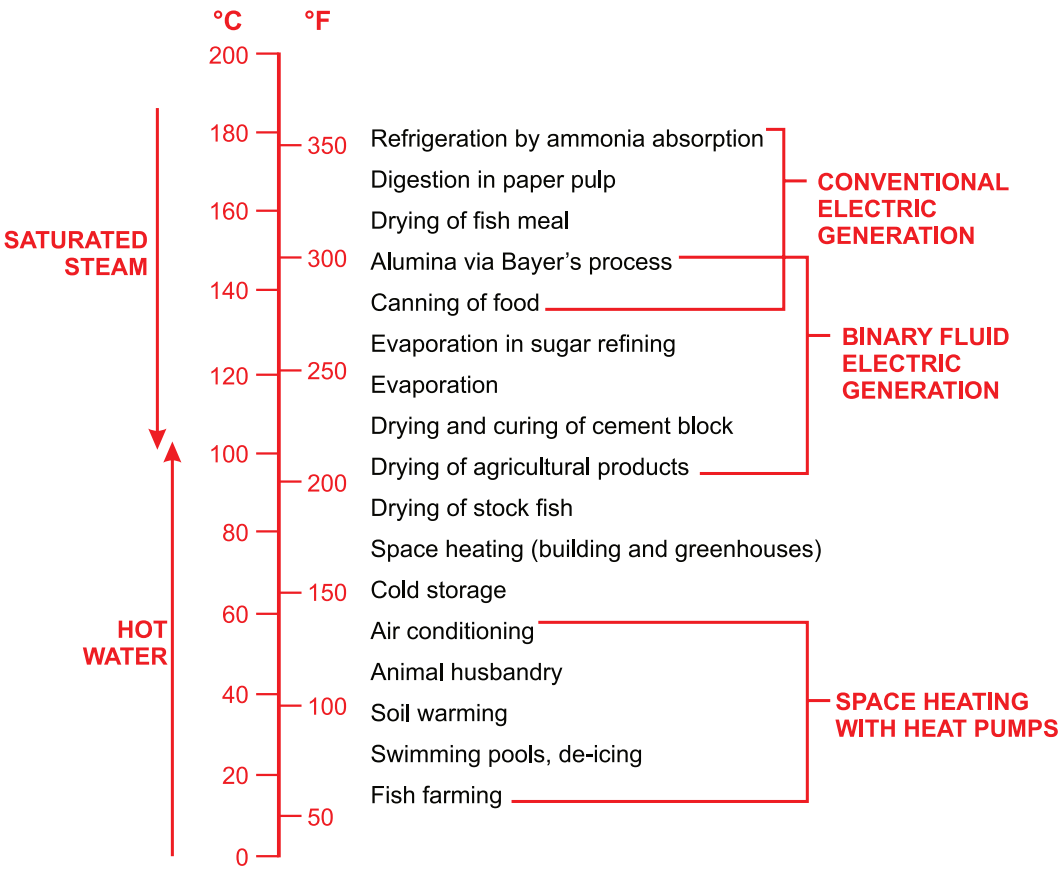

Figure 2.1: Possible applications for direct use of geothermal energy suggested by Lindal (1973), as cited by Fridleifsson (1998).

Direct use of geothermal energy can involve a wide range of applications. The technology, reliability, economics and environmental acceptability of direct-use geothermal energy has been demonstrated throughout the world. Direct-use applications can use both high and low temperature geothermal resources and are widely deployed. Direct-use applications are however much more site specific since the heat carrying fluid (water) is dense and expensive to transport. Therefore direct-use exploitation of geothermal reserves requires a close geographic match between the location of the reserves and the intended market application. A given direct-use application has a temperature working range which needs to be taken into account when exploring for suitable geothermal resources and a great diversity of applications are possible for a given temperature range. Some direct-use applications have a narrow working temperature window whereas others are widespread. Therefore the sophistication employed in the temperature analysis and thermal characterization of the geothermal reservoir must match the flexibility/complexity of the temperature requirements of the envisaged direct use application(s).

Aside from heat extraction applications, sedimentary basins have been the focus of thermal energy storage. The storage of thermal energy in the subsurface allows reservoir managers to balance fluctuations in supply and demand of low temperature energy. ATES systems utilize low-temperature geothermal aquifer resources. In an ATES system, groundwater is pumped out of the ground, passed through a heat exchanger and re-injected in a similar manner as in a HSA geothermal plant. ATES systems are used for the seasonal storage of heat energy mainly for the purpose of heating and/or cooling residential and industrial buildings (Paksoy, 2007). Since the first demonstration projects in the early 1980's in the U.S.A., China, Switzerland and Denmark, ATES has become a well-established and documented technology (Lee, 2010, Paksoy, 2007).

Another important aspect of the direct use of geothermal energy is cascading and combining uses toward the optimization of the energy extraction (Gudmundsson, 1988).

2.3 Geothermal exploration

Geothermal exploration aims to locate and confirm geothermal reservoirs in areas both economically and technically viable for geothermal energy exploitation. Usually, geothermal exploration programs are developed on a step by step basis and are similar to the programs of conventional oil and gas exploration and exploitation. A typical geothermal exploration program can be described as follows:

1. An initial phase aimed at selecting the most promising areas based on the geology and the available temperature data.
2. A pre-feasibility phase, during which surface investigations (geology, geophysics etc.) take place.
3. An early exploration stage, where the resource/reserve assessment is largely qualitative and addresses both the temperature of the reservoirs and the flow rates (both being necessary for the estimation of recoverable power from the reservoir). At that stage, a first step of compilation of all available data for the region of interest is necessary (Huenges, 2010).
4. An analysis of the thermal regime and thermal characterization phases where the regional temperature field is investigated using lithology and temperature data. This analysis provides valuable information on the possible prospects at the regional scale (Cacace et al., 2010).

This guides the decision maker towards the feasible geothermal uses. During that stage, the characterization of the reservoir rock contributes to the assessment of the achievable flow rate and the sustainability of the reservoir.

At the exploration stage (3), data acquisition, interpretation and modelling studies focus on providing a consistent understanding of the reservoir that includes available geological, geophysical and hydrothermal knowledge. The gaps and uncertainties are then addressed in the risk assessment and the mitigation plan inherent in the exploration protocol. The reservoir study fits the level of details and complexity required within the risk framework to address the problem of reserve estimation.

2.4 Reservoir development

Reservoir development often starts with the drilling of a geothermal exploration well (Manning et al., 2007). This well provides the necessary information for accurate reserve estimates and field development planning if resources are confirmed. The geothermal drilling target is generally inferred from offset wells or estimated in connection with regional or local geological knowledge. The target definition is governed by geological and geophysical models that illustrate the geometrical constraints of the field and their properties if available. Once the resource is confirmed for a given project lifetime, geothermal reservoir engineering proceeds to developing the most suitable development plan for the reservoir, determining the number and nature (e.g. producer or injector) of wells necessary to reach the recoverable power target, determining the recovered heat and evaluating the reservoirs intervals. The outcomes are suggested production intervals with estimated production rates, numbers of well necessary and best locations for those wells. Production considerations include recoverable energy, production power, working temperature and sustainability of the flow rate and the avoidance of thermal breakthrough. The tools used for field development are often analytical, lumped or numerical reservoir models. The field development commonly used for low temperature direct-use geothermal projects is the ‘well doublet’ defined by Gringarten (1978). A well doublet development is composed of a well for production and a well for injection. The hot water is produced, then circulated into an heat exchanger and then re-injected using the injector well.

2.5 Reservoir management

Once the reservoir is developed and in production, reservoir management aims to (i) maintain the level of production according to the energy/power demand at the surface and to (ii) alter the production if required. The temperature disturbance caused by the injection of cooled water is often called a thermal plume or thermal contamination. The migration of thermal plumes over time can be critical to the sustainability of a geothermal project. Indeed, if the thermal plume reaches a producer (a process known as thermal breakthrough) it will reduce the thermal power produced by the well and therefore will reduce the recovered power of the plant. Similarly, the thermal plume can affect other subsurface uses in the vicinity. The study of thermal contamination is critical for reservoir production sustainability (Banks, 2009a,b, Gringarten and Sauty, 1975; Stopa and Wojnarowski, 2006). The need to avoid, limit or delay thermal breakthrough is used to constrain the minimum distance between the wells in the geothermal field development plan.

Reinjection of fluid into a geothermal reservoir may lead to losses of injectivity over time. According to Ungemach (2003), the causes of injectivity decline are:

- Scaling resulting from chemical incompatibility between injected and formation (native) fluids, often driven by temperature differences
- Clogging resulting from microbiological effects, suspended solids (fines, corrosion products, scale), fines migration within the receiving formation

The use of well doublets brings issues of well connectivity into focus. If well connectivity is too high, thermal breakthrough will occur rapidly and the reinjected cool water will be produced to the above-ground application, resulting in a reduction of system viability. If the connectivity is too low or absent, as may occur if the re-injection occurs within a different reservoir compartment, pressure support may not be present and the system may not support the desired flow rates over the full project lifetime.

Aside from the considerations linked to well doublet connectivity, the zone of influence of each well will have to be considered in order to optimise overall reservoir production. An optimal well location will have good formation connectivity in its vicinity to guarantee the productivity or the injectivity, and a moderate to low inter-well connectivity to guarantee pressure support without promoting thermal breakthrough. Optimization of the productivity/injectivity of the reservoir is often required at the management stage.

2.6 Geothermal projects in Western Australia

Geothermal exploration and production have taken place in Western Australia since the beginning of the 20th century. While geothermal exploration projects now occur all over the state, geothermal production has so far been located in the Perth Metropolitan Area.

2.6.1 Geothermal exploration

Recent geothermal exploration activities in Western Australia focused on heat flow estimations. Bestow (1982) presented an extensive compilation of temperature gradients and heat flows for every basin in Western Australia (Figure 2.2). This study concluded that the geothermal resources are suitable for direct-use projects such as air conditioning and industrial use with expected drilling targets at 2000 – 3500 m depth and temperature between 65 °C and 85 °C. Crostella and Backhouse (2000) investigated the regional geothermal gradient of the Perth Basin with focus on petroleum generation and prospectivity. These authors noticed that low temperature gradients are linked to the high thermal conductivity of Middle Triassic to Upper Jurassic sediments for the northern and central part of the Perth Basin and the entire stratigraphical section in the southern part.

Further temperature analysis was performed by Chopra and Holgate (2007). These authors analysed deep temperature measurements from 180 wells in the Canning, Carnarvon and Perth basins. For these wells, they corrected the temperature data to estimate true formation temperature when sufficient suitable temperature data were available. They also calculated temperature gradient from surface to total depth, predicting temperature at the top of the basement and the depth required to reach 200 °C.

More recently, thermal conductivity measurements, heat flow estimations, and estimations of depths to isotherms and temperatures at the top of the basement were made for the Perth Basin (Hot Dry Rocks Pty Ltd, 2008), the Canning Basin (Hot Dry Rocks Pty Ltd, 2009), the Bonaparte (Hot Dry Rocks Pty Ltd, 2010a), the Browse Basin (Hot Dry Rocks Pty Ltd, 2010b), the Carnarvon Basin (Hot Dry Rocks Pty Ltd, 2010c) and the Officer Basin (Hot Dry Rocks Pty Ltd, 2010d). In these studies, the mechanism of heat transfer was assumed to be vertical conduction and the core thermal conductivity measurements sampled from the whole basin were used to estimate thermal conductivities at the formation scale. The above analyses of well data interpreted the temperature data from the different wells independently without any correlation with other nearby temperature measurements.

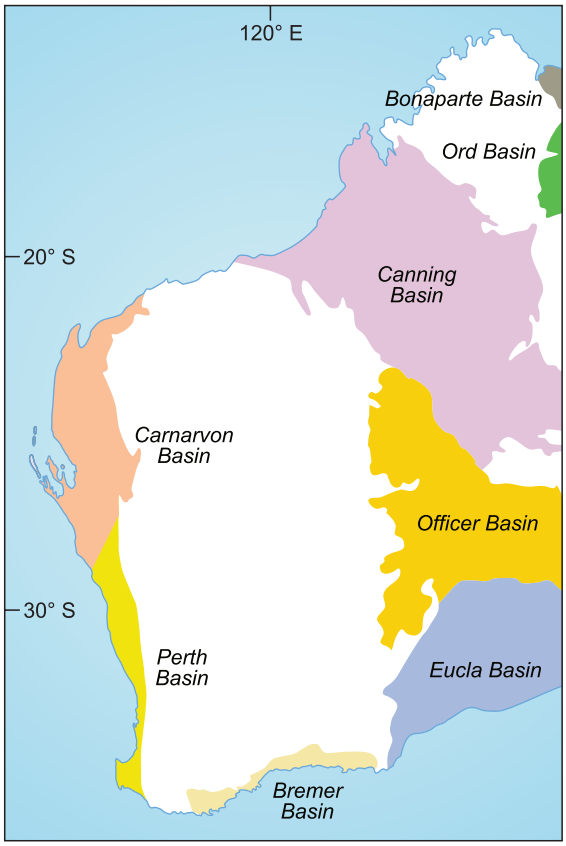

Figure 2.2: Sedimentary basins of Western Australia.

The first hydrothermal modelling study in Western Australia was performed by Swift (1991) for the Exmouth plateau of the Carnarvon Basin. He studied two-dimensional cross-sections and concluded that lateral variations of thermal conductivity produce high horizontal temperature gradients which drive natural convection in the region.

Finally, a three-dimensional conduction modelling study was performed recently for the North Perth Basin (Geointrepid, 2011). This study provided the first three-dimensional understanding of that area (Figure 2.3 Left blue area). It also pointed out an important disconnection between areas of high modelled heat flow and zones of temperature anomalies.

2.6.2 Perth Basin settings

As discussed by Timms et al. (2012), the Perth Basin is a sedimentary rift basin (Figure 2.3, left) approximately 1000 km long extending in a north-northwesterly direction between latitudes 27°00'S and 34°00'S. The central Perth Basin or Perth Metropolitan Area (Figure 2.3, right) comprises a thick sequence of sedimentary rocks, bounded by the Darling Fault to the east and the continental slope to the west. Basement lithology consists of Precambrian rocks of the Pinjarra Orogen (Mory and Iasky, 2005). Early Permian to Late Cretaceous sedimentary sequences up to 15 km thick occupy the series of sub-basins, troughs, shelves and ridges comprising the basin (Figure 2.4). Native permeabilities of the aquifer sediments throughout the Perth Basin are high (Davidson and Yu, 2008), thus facilitating groundwater circulation through these aquifers at relatively shallow depths. Descriptions of the

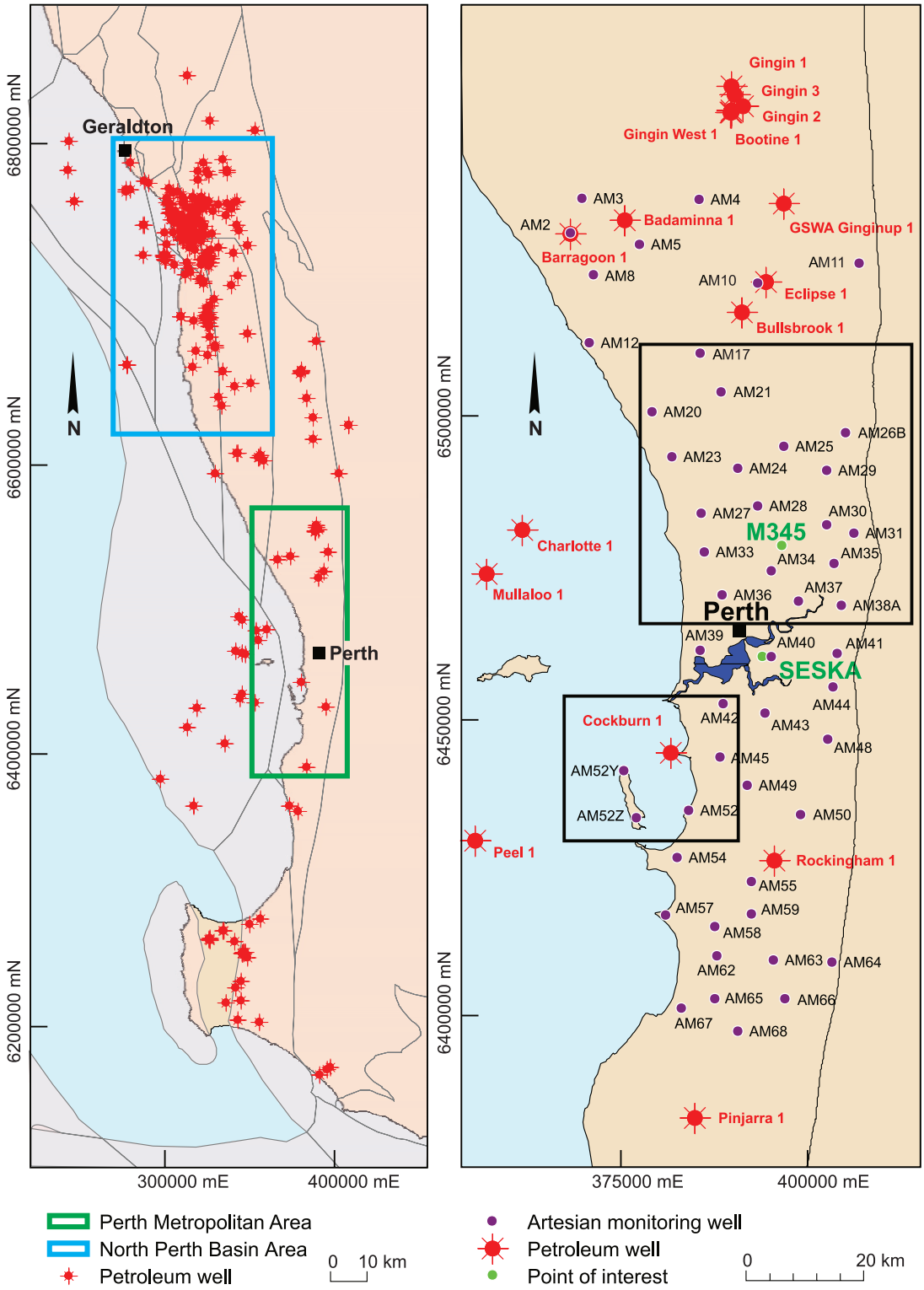

Figure 2.3: Left, Perth Basin situation map with petroleum wells and selected areas of interests. Right, Perth Metropolitan Area with Artesian Monitoring and petroleum wells, with selected areas of interests developed further in the report.

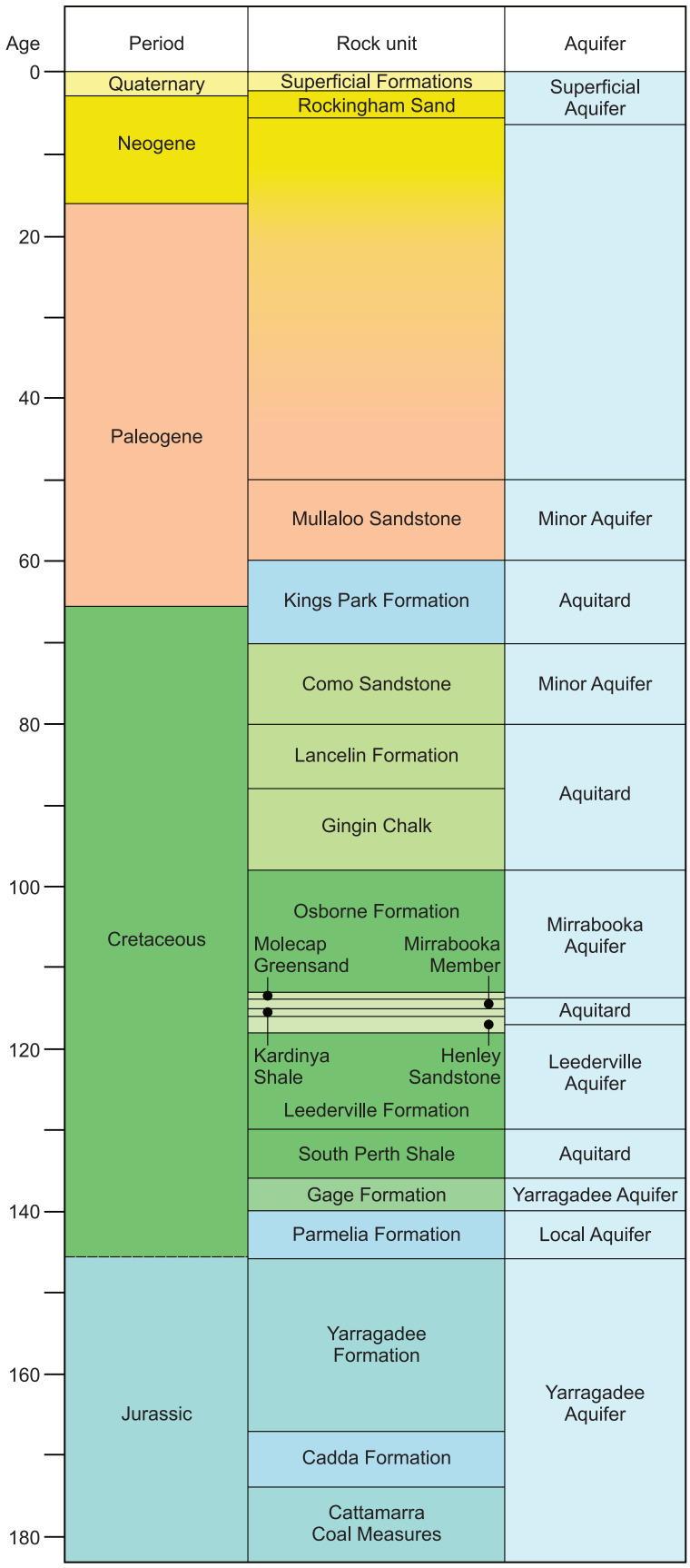

Figure 2.4: Generalized stratigraphy of the Perth Basin, showing the distribution of aquifers (data from Davidson 1995 and Turner et al., 2009).

shallow (<1 km) stratigraphic units (Figure 2.4) of the Perth Region are provided in Davidson (1995). The shallow portion of the Perth Basin comprises three major aquifers: the Superficial, Leederville and Yarragadee aquifers used for public and industrial water supply; as well as several minor aquifers: the Rockingham, Kings Park, and Mirrabooka aquifers.

2.6.3 Geothermal projects in the Perth Metropolitan Area

Since the early 20th century, the Perth Metropolitan Area has been explored for heat and water production. The first and now obsolete geothermal direct-use projects in Perth were the Claremont laundry, Jandakot Wool Scourers, Graylands Old Men's Home, Crawley warm baths and the reptile enclosure of the South Perth Zoological Gardens (Pujol, 2011). Currently, there are six HSA geothermal projects in production status (Pujol, 2011). These projects are direct-use swimming pool heating applications with some component for space heating. The six existing geothermal projects (Figure 2.5) are: Bicton Pool, Claremont Aquatic Centre, Craigie Leisure Centre, Challenge Stadium, Christchurch Grammar School and St Hilda's Anglican School. Two other projects are at the development stage. These geothermal projects are targeting the Yarragadee Formation and/or the overlying Gage Formation (Pujol, 2011) to a maximum depth of 1000 m directly in the Perth Metropolitan Area.

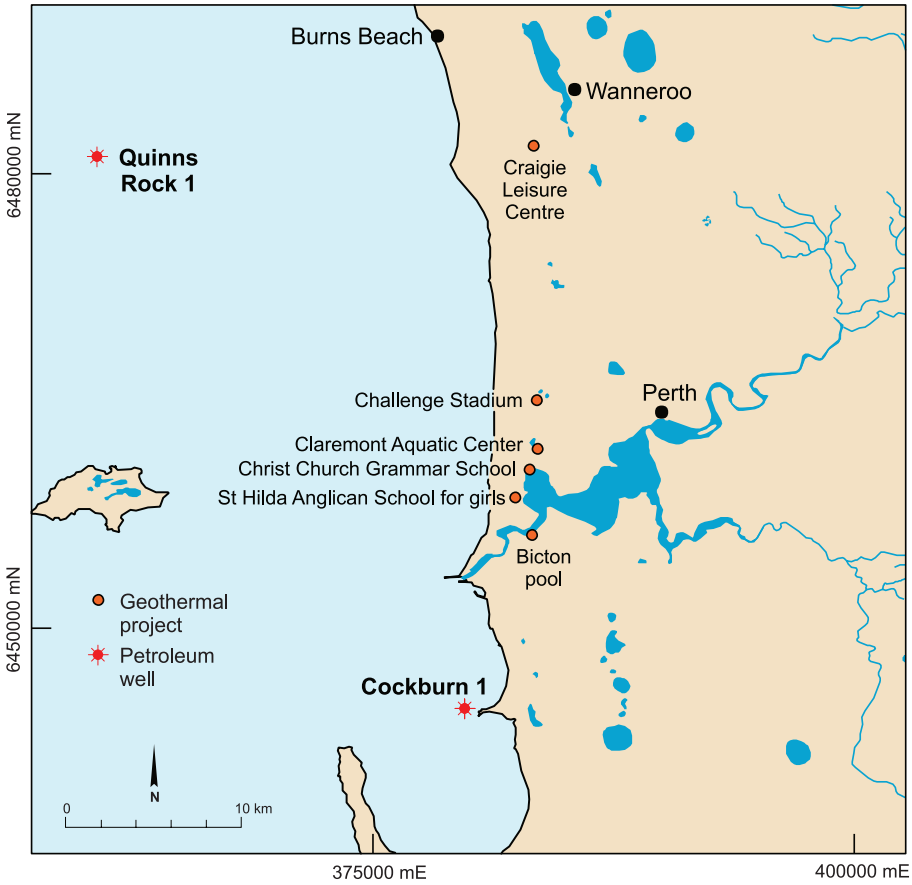

Figure 2.5: Existing geothermal projects in the Perth Metropolitan Area.

Oldmeadow and Marinova (2011) reviewed the Challenge Stadium project in Perth consisting of three outdoor and indoor swimming pools where a total water volume of 11 ML is geothermally heated. Challenge Stadium is now the site of Australia's most successful operating low temperature geothermal project. In essence, the system works by abstracting 42 °C water from the target aquifer, running the warm water through a heat exchanger, then reinjecting the cooled water (at approximately 30 °C) to the same aquifer so as to maintain a neutral water balance. With a 30% contingency the peak daily energy requirement for the system to heat the swimming pools to 26 °C is 1755 kWh. It operates with a maximum abstraction capacity of 50 L/s and maximum reinjection capacity of 30 L/s.

2.7 Concluding remarks

Geothermal energy exploitation in Western Australia has benefited from the extensive knowledge of the shallow aquifers of the Perth Basin gained through public water supply activities over the past century. On the other hand, geothermal exploration has been pursued from a petroleum exploration angle due to the desire to tap higher temperature reservoirs in deeper formations. In sedimentary basins, geothermal reservoirs are part of a broad and complex geological, geochemical and hydrothermal system.

As the spectrum of possible direct-use geothermal applications embodies a diverse range of working temperatures and flow, geothermal reservoir exploration, development and management approaches have to address the geothermal system complexity and generate solutions specific to the intended direct-use application.

To meet the needs of a growing geothermal industry in Western Australia, new techniques and understandings are required. This report describes advances made by WAGCoE in

- developing geothermal exploration techniques consistent with the geological and hydrothermal knowledge which identify exploration targets for selected direct-use applications,
- providing new tools and demonstrated approaches for the interpretation of temperature data,
- contributing to the development of a major geothermal demonstration project in the Perth Metropolitan Area,
- boosting the understanding and optimization of geothermal energy management systems within the Perth Metropolitan Area and sedimentary systems worldwide.

3. NEW RESERVOIR EXPLORATION METHODS

This section deals with several reservoir exploration studies performed by WAGCoE. The objectives of the first study presented here are to perform an integrated reservoir modelling study based on existing publicly available data, to identify possible geothermal targets and to propose possible direct-use applications for the targets. This study is based in the Canning Basin, Western Australia. The structural geology and hydrogeology components of this work are presented in Reid et al. (2012); only the reservoir engineering component is presented here.

The second study presents a joint stratigraphic forward modelling/reservoir engineering investigation of the Perth Metropolitan Area. The basis for the Sedsim sedimentary models employed here is discussed more fully in Timms et al. (2012).

3.1 Noonkanbah, Canning Basin

This Canning Basin case study seeks to identify potential HSA targets in the vicinity of Noonkanbah using coupled fluid and heat flow simulations at sub-basin scale and then to test the feasibility of these targets via smaller reservoir scale simulations. Because this study was a preliminary assessment using only limited data, the modelling focused on simple descriptions of geometry and physical processes. The geologic modelling was performed with the modelling package SKUA®, the sub-basin scale simulations using FEFLOW, and the reservoir scale simulations using TEMPEST MORE. This workflow (Corbel et al., 2011a; Reid et al., 2010; Ricard et al., 2010) is demonstrated on a case study in the Fitzroy Trough, Canning Basin, Western Australia (Figure 3.1).

3.1.1 Structural and hydrothermal modelling

A 3D geological structural model was built using the modelling package SKUA. Main faults were identified and then modelled along with aquitards and aquifers. This sub-basin scale geological model was developed using available data including interpreted seismic lines, well data and publicly available reports. The resulting geological model covers an area of 84 km x 172 km and extends to a depth of 3000 m below sea level. Faults are critical in geothermal exploration as they determine the volume and the recharge of the reservoirs. For the sub-basin scale model only faults compartmentalizing the model or creating major offsets were considered. The hot aquifers considered in this study are the Grant Formation and the Poole Sandstone aquifers (Table 3.1). The Grant Formation aquifer overlay a major regional unconformity. As this unconformity lies at the lower depth limit for economic drilling for HSA, we decided to only model the formations above that unconformity.

Using this geological structural model, a hydrothermal model was created to define temperature distributions, provide heat-in-place estimates, and identify prospective targets inside the geothermal reservoir. In this hydrothermal study, rock and fluid thermal and flow properties as well as boundary conditions were defined using available data and understanding of the geothermal reservoir. Rock properties were assumed to be constant by formation across the sub-basin-scale model. The 3D geological model was then populated with those properties and coupled heat and flow simulations were run to identify potential targets of smaller scale.

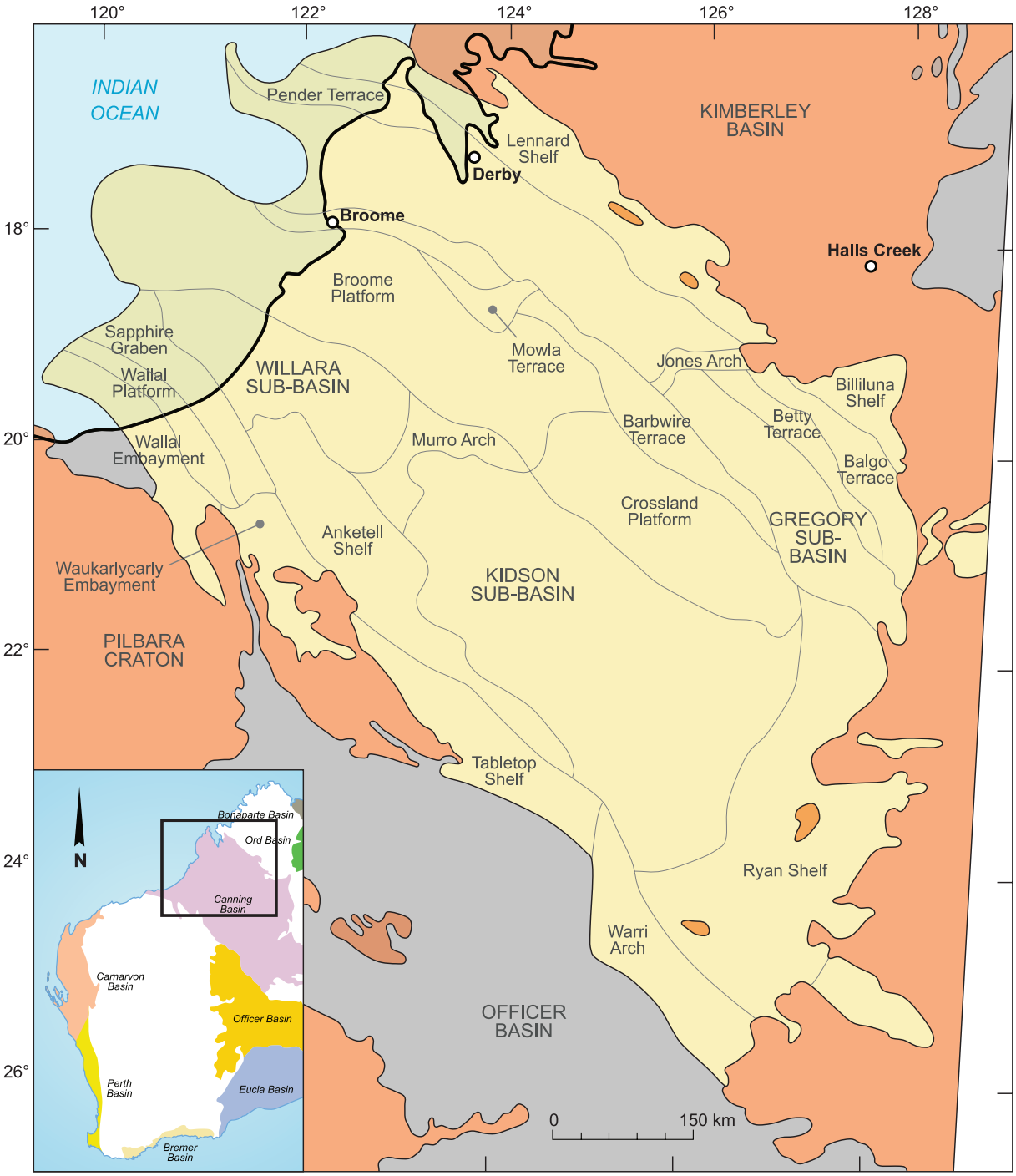

Figure 3.1: Location map of the Fitzroy Trough within Western Australia. The Canning Basin is delimited by the yellow colour. The sub-basin-scale model area is shown with a black rectangle in the Fitzroy Trough of the Canning Basin.

Age	Stratigraphic unit		Lithology	Aquifer potential
Early Permian	Surficial formations			
	Noonkanbah Formation		Mudstone interbedded with sandstone	Aquiclude
	Pooles Ss	Tuckfielfd Member	Sandstone, minor siltstone	Major
		Nura Nura Member	Calcareous quartz sandstone and sandy limestone	Aquiclude
	~~Unconformity~~~~~			
	Grant Gp	Carolyn Formation	Sandstone, conglomerate and mudstone	Major
		Winifred Formation	Siltstone, minor limestone	Aquiclude
		Betty Formation	Sandstone and conglomerate/diamictite, minor siltstone	Major
	~~Unconformity~~~~~			
Late Carboniferous	Reeves Formation		Sandstone, mudstone, and diamictite	Major?
	~~Unconformity~~~~~			

Table 3.1: Stratigraphy of the Fitzroy Trough, modified from Geological Survey of Western Australia and Petroleum Division (2004).

The hydrothermal model was run to steady state conditions. The final steady-state model temperature and pressure distributions are shown in Figure 3.2. Based on reservoir thickness, reservoir quality, and temperature distributions, two smaller reservoir-scale prospects in the Carolyn Formation were identified for further study (Figure 3.2).

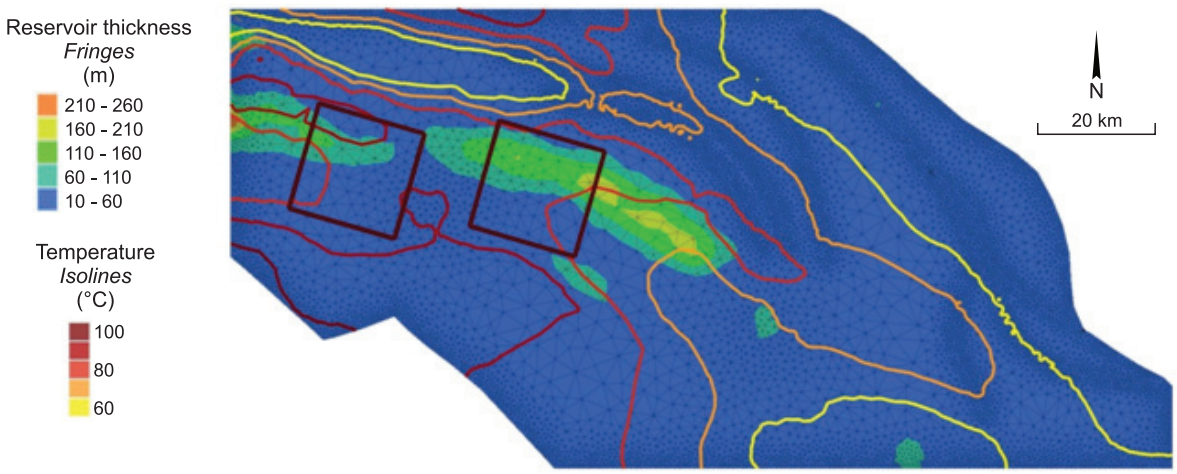

Figure 3.2: Selection of reservoir models (maroon squares) from Carolyn Formation, showing thickness and modelled temperature. This sub-basin model area is located within the black rectangle of Figure 3.1.

Further details on the geological and hydrothermal studies are available in Reid et al. (2012).

3.1.2 Reservoir modelling

The aims of the reservoir study at this early stage of geothermal exploration were: (i) to characterize the different reservoirs, (ii) to evaluate the possible geothermal applications, and (iii) to propose the best location for geothermal development.

The reservoir study is demonstrated in the right target isolated in Figure 3.2. The reservoir model (Figure 3.3), a 25 km x 25 km subset of the sub-basin-scale model, contains three formations, all in the Grant Group, from bottom to top: Betty Formation (aquifer), Winifred Formation (aquitard) and the Carolyn Formation (aquifer). Temperature and pressure data were imported from the FEFLOW hydrothermal model into the TEMPEST MORE reservoir model. The Carolyn and Betty formations both have mainly sandstone while the Winifred Formation is considered to consist mostly of siltstone. The reservoir model was meshed on 49x49x39 corner point geometry (CPG) cells. Typical cell sizes are 500 m x 500 m laterally and vary from 9 to 250 m in the vertical direction.

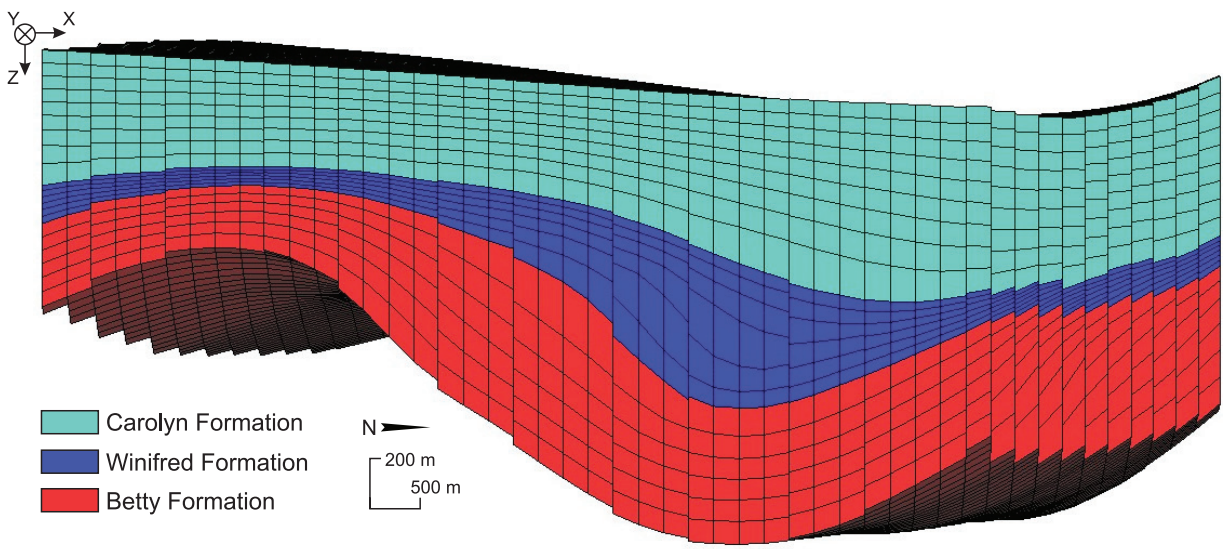

Figure 3.3: Reservoir model coloured by lithology, in light blue the Carolyn Formation, in dark blue the Winifred Formation, in red the Betty Formation. The model extents are located in Figure 3.2 by the right maroon square.

The thickness of the Carolyn Formation ranges from 386 to 802 m with an average of 553 m. The thickness of the Betty Formation ranges from 207 to 778 m with an average of 492 m. The temperature in the Carolyn Formation ranges from 60 to 84 °C with an average of 71 °C. An average formation temperature map was calculated and then projected to the surface assuming 5 °C/km^{-1} temperature losses (Figure 3.4a). The temperature in the Betty Formation ranges from 76 to 110 °C with an average of 93 °C. An average formation temperature was calculated and then projected to the surface assuming 5 °C/km^{-1} temperature losses (Figure 3.4b).

The reservoir pressure was predicted to be close to the hydrostatic condition, so no over-pressure is expected. Geothermal production of the aquifer water will require pumping. At this stage, the temperature range of both aquifers is suitable for a large variety of direct-use applications.

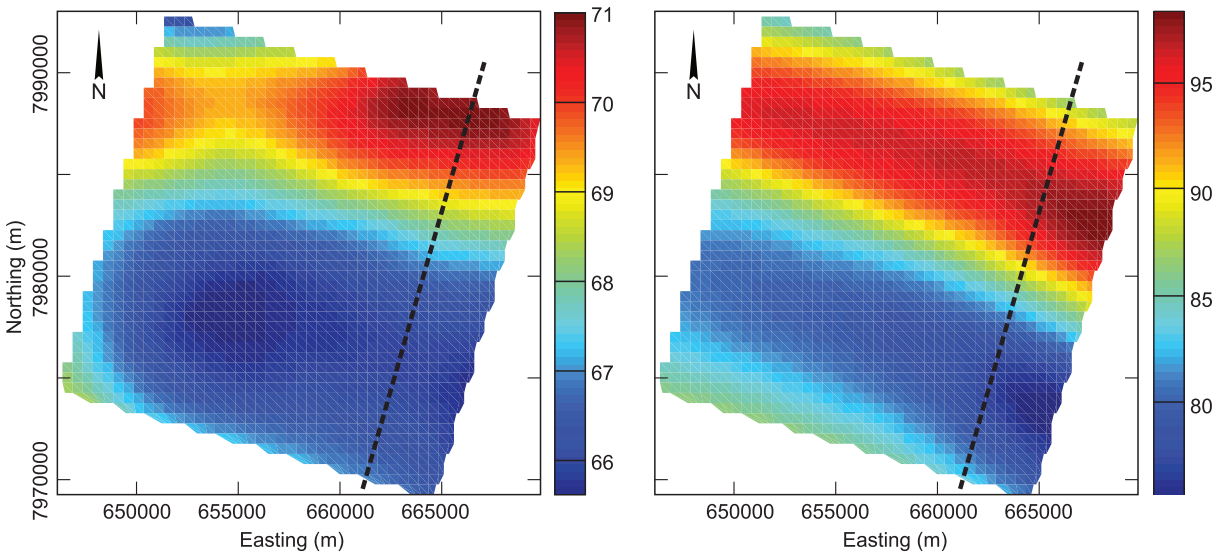

Figure 3.4: Projection to the surface of the average formation temperature for (a) the Carolyn Formation, (b) the Betty Formation.

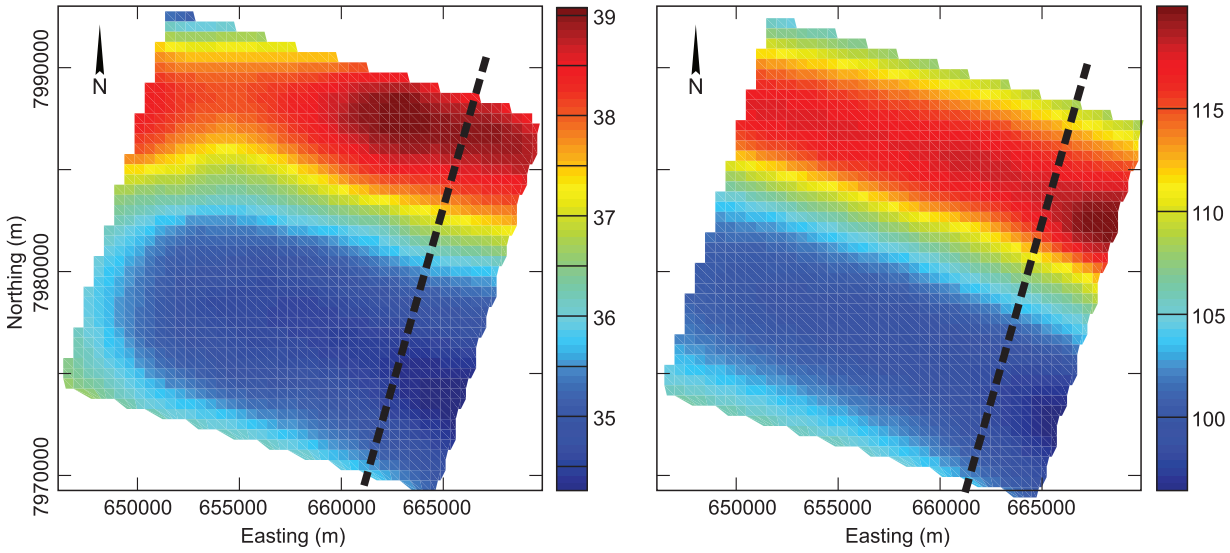

Figure 3.5: Normalised formation flow rate for (a) the Carolyn Formation, (b) the Betty Formation.

Assuming a maximum reservoir pressure loss ΔP of 200 kPa due to production, a surface temperature extraction of 20 °C and a well doublet distance of 2000 m, the flow rate and the extractable energy could then be calculated on each cell of the model. As the rock properties were assumed to be constant per formation, the spatial variation of the flow rate was directly linked to the spatial variation of the formation thickness, assuming production over the whole formation thickness, and the water viscosity. The water viscosity varied due to the temperature increase with depth. To make comparisons within an aquifer and between the two aquifers, the flow rate was integrated vertically and then divided by the aquifer thickness. We defined the result as the normalized vertical

formation flow rate. For a given pressure difference, well doublet distance and well radius, this parameter varies within a formation due to the impact of temperature on the viscosity of the fluid. The normalized vertical flow rate parameter allows us to compare the geothermal potential of both aquifers (Figure 3.5). Within the Carolyn Formation, this parameter varies by approximately 14%. In the Betty Formation, this variation is approximately 6%. The normalized formation flow rate is about three times higher in the Betty than in the Carolyn Formation. This can be explained by a higher permeability of the Betty Formation and by a higher temperature (and hence lower fluid viscosity).

Finally, the Betty Formation was the subject of a geothermal reservoir modelling investigation with a well doublet (producer and injector) positioned at the location of the highest normalised flow rate values; this location also displays the highest temperature.

The geothermal target was assessed in terms of several constraints on production intended to reflect requirements of feasible geothermal applications. The production requirements applied were as follows:

i. a well doublet composed of a producer and an injector,
ii. a working flow rate of 70 L/s,
iii. a production/injection interval of 300 m,
iv. the fluid is produced at reservoir temperature and re-injected at 60 °C,
v. an operation lifetime of 20 years (before thermal breakthrough).

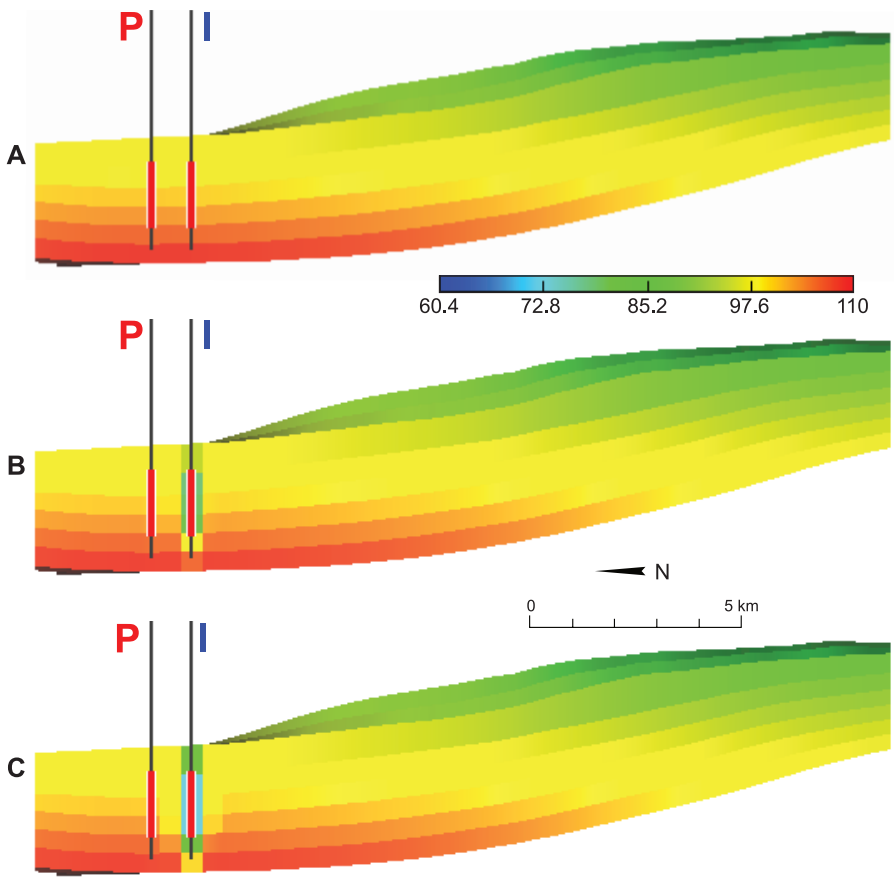

Figure 3.6: (a) initial temperature, (b) temperature after 20 years of production and (c) temperature after 40 years of production. Producer and injector wells are denoted by P and I, respectively. The cross-section is illustrated in Figure 3.4(a) by a dashed line.

Figure 3.6 shows cross-sections of the temperature in the reservoir model at various production times. The reservoir temperature is affected by the plant production around the injection well. However, with a 2 km distance between the two wells, the injected cold water did not cool the producer after 40 years of continuous production (Figure 3.6). The produced temperature at the bottom hole is constant over time, slightly over 100 °C. Taking into account the heat losses in the well, the wellhead temperature should be less than 100 °C. The production of electricity, which requires a minimum temperature of 95 °C, is therefore possible but quite unlikely due to other above-ground losses. However, the geothermal resource seems to be well adapted for direct-use applications.

3.1.3 Discussion

An integrated modelling study incorporating structural geology, reservoir engineering and regional hydrothermal modelling, has been performed with application to the Noonkanbah area in the Canning Basin, Western Australia. This integrated modelling study focused on the consistency of the dataset at different scale and different resolution. The structural modelling allowed defining the boundaries and the volume of the reservoirs while the regional hydrothermal study gives the initial input for the resources evaluation. Based on that, reservoir modelling areas were defined and possible geothermal direct use applications were investigated. The results showed that the two aquifers have potential for direct use applications with temperature about 65 °C in the Carolyn Formation at an average depth of 1000 m and temperature of about 74 °C to 92 °C in the Betty Formation at an average depth of 2300 m. The deeper Betty Formation appears to be a better production target than the Carolyn Formation at this location. Mapping of the normalized vertical flow rate provides a tool for best well implementation. Finally, a simple reservoir modelling study based on a well-doublet project design was performed at the best well location and shows the sustainability of the geothermal project in term of thermal breakthrough for the planned lifetime of the project.

3.2 Reservoir assessment via stratigraphic forward modelling

The major aquifer and low-temperature geothermal target in the Perth Basin, the Yarragadee Aquifer, provides a major portion of Perth's drinking water. Although the shallow part of the Yarragadee Aquifer has been well studied by hydrogeologists, the deeper part is still poorly characterized. Stratigraphic forward modelling (SFM) is a process simulation approach that attempts to replay the deposition of sediments. Using the stratigraphic forward modelling package Sedsim, the sedimentation of the Yarragadee Formation was simulated over a period of 15.8 Ma, from 160 Ma to 144.2 Ma. More details on this stratigraphic forward modelling study on the Yarragadee formation of the Perth Basin are presented in details in Timms et al. (2012). This section (Corbel et al., 2011b; Corbel et al., 2012) presents the second part of this joint geothermal reservoir characterization study.

Once the sedimentary simulation of the Yarragadee Formation was achieved via Sedsim, the identification of geothermal reservoirs was the next step. This required the investigation of the ability of the subsurface to deliver the energy required for a target geothermal application. Here, based on simple physical assumptions such as thermal conduction, uniform geothermal gradient, and using

pre-defined geothermal production design settings such as flow rate and maximum pressure drop, parameters such as reservoir temperature and reservoir producible power were evaluated. As the various possible geothermal applications have differing subsurface requirements, reservoirs are sequentially investigated for a given geothermal application. This methodology has been developed to allow rapid investigation of the local geothermal potential while changing the surface geothermal application requirements. It is recognized that this methodology is a first-pass approach, as it does not account for non-conductive processes that have been shown to be significant in the Perth Metropolitan Area (Reid et al., 2011).

3.2.1 Reservoir assessment methodology

The assessment methodology was divided into three steps. First, temperature, water density, heat capacity and flow rate were computed using the stratigraphic forward model outputs (porosity, permeability, cell thickness) and the geothermal project design (pumping pressure difference), for each grid cell of the model.

Subsurface temperature in the Perth Basin was computed assuming a vertical conduction heat transfer, a constant geothermal gradient of 25 °C km^{-1} (Reid et al., 2011) and a constant ground surface temperature of 20 °C. Water density and heat capacity were computed as functions of temperature only and the flow rate was determined using the doublet flow rate equation (Gringarten, 1978).

Geothermal reservoirs were then defined by vertical summation of the flow rate and thermal energy, up to a given reservoir thickness. For each of the reservoirs, average temperature, cumulative flow rate and the energy that can be extracted from the geothermal fluid for a given geothermal application were also computed. The reservoir thickness determines the range of feasible geothermal applications. To assess the impact of the screening interval planned for an application, it is easy to simply modify the reservoir thickness and check the effect on the flow rate.

The power extractable from a geothermal flow, Pth (in MWth), is computed using the following equation:

$$P_{th} = COP\ \rho\ C_p\ Q\ \Delta T \qquad (3.2.1)$$

where COP is the coefficient of performance of the geothermal infrastructure
Q is the production flow rate of the geothermal fluid in $m^3\ s^{-1}$
ρ water density in kg m^{-3}
C_p water heat capacity in kJ $kg^{-1}\ K^{-1}$
ΔT temperature difference between extracted and reinjected water in degress Celsius.

Finally, optimal locations for a given geothermal application can be identified using thresholds on the reservoir temperature, flow rates or extractable power. The thresholds can be quickly modified depending on the main parameters of the geothermal application and the appropriate locations quickly updated.

3.2.2 Reservoir assessment for absorption chiller applications

The above methodology has been applied to assess the prospectivity of direct-use geothermal applications within the Yarragadee Formation in the Perth Metropolitan Area.

As mentioned before, swimming pool heating has already been proven successful in the Perth Metropolitan Area, therefore we decided to look at another direct-use application, air conditioning. We are taking the example of an absorption chiller to see what cooling load could be met with the following characteristics:

First, in order to locate suitable reservoirs, a threshold on the reservoir temperature was applied based on the application working temperature. Then, the flow rate and energy were calculated over a maximum screened interval of 300 m. The results are presented in map view and along a North-South cross-section on Figure 3.7. Those results are first-order estimations and must be treated with care. Although they give a preliminary idea of the feasibility of a relevant absorption chilling application, as defined in Table 3.2, further work including economic studies linked to pumping costs must be done before taking any decision to invest. Nevertheless, the concept of reservoir assessment linked to SFM predictions has been demonstrated.

Plant design	Air conditioning
Inter-well distance, half distance of an horizontal cell, d_{well} = 1855 m	Working temperature, 75°C - 85°C
Well radius, r_{well} = 0.15 m	Coefficient of Performance = 0.67
Production interval, H = 300 m	Temperature difference, ΔT = 20°C
Maximum reservoir pressure losses ΔP = 200 kPa	Minimum extractable power = 1 MW_{th}

Table 3.2: Geothermal application parameters: Air Conditioning via Absorption Chilling.

Testing different application settings is quite easy with this methodology, as the flow rates and extractable energy values can be computed readily. Although Figure 3.7 shows only the upper (Yarragadee) reservoirs fulfilling our application criteria, deeper reservoirs might be located in the same area with different extractable flow rates and energy.

3.2.3 Discussion

Stratigraphic Forward Modelling was successfully applied to characterize the unexposed and poorly quantified Yarragadee Formation in the Perth Basin. It proved its efficiency at predicting grain size and porosity distributions based on geological reasoning rather than interpolation between sparse data. It provided insight into, and numerical predictions of, the distribution of sediments and their properties below ground, based on an understanding of the depositional processes involved.

SFM was then used to estimate rock properties for input to a regional thermal model. Assuming a temperature distribution over the regional model, flow rate and thermal power were calculated, compared and plotted. This simple technique allows the potential for various candidate direct-use applications to be evaluated quickly. It provides a regional scale view of the spatial distribution of possible reservoirs and their geothermal potentials. This screening technique would benefit from better descriptions of the subsurface temperature and pressure distributions. The method would also

benefit from inclusion of the non-hydrostatic pressure data as an important parameter for pressure losses and therefore pumping power demands. Ultimately, this SFM-based method informs risk assessment and risk mitigation processes for direct-use geothermal exploration.

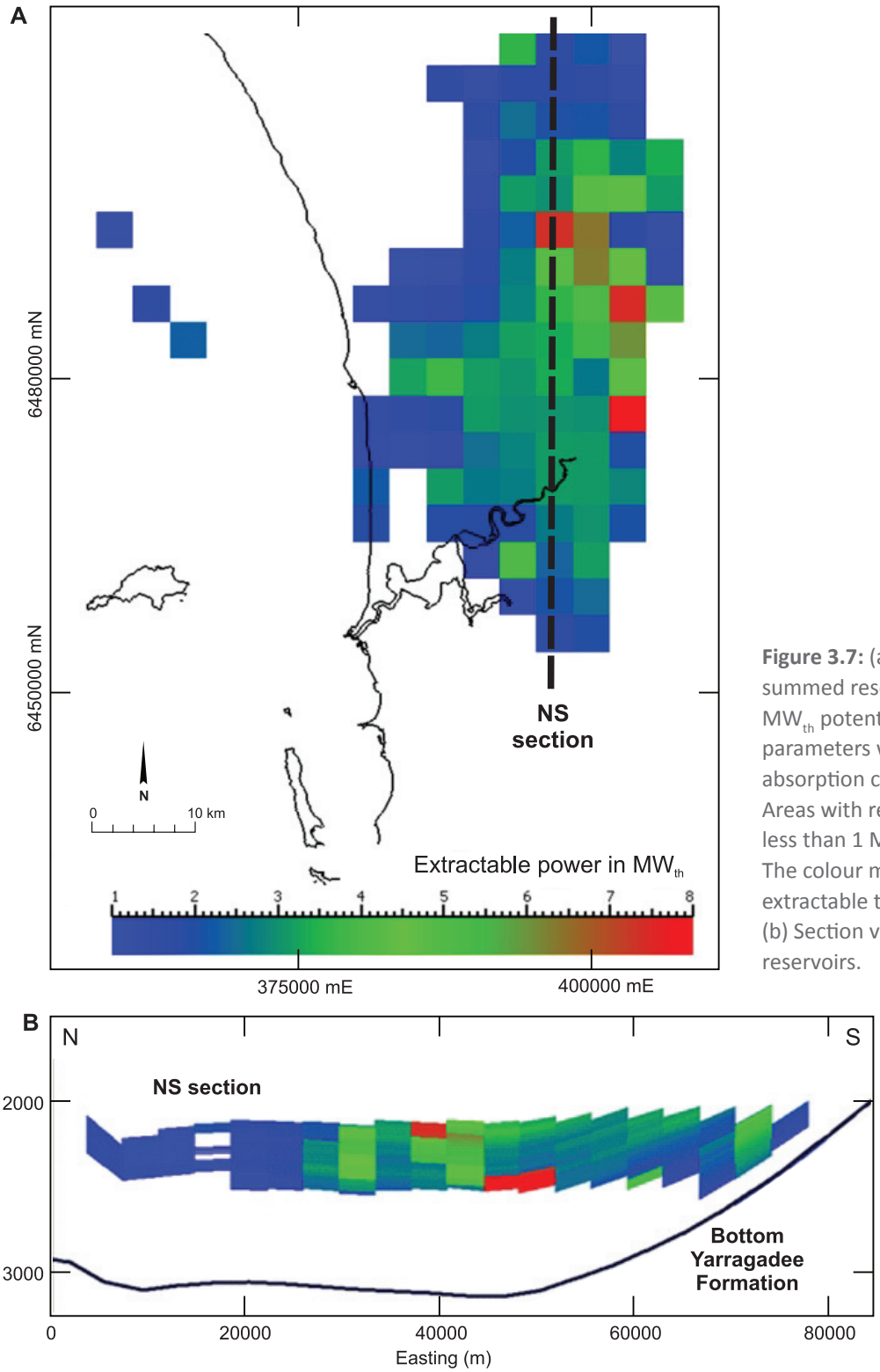

Figure 3.7: (a) Map view of summed reservoirs above 1 MW_{th} potentially fulfilling the parameters we defined for absorption chiller applications. Areas with reservoirs producing less than 1 MW_{th} are left white. The colour map shows the extractable thermal power. (b) Section view of target reservoirs.

3.3 Conclusions

In this section, we addressed several issues regarding the exploration for geothermal reservoirs. One of the key issues for low-temperature geothermal exploration is to develop its risk assessment and mitigation framework. Starting from the intrinsic definition of a direct-use geothermal plant, we proposed an innovative way to evaluate the geothermal potential of an area. From existing and publicly available datasets, we performed an integrated exploration study from structural geology to reservoir engineering and resources evaluation in the Canning Basin. This work allowed us to compare different aquifers to each other and also to target the locations of best productivity. The second study presented in this report is also based only on publicly available data. In this second study, the specific requirements of a surface geothermal application were taken into account to define suitable target reservoirs in the Yarragadee aquifer of the central part of the Perth Basin. This was achieved by using modelling workflow similar to the first study, but with better geological constraints in the subsurface.

4. THERMAL CHARACTERIZATION OF THE PERTH BASIN

The spatial distribution of subsurface temperature and its evolution through time is an important parameter for resource evaluation and production sustainability estimates of geothermal projects.

Existing temperature measurements in Western Australia are the results of groundwater and petroleum exploration and production activities. While sparse temperature data are available at great depth (more than 1 km), records of continuous temperature logging are rare or mostly available only at shallow depths (less than 1 km). In most cases temperature measurements are acquired in the wellbore shortly after drilling. The observed temperature can differ significantly to the undisturbed rock formation temperature as a result of thermal perturbation during the drilling process. Correction of temperature data is an important enabling step for subsequent geothermal reservoir analysis.

This section addresses the following aspects of thermal characterization of the Perth Basin performed by WAGCoE:

- Development of a thermal data analysis tool, GeoTemp™ (Ricard and Chanu, 2012),
- Correction of temperature measurements of the Perth Basin,
- Mapping and distribution of temperatures in shallow formations of the Perth Metropolitan Area,
- Investigation of the Gnangara Mound shallow low-temperature anomaly,
- Fine-scale vertical heterogeneity of flows in the Leederville Formation, observed during the M345 Aquifer Storage and Recovery project,
- Deep temperature estimates, based on Cockburn-1 logging data.

4.1 GeoTemp™

Geothermal exploration and exploitation requires tools and workflows to process, assess, interpret and visualise temperature data. To handle these tasks, WAGCoE has developed the GeoTemp™ data analysis tool.

GeoTemp™ (Ricard and Chanu, 2012; Ricard et al., 2011a; Ricard et al., 2011b) embodies an integrated graphical workflow for inferring underground temperature profiles and estimating rock thermal parameters based on the analysis, interpretation and modelling of wireline temperature logs and core sample data. Version 1.0 of the software (Ricard and Chanu, 2012) presents the foundation of this workflow and includes data loading, interpretation and one-dimensional vertical conduction modelling procedures.

Temperature data are available in two fundamentally different formats: wireline temperature logging measurements or sparse temperature observations. GeoTemp™ handles the interpretation of these data formats by using three distinct components as described succinctly below:

i. Wireline logging workflow is formed by several modules corresponding to different steps of the analysis: Processing, Data Evaluation, Heat Production, Conduction, Modelling and Risk.
ii. Wireline workflow support provides four additional modules for data handling: Viewer, Formation Management, Guided Analysis and Regional Assessment.
iii. GeoTemp Sparse temperature viewer represents its own module for sparse data analysis.

GeoTemp™ is a platform independent software which can be run conveniently on Windows, Linux and Macintosh operating systems. The software package is composed of an executable file, some tutorial examples and a detailed technical user manual. Executable files, tutorial examples and the user manual can be downloaded free of charge from the CSIRO website (: http://www.csiro.au/en/Organisation-Structure/Divisions/Earth-Science--Resource-Engineering/GeoTemp.aspx). A detailed description of GeoTemp™ can be found in Ricard and Chanu (2012).

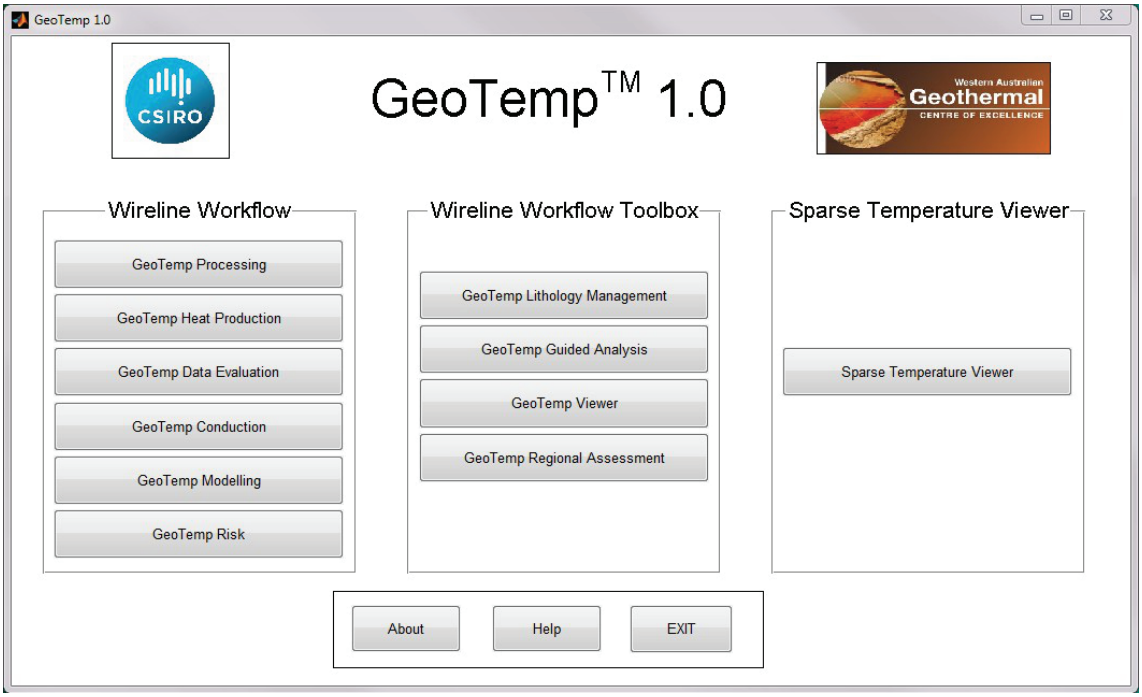

Figure 4.1: GeoTemp™ 'Framework'. The interface is subdivided into three panels, one for each component. In those panels, each button links the main interface to the respective component module.

4.2 Perth Basin temperature corrections

In sedimentary basins, the temperature normally increases with depth (neglecting thermal perturbations due to non-conductive processes). Exploration for geothermal heat extraction systems requires observations and information on the temperature at depth. The deepest existing temperature measurements were usually collected during petroleum exploration and were thus acquired using a range of methodologies, often shortly after the wells were drilled. Some common methods for temperature data acquisition and standard terminology include:

- wireline logging - produces bottom hole temperatures (BHT) at the deepest point
- drill stem test (DST) - pumps significant quantities of water from the formation
- formation evaluation (WFT) - a small-scale sampling method
- continuous temperature logging

Deep temperature measurements are geographically sparse, made by different techniques and engender different levels of reliability; nevertheless they remain the only information available on

reservoir temperatures at depth. We focus on the processing and interpretation of sparse and deep temperature measurements within the Perth Basin, Western Australia (Ricard et al., 2012a). We present a simple temperature study based on existing corrected and non-corrected temperatures for the Perth Basin. All results are combined and conclusions are made on the impact of the temperature corrections on geothermal exploration in the Perth Basin.

4.2.1 Non-corrected temperatures

The Perth Basin has been subject to intense petroleum exploration, both onshore and offshore. As part of this exploration program, deep temperature measurements were taken; many of those are available in the PressureDB database (CSIRO, 2007). In this study, we used 59 Perth Basin wells present in the PressureDB database, representing a total of 491 temperature observations. The data comprised 270 BHT, 21 corrected BHT, 6 drill stem tests, 170 wireline formation tests, and 6 unknown measurement types. Temperature data are mostly BHT measurements and therefore are considered as having low reliability.

Thermal regime characterization at shallow depths in the Perth Metropolitan Area (Reid et al., 2011) showed that heat production from the sedimentary column above 700 m depth is less than 1% of the total heat budget. A temperature gradient was calculated from the measurements assuming no radiogenic heat production and a vertical conduction thermal regime over the entire basin. Previous studies by Chopra and Holgate (2007) and Hot Dry Rocks Pty Ltd (2008) calculated the temperature gradient in wells using the same assumptions, and created interpolated maps of temperature at depth for the Perth Basin.

The temperature dataset compiled here is plotted against depth of measurement in Figure 4.2 both with a 26 °C km^{-1} temperature gradient slope with maximum temperature varying from 80 to 130 °C, at 3000 m. From surface to 3000 m, the dataset exhibits a linear trend with a 73% correlation. The discontinuity of the linear trend at 3000 m is of particular interests for deep geothermal

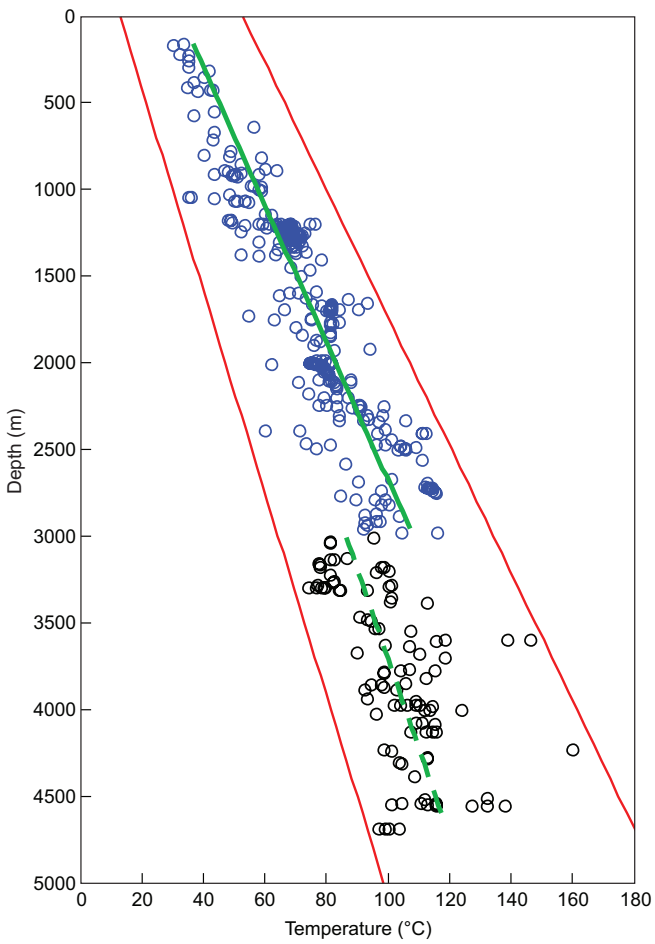

Figure 4.2. Temperature measurements in the Perth Basin with correlation line in green and lower and upper bounds in red (a) for the entire dataset (b) only from surface to 3000 m.

exploration, although no explanation for the discontinuity has yet been found. The part of the dataset below 3000 m exhibits a poor correlation of 41% to a linear trend with a temperature gradient of 18 °C km^{-1}. The entire basin dataset can be bounded by a lower temperature gradient of 17 °C km^{-1} and an upper gradient of 26 °C km^{-1}. The deeper temperature data are likely to be more unreliable if they are uncorrected.

4.2.2 Corrected temperatures

In this section, we perform an analysis of corrected temperature measurements in the North Perth Basin, with the additional goal of providing reliability estimates. The uncorrected temperatures shown in the previous section suffer from uncertainties which increase with depth. In order to reliably utilise temperature measurements for prediction and calibration of numerical models, corrections to true formation temperatures (TFT) are necessary, along with some measure of the uncertainty in the correction.

Here we use a technique to correct measured temperatures and estimate standard deviations (σ) for the derived true formation temperatures. The analysis assumes that the errors on final TFT estimates are normally distributed:

- For drill stem tests, no mean correction is required and σ = 2.5 °C (Hermanrud et al., 1990).
- For Horner corrected temperatures, the mean offset is assumed to vary proportionally to the measured temperature (Holgate and Chopra, 2005) with the correction equal to 4% of the Horner Plot temperature estimate, which was the value derived for South Australian measurements.
- For Horner corrected temperatures, the standard deviation is proportional to the measured temperature and varies with the number of extrapolation data points (Waples and Ramly, 2001). For two measurements σ=4.9% of the Horner Plot temperature estimate, and for three or more BHTs, σ=6.9% of the Horner Plot temperature estimate.

The uncertainties produced by these formulae agree well with the average standard deviations estimated by Forster (2001) and Corry and Brown (1998). The final temperature data is available in Table 4.2 of the companion report of Project 3, Reid et al. (2012).

Temperature measurements from 97 wells, mostly onshore, in the Perth Basin (Figure 4.3) have been processed with the above corrections and uncertainties in view of the three dimensional heat conduction modelling study performed by Reid et al. (2012). An area under active geothermal exploration, the North Perth Basin, was specifically investigated. An overview of the 236 temperature observations with their corrections and associated uncertainty is shown in Figure 4.4. The North Perth Basin wells have generally higher temperatures at depth than those from the rest of the Perth Basin, although many northern measurements show significant uncertainty.

Average geothermal temperature gradients were calculated from mean annual temperature (MAST) estimates on the ground surface and the corrected temperature values. Standard deviations on temperature gradient were assumed to represent the same percentage of error than the standard deviation of corrected temperature. Temperature gradients are plotted at their depth measurement

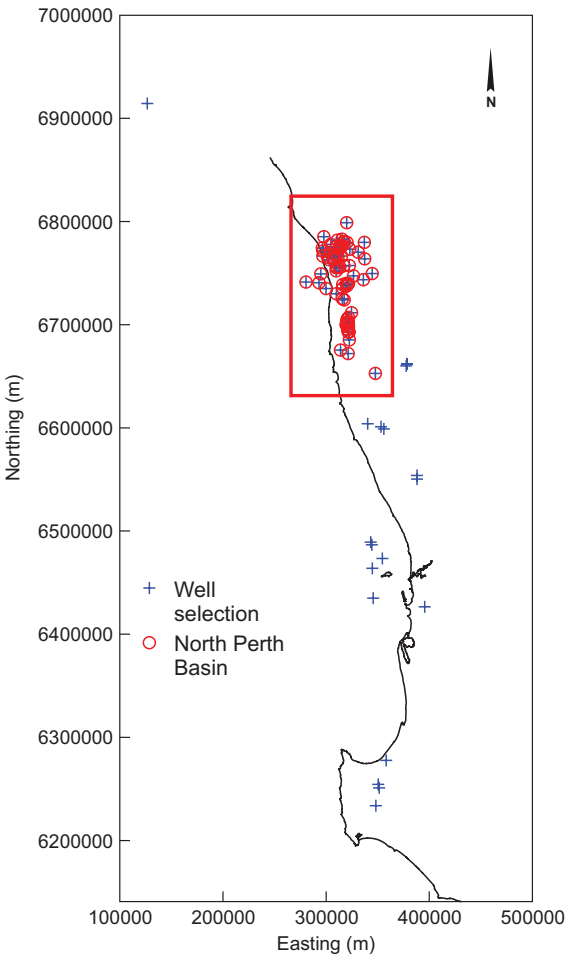

Figure 4.3: Location map of Perth Basin wells with deep temperature measurements.

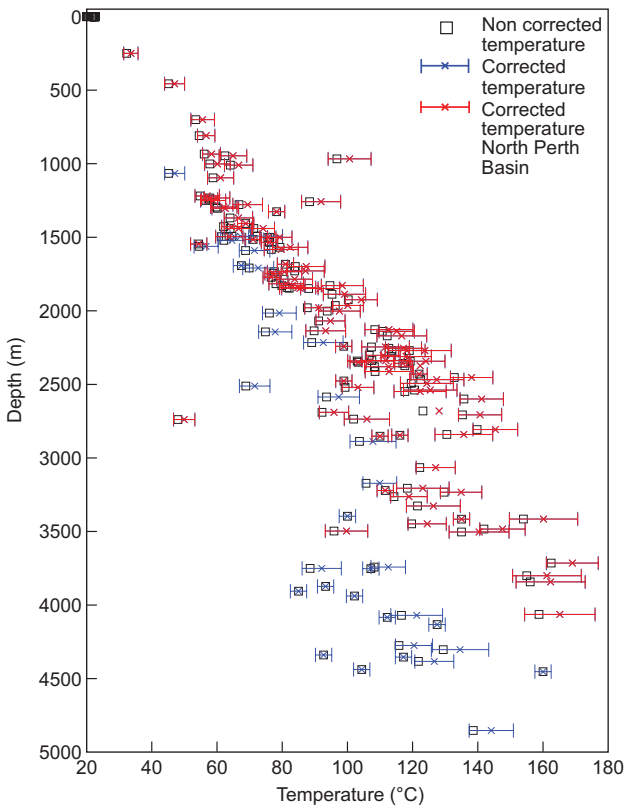

Figure 4.4: Temperature corrections at depth for wells from the Northern (red) and rest (blue) of the Perth Basin. The non-corrected data is shown with a square, while the corrected temperature is indicated in the midpoint of the uncertainty range.

in Figure 4.5. It is clear that average temperature gradients decrease with depth for the entire Perth Basin dataset. However, the North Perth basin subset exhibits a constant temperature gradient. Near the surface, average temperature gradients can show large variability and uncertainty and are generally higher than gradients deeper in the sedimentary sequence. Both of these conclusions point out the necessity of not relying on shallow temperature measurements to predict temperatures at depth, as over-prediction may result. Average temperature gradients for all wells from the surface to 3000 m are mostly between 25 to 50 °C km^{-1}. Deeper, they range from 15 to 45 °C km^{-1} for the entire Perth Basin and between 30 to 45 °C km^{-1} for the North Perth Basin area.

A frequency chart for the entire Perth Basin is shown in Figure 4.6 for the average geothermal gradient calculated from the corrected TFT temperature and from the raw BHT measurements. The difference between the two estimates is charted in Figure 4.7. The temperature gradient correction

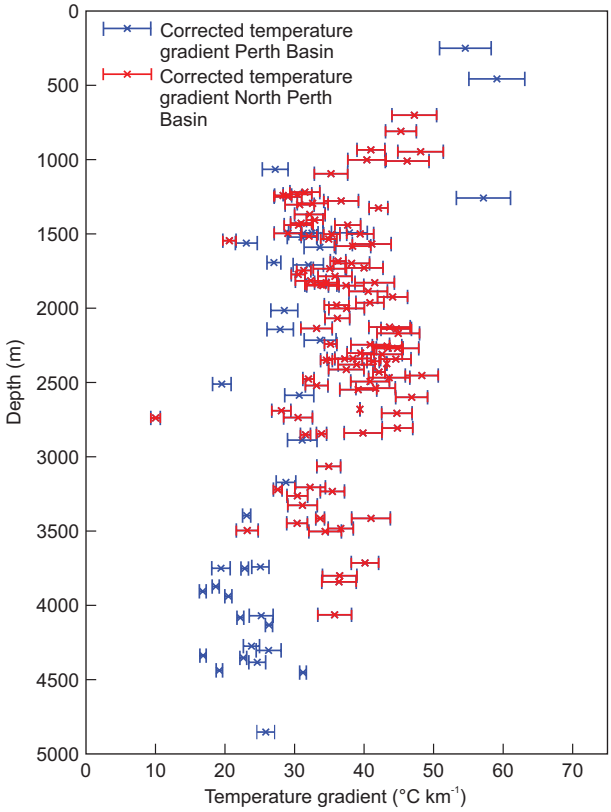

Figure 4.5: Temperature gradient reported to the depth of the wellbore temperature measurements.

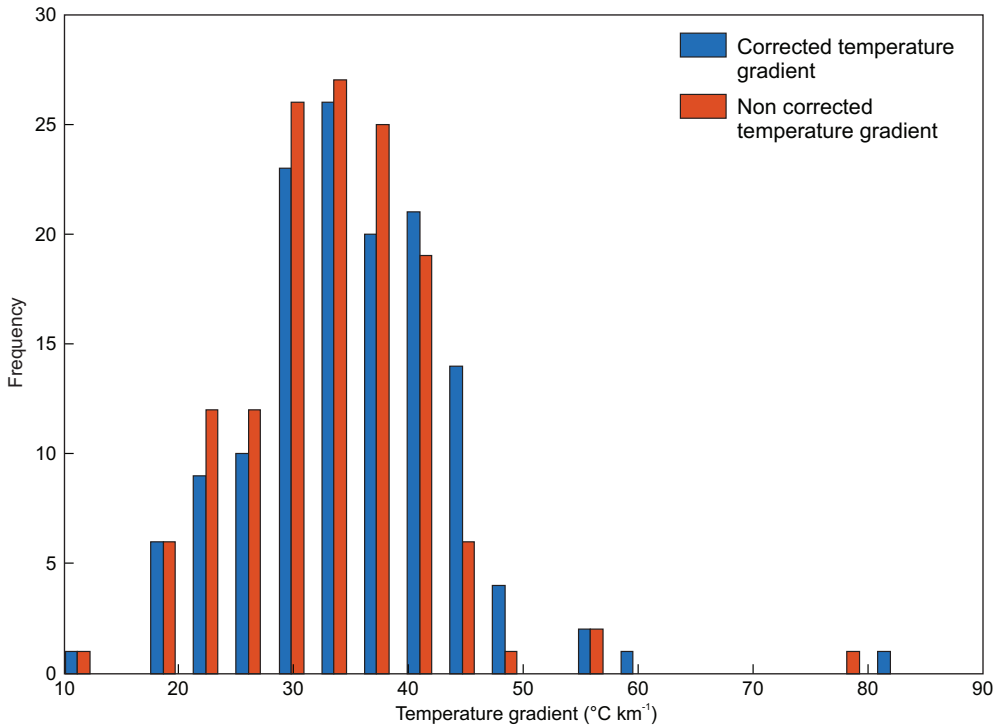

Figure 4.6: Histogram of temperature gradient.

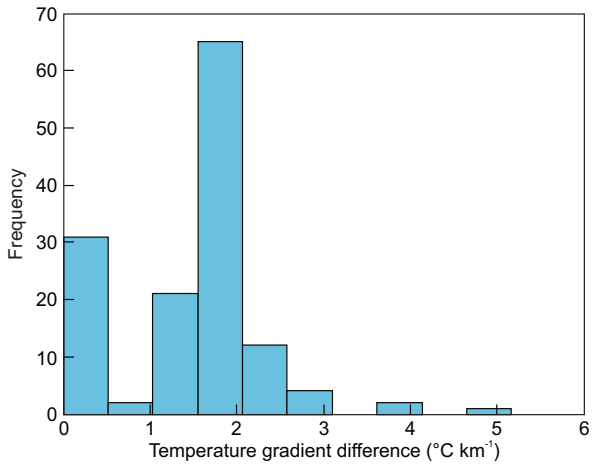

Figure 4.7: Temperature gradient correction.

Figure 4.8: Depth averaged temperature gradient (°C km^{-1}) distribution map for the North Perth Basin Area with well locations.

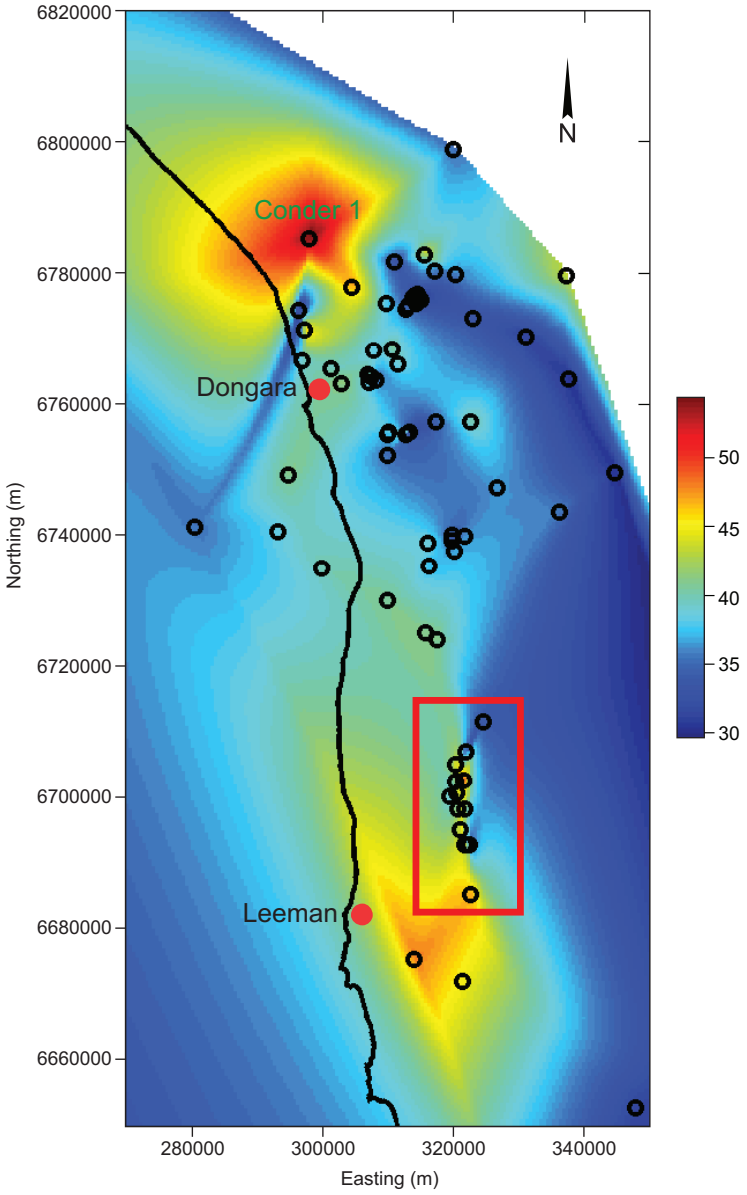

shows a difference up to 5 °C km^{-1} with a mean at 2 °C km^{-1}. This means that measurements without corrections could under-predict the formation temperature by 8 to 20 °C at 4000 m depth.

Figure 4.8 shows a temperature gradient map for the North Perth Basin. The overall background temperature gradient seems to lie between 30 to 35 °C km^{-1} with two major anomalies, one in the northern part and one in the southern part. The northern anomaly is linked to a single temperature gradient value calculated from a measurement at 250 m depth at the Conder 1 well. This high temperature gradient is not confirmed within the other selected wells at this location. The southern anomaly is linked to the temperature measurements at three wells. There are several small temperature gradient anomalies in the North Perth Basin, which appear to be linked to single well values.

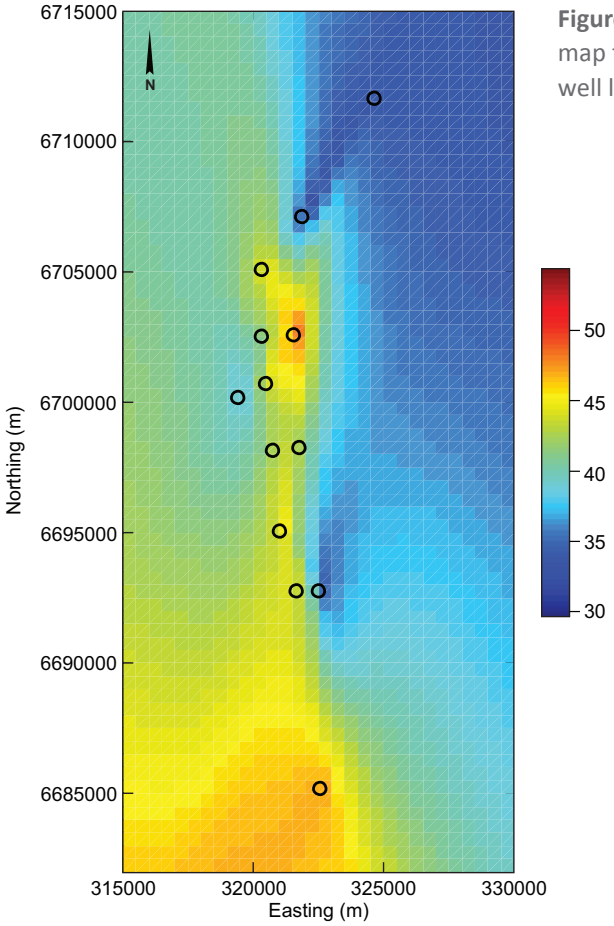

Figure 4.9: Temperature gradient (°C km^{-1}) distribution map for a subset of the North Perth Basin Area with well locations.

A more significant anomaly is located in the southern part of this dataset, highlighted by a red square in Figure 4.8 and depicted in detail in Figure 4.9. This area has 13 wells. The temperature measurements for those wells are above the Perth Basin trend and mostly between 2000 and 3000 m (Figure 4.10). The temperature gradient for 17 of the 21 measurements is between 40 to 50 °C km^{-1}. The remaining four temperature gradient estimates are around 30 to 35 °C km^{-1}. It is to be noted that the wells are aligned along a North-South lineament with wells with low temperature gradient to the east. The variability of the temperature gradient within this small area of 3000 m x 500 m suggests that this thermal anomaly should be investigated further.

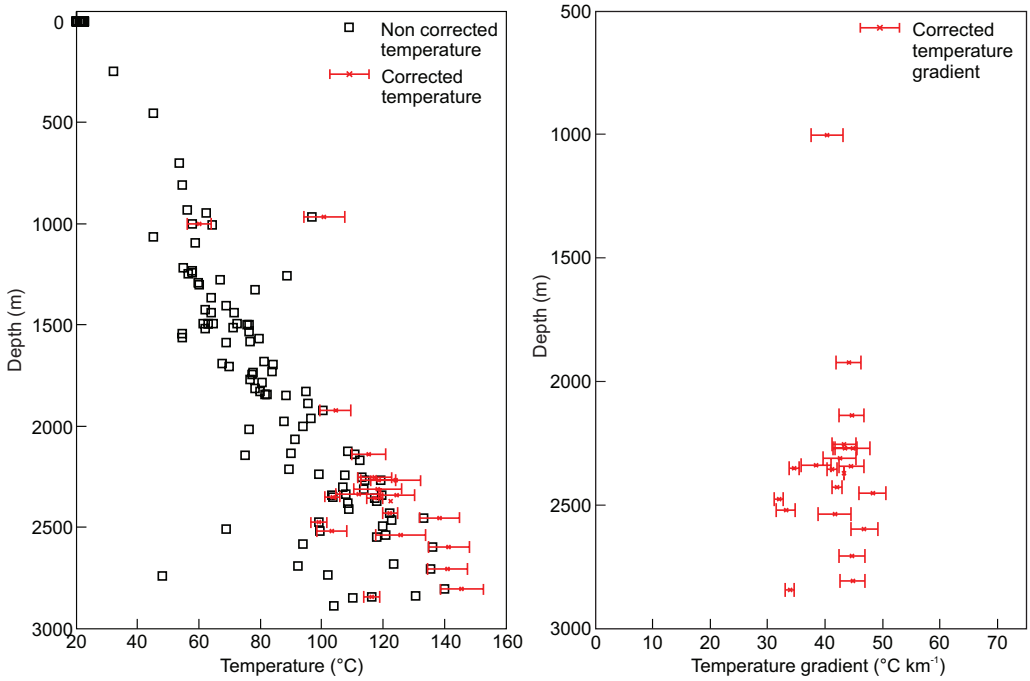

Figure 4.10: Temperature (top) and temperature gradient (bottom) versus depth for the southern anomaly in the North Perth Basin Area.

4.2.3 Discussion

Careful processing of sparse temperature data is required to support accurate thermal interpretations. In the case of the Perth Basin, temperature observations seem to be confined inside a gradient envelope that leads to temperatures varying from 80 °C to 100 °C at 3000 m depth. These conditions are favourable for a variety of direct-use geothermal applications. Corrections to temperature measurements are significant, and favourable, at higher temperatures, but uncertainty estimates should be performed for average geothermal gradient calculations. The North Perth Basin exhibits a constant temperature gradient trend with two anomalies. Small anomalies appear to be linked to temperature measurements at single wells, such as the Conder 1 well. An area in the southern part of the North Perth Basin with 13 wells shows high variability of temperature gradients within a small geographical area. While this area could represent an attractive geothermal target due to high temperature and temperature gradient, sharp horizontal temperature gradients imply that some risk is associated with geothermal resource predictions in this location.

4.3 Temperature of shallow formations in the PMA

In the Perth Metropolitan Area, temperatures suitable for direct-use applications are provided by hot groundwater in sedimentary aquifers. Although several commercial projects utilise hot water from the Yarragadee Aquifer (Pujol, 2011), there has yet been no systematic study of subsurface geothermal conditions in the PMA to support the development of direct-use geothermal projects in shallow formations.

Exploration of Perth's shallow temperature distribution was performed by WAGCoE (Reid et al., 2011). In this section we consider the estimation of true formation temperatures in shallow sediments by detailed temperature and gamma ray logging within water bores up to 800 m deep.

4.3.1 Data collection and collation

Detailed vertical temperature and gamma ray logging of seventeen WA Department of Water (DoW) Artesian Monitoring (AM) wells was performed throughout the PMA. Logging equipment was provided by Geoscience Australia.

Down-hole temperature logging was conducted at 5 cm intervals with a 5 m min^{-1} descent. The data were recorded as digital LAS files and are stored in the WAGCoE Data Catalogue (Corbel and Poulet, 2010; Poulet and Corbel, 2012). The temperature probe was calibrated before and after logging. Data was quality controlled by correcting for effects of basal silting, water table elevations, and seasonable ground surface temperature fluctuations (Reid et al., 2011).

In addition to the direct measurements, temperature logs from fifty-three DoW AM wells measured in the 1980s were digitised into LAS format (Reid et al., 2011). The digitised data were calibrated to temperature point values recorded at the time. These wells greatly extend the spatial scope of data available in the PMA.

4.3.2 Shallow temperature distribution

The temperature logs provide a picture of true formation temperatures within shallow sediments in the Perth Basin. A three-dimensional model of the temperature distribution was created and used to produce maps of temperature at depth and within the major aquifers. Figure 4.11 shows the temperature distribution at 250 m below the ground surface. Figure 4.12 shows temperatures at the top of the Neocomian Unconformity, an erosional surface roughly representing the top of the Yarragadee Formation. Three dimensional models in PDF format of the subsurface temperatures are available online at http://www.geothermal.org.au/Catalogue.htm.

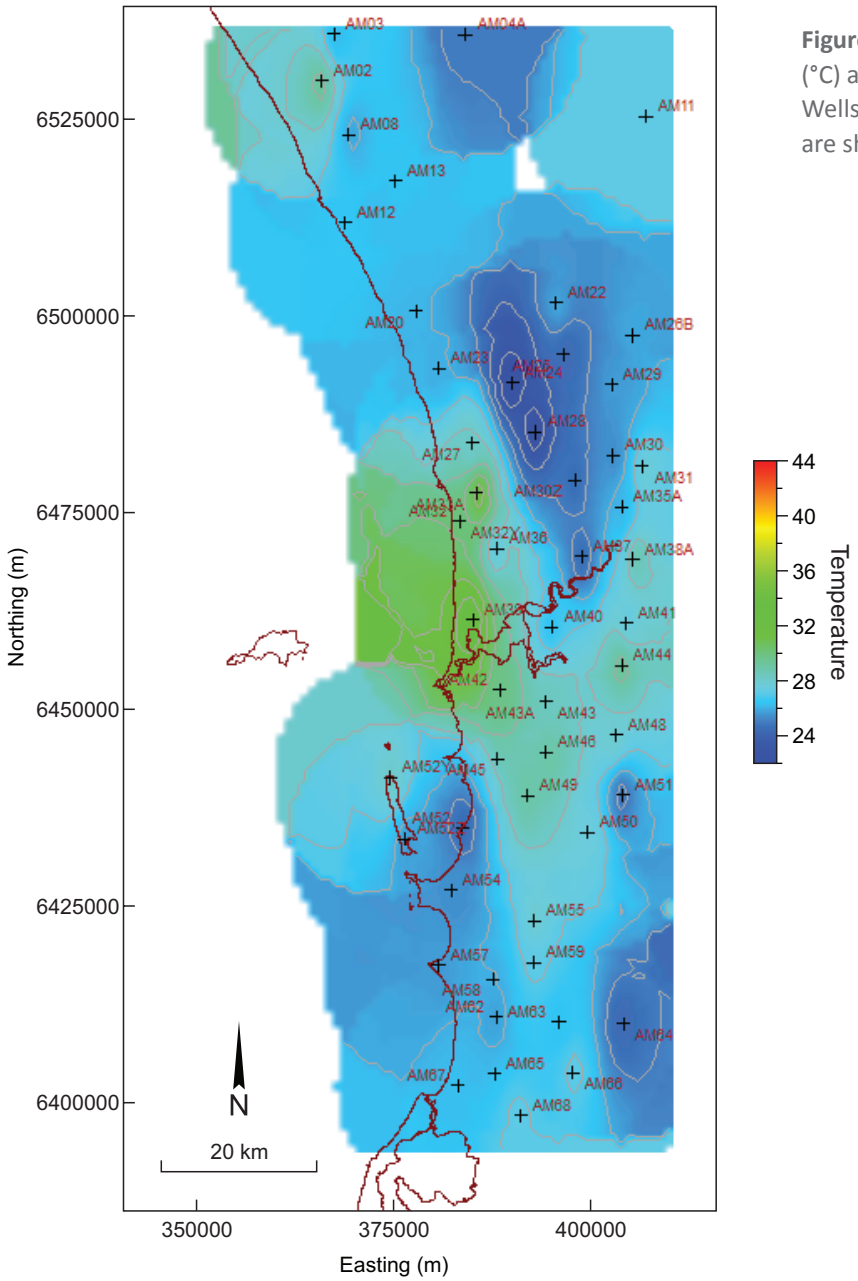

Figure 4.11: Temperature (°C) at 250 m below AHD. Wells used in the analysis are shown.

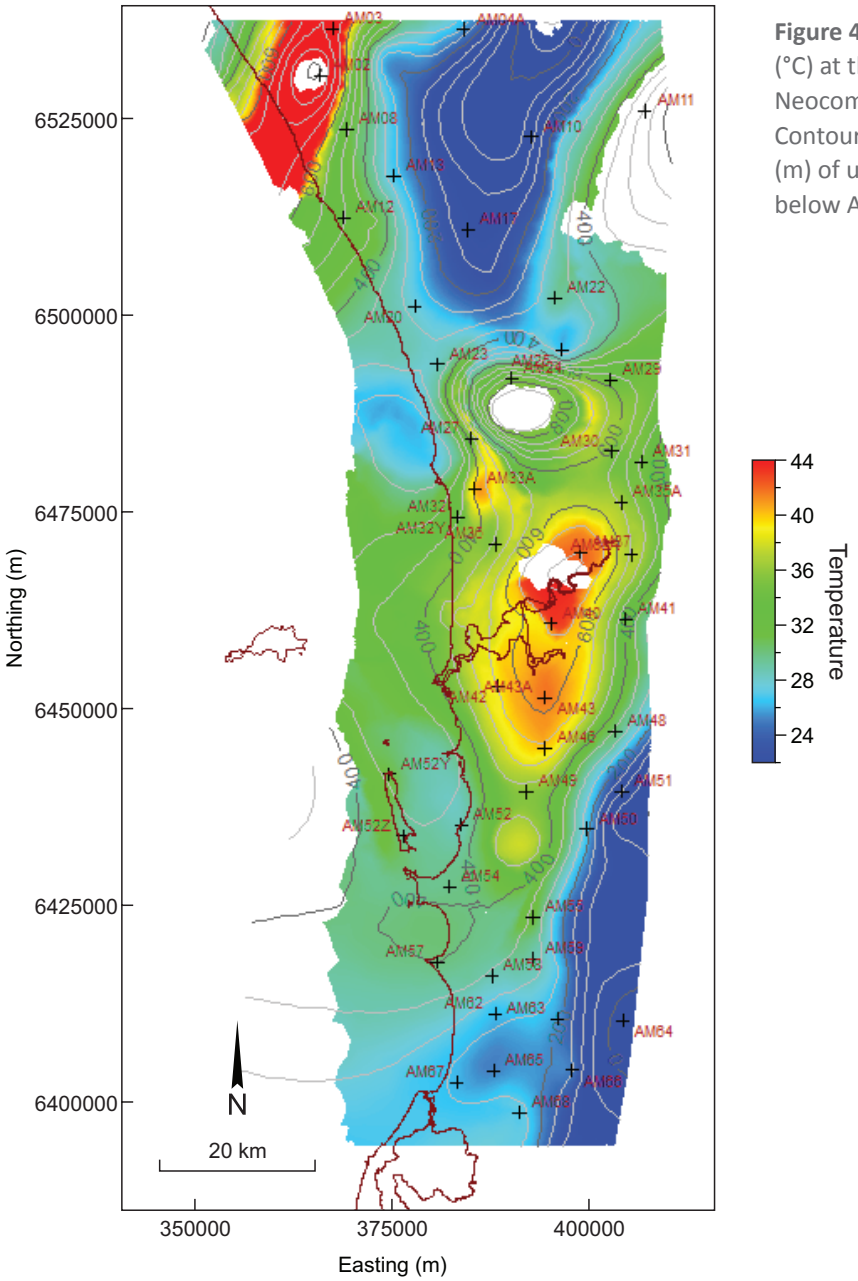

Figure 4.12: Temperature (°C) at the top of the Neocomian Unconformity. Contours indicate depths (m) of unconformity below AHD.

4.3.3 Thermal regime analysis

As radiogenic heat productions are negligible in the Perth Metropolitan Area (Reid et al., 2011), a detailed temperature gradient analysis was performed. The temperature data were interpreted with a one-dimensional conductive heat model using the GeoTemp™ package (Ricard and Chanu, 2011a and 2011b). Differences between the conductive heat model and the observations greater than 5% were deemed indicative of heat moving via non-conductive mechanisms, such as advection or convection. Evidence of non-conductive or advective heat flow was found in most formations in the PMA, with significant effects in the aquifers (Reid et al., 2012). Average geothermal gradients were calculated for each formation from the logged and digitised data and are shown in Table 4.1. In

Formation	Geometric Mean (°C km^{-1})	Std. Deviation (°C km^{-1})	Fraction of wells used
Superficial	11.4	6.9	19/40
Rockingham sand	15.5	5.6	7/8
Kings Park Formation	27.4	13.2	10/10
Mullaloo Sandstone Member	23.3	16.8	4/6
Como Sandstone Member	28.4	3.7	3/4
Lancelin Formation	24.7	6.0	3/4
Poison Hill Greensland	16.0	2.6	6/6
Gingin Chalk	16.8	12.1	7/10
Molecap Greensland	20.8	7.01	8/11
Mirrabooka Member	24.5	3.1	5/6
Kardinya Shale Member	29.8	9.7	22/36
Henley Sandstone Member	22.7	7.7	18/29
Pinjar Member	25.2	8.9	32/47
Wanneroo Member	25.1	6.9	55/62
Mariginiup Member	30.8	7.9	51/53
South Perth Shale	38.3	8.4	42/46
Gage Formation	25.0	5.7	34/37
Parmelia Formation	36.1	13.6	2/3
Yarragadee Formation	25.1	4.7	26/31
Cattamarra Coal Measures	23.8	3.2	6/9

Table 4.1: Average geothermal gradient by formation.

general, the gradients vary with lithology, with sandstone formations exhibiting average gradients of approximately 25 °C km^{-1}, while insulating silt/shale formations show higher average gradients of over 30 °C km^{-1}. For this gradient analysis, vertical conductive heat flow was assumed and wells exhibiting advective flow in that formation were excluded from the calculation. The last column of Table 4.1 indicates the fraction of wells crossing each formation included in the average conductive geothermal gradient estimates.

4.3.4 Discussion

For the first time, an extensive database of temperature measurements and maps of the temperature distribution in three dimensions in the Perth Metropolitan Area are available. Average geothermal gradients of 25 °C km^{-1}, to 30 °C km^{-1} indicate that subsurface temperatures can be reasonably well predicted for direct use applications. However, non-conductive heat flow is widespread across the area. Geothermal gradients and estimates of conductive vertical heat flow exhibit considerable variability within formations, which points out the need for mapping of thermal rock properties. Radiogenic heat production rates for Perth Basin sediments have been shown to be an insignificant part of this variability (Reid et al., 2011).

Non-conductive heat transfer has been further investigated for identification of advective heat transport in the Leederville in Reid et al. (2012).

4.4 Characterisation of the Gnangara Mound low temperature anomaly

Temperature and gamma-ray logging of artesian monitoring wells owned by the Department of Water (DoW) has indicated several temperature anomalies (both high and low) in the Perth Metropolitan Area (Figure 4.13). High temperature anomalies may be attractive for geothermal heat extraction applications whilst low temperature anomalies may be of interest for geothermal heat rejection projects. Characterisation of temperature anomalies will provide a better understanding of geothermal systems in the Perth metropolitan area.

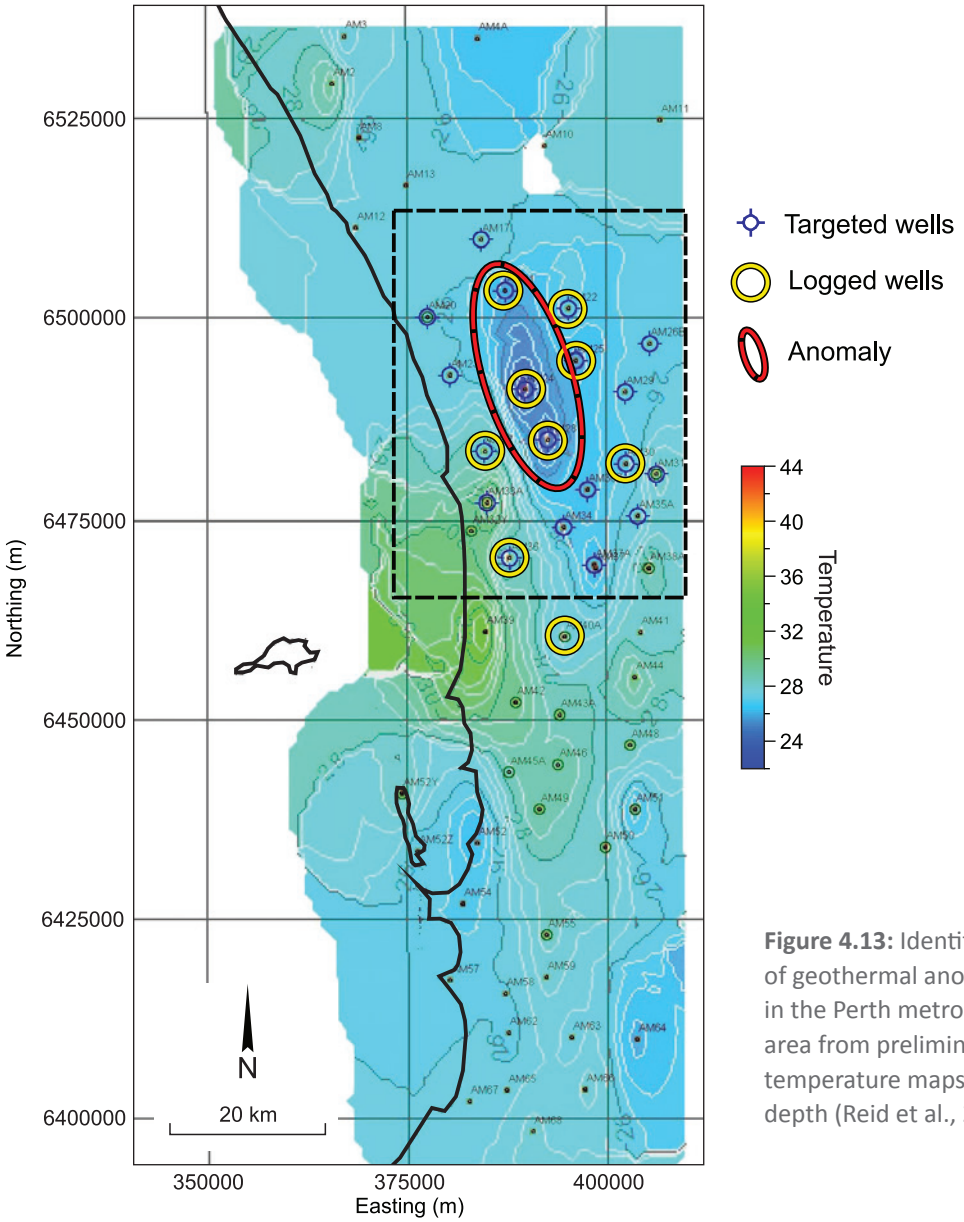

Figure 4.13: Identification of geothermal anomalies in the Perth metropolitan area from preliminary temperature maps at 250 m depth (Reid et al., 2011).

A low temperature anomaly located at the south of the Gnangara Mound, highlighted by a red ellipse in Figure 4.13, was indicated by measurements at, at least, two separated wells, AM24 and AM28. The temperature interpolation at this location was generated from digitised temperature logs only.

The investigation of shallow temperature anomalies based on these preliminary maps is difficult due to the uncertainties associated with interpolation from digitised data. In these cases there is potential for systematic errors resulting from insufficient documentation, at the date of logging of those datasets (1980s). Insufficient spatial resolution also affects the analysis of the thermal anomaly extent.

4.4.1 Logging campaign

A temperature and gamma-ray logging campaign in 2011 targeted this shallow low temperature anomaly. Eight artesian monitoring wells and a reference well were logged (see Figure 4.13) to characterise the thermal anomaly and assess the quality of data from previous logging campaigns. A comparison of temperature logs acquired between 1980 and 2011 has indicated differences on the order of 1 to 2 °C between digitised and newly acquired measurements probably due to the measurements errors and the digitization process (Figure 4.14). The new temperature measurements confirmed the apparent low-temperature anomaly seen in the 1980s data set. Moreover, the new temperature and gamma-ray logging has confirmed clearly anomalous temperatures to 250 m depth and defined a north-south extent of approximately 34 to 38 km from north of Pinjar to Mirrabooka and an east-west extent of 7.4 to 10.4 km centralised over the Gnangara-Moore River state forest. Temperature anomalies vary between -2.4 and -6.7 °C from regional temperature averages (i.e. 23.8 °C) at 100 and 500 m depth, respectively.

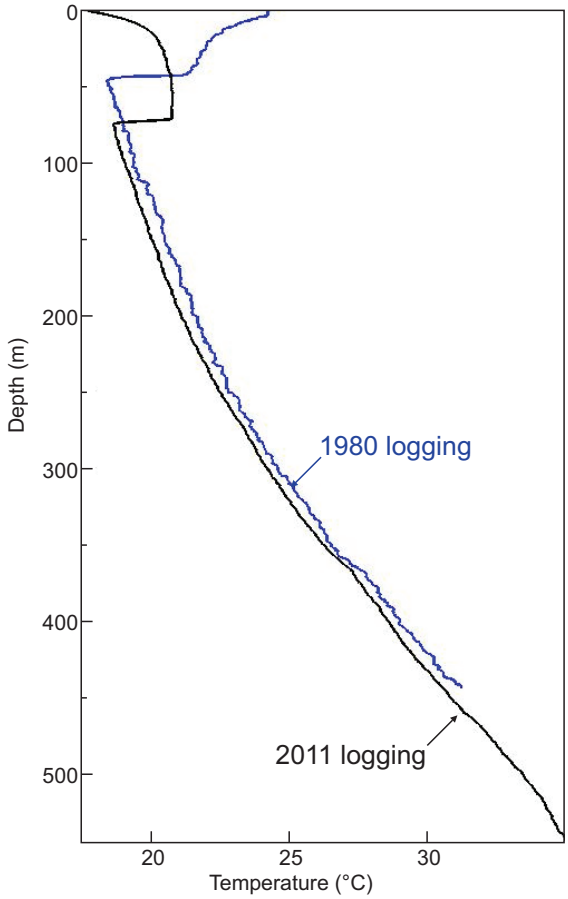

Figure 4.14: Comparison of temperature logs at AM22 between 1980 and 2011.

4.4.2 Possible fault controls

Despite the fact that the Gnangara Mound area exhibits high levels of recharge from the Superficial Aquifer to the Mirrabooka and Leederville aquifers from local hydraulic contacts (Davidson, 1995), no advective pattern in the temperature profiles over those aquifers has been identified. A detailed temperature analysis, performed using GeoTemp™ and presented in detail in Tressler (2011), indicated a vertically conductive thermal regime. The analysis of fault networks in the Perth Metropolitan Area, presented in Timms et al. (2012), highlighted the presence of several faults in the Gnangara Mound area which match the extent of the temperature anomaly (Figure 4.15).

This analysis confirms the low temperature anomaly of the Gnangara Mound area, which represents a possible target for geothermal heat rejection. The origin of the low temperature anomaly is yet to be explained but may be related to the complex local geology and hydrogeology (i.e. aquifer recharge and faulting).

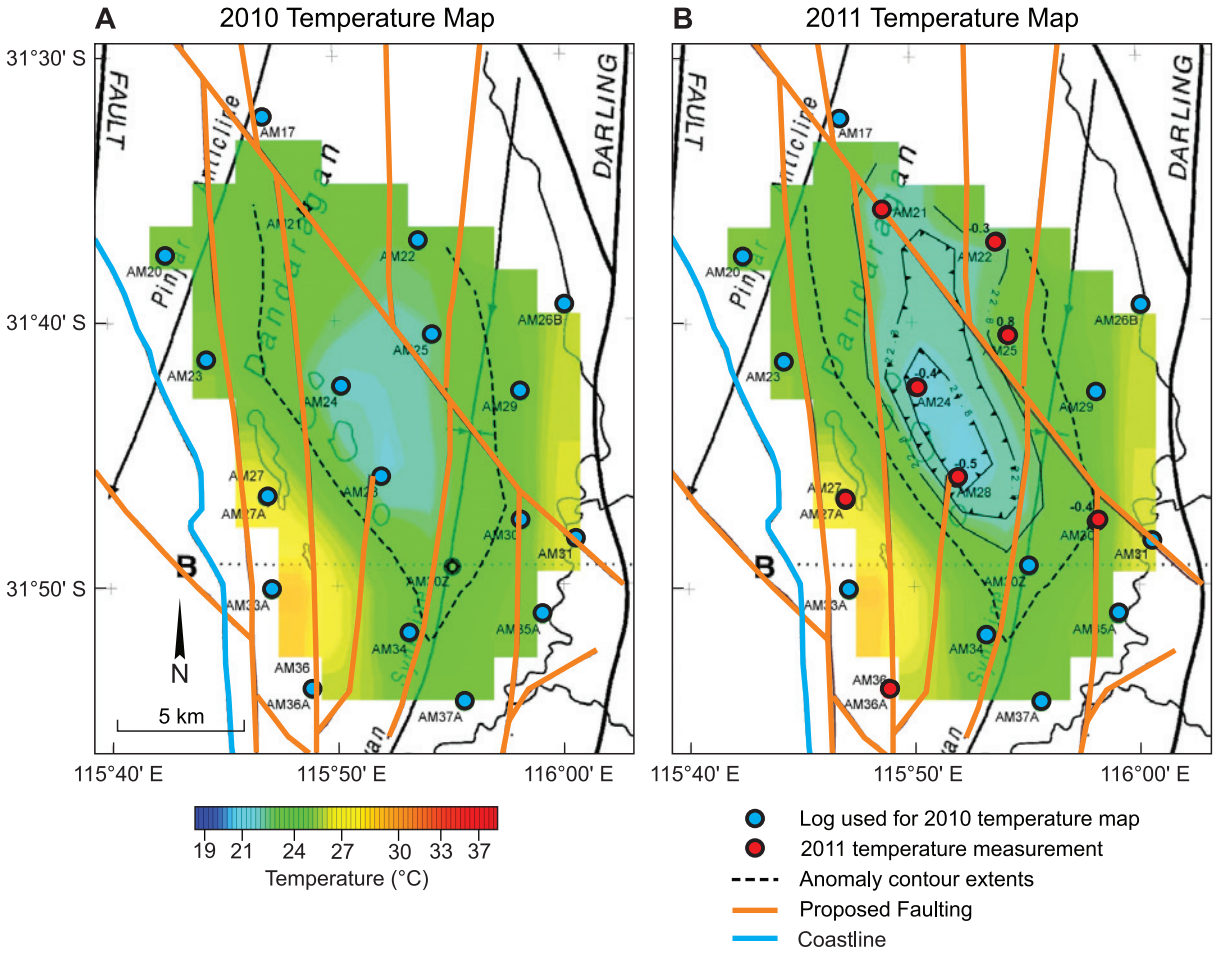

Figure 4.15: Localisation of the Gnangara Mound with faults and artesian monitoring wells, the area extent is within the orange square in Figure 4.13. On the left, the temperature distribution map at 250 m depth generated from the 2010 dataset with indication of the anomaly extent. On the right, the temperature distribution map at 250 m depth generated from the 2010 and the 2011 datasets with indication of the anomaly extent.

4.5 M345 Aquifer Storage and Recovery

The Water Corporation of Western Australia operates an Aquifer Storage and Recovery (ASR) trial site near the Mirrabooka bore field (M345) (Figure 4.16). ASR has been identified as a potentially significant operating strategy for water sourcing and distribution within the Perth Metropolitan Area. Potable water is injected into a groundwater aquifer during times of water excess for storage, minimising water losses and keeping the water available for subsequent drought periods. The ASR operation has potential benefits for issues such as drought management, improvement of groundwater quality, source enhancement, maintenance of groundwater levels, and protection of

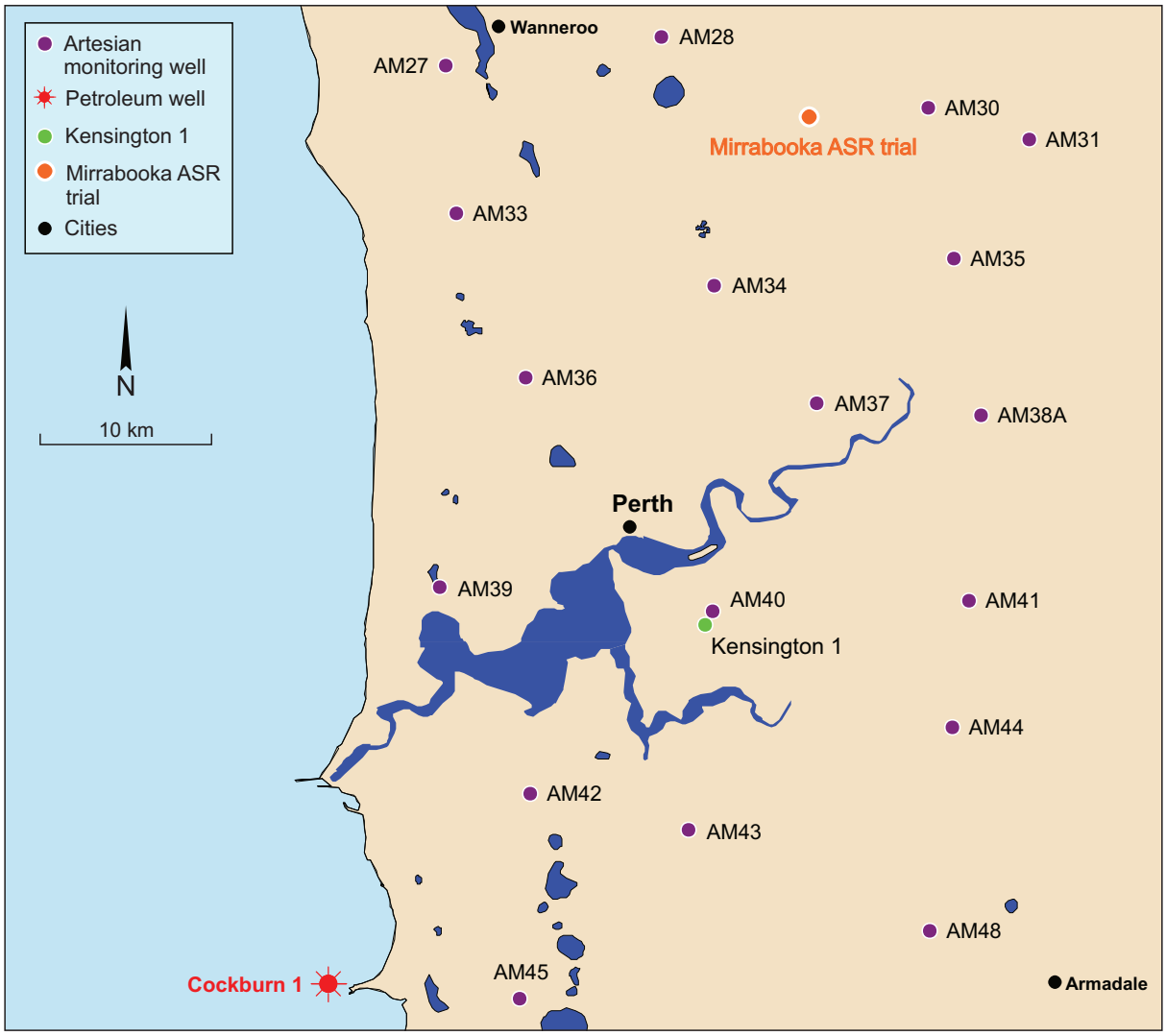

Figure 4.16: Mirrabooka ASR trial site location in the Perth Metropolitan Area shown as red square, reproduced from Malajczuk (2010).

groundwater-dependent vegetation. At Mirrabooka, the test trial is run in cycles alternating injection, storage and production, mimicking 'real life' conditions to better understand potential hazards and the limits of ASR. The M345 ASR trial site is equipped with six wells (Figure 4.17): the production well 2/07 (acts as injector and producer depending on cycle), and five monitoring bores 1/08, 2/08, 3/08, 4/08 and 1/09. Within the monitoring bores, screens have been located at distinct depth intervals. Monitoring screens in wells 1/08-4/08 are located in the first injection interval while the screen in 1/09 delivers insight into the second and deeper part of the injection zone. The trial has been subject to extensive baseline and monitoring data acquisition (Rockwater Pty Ltd, 2009, Rockwater Pty Ltd, 2010). The objective of the study (Ricard et al., 2012b) presented here was to investigate the benefit of time-lapse temperature observations from the Mirrabooka Trial Site to reservoir characterization.

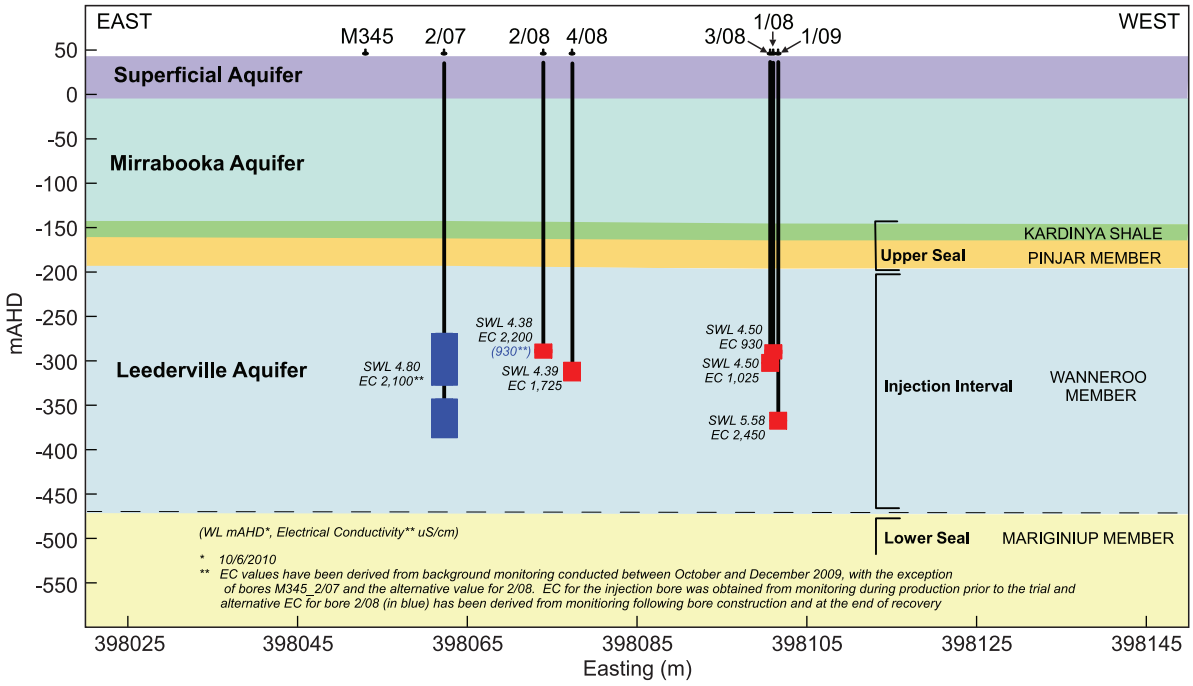

Figure 4.17: Lithology at M345 with the injection screens shown in blue and the monitor screens in red, adapted from Rockwater (2010).

4.5.1 Geophysical data collection

Data collection during the trial was extensive, with geophysical logging prior to and during the trial, coring, vertical seismic profiling, water sampling, and production monitoring at surface. In the following discussion, only measurements related to the present geothermal study are considered.

4.5.1.1 Static measurements

Gamma-ray logging (Figure 4.18) was performed in the 2/07 and 1/09 wells. The logging measurements correlate very well across the two bores, indicating uniform connected sedimentary layers throughout the M345 trial site. Thus, an assumption of horizontal confined layers in the Mirrabooka region can be verified. However, the Wanneroo Member shows strong vertical heterogeneity.

Permeability and porosity measurements were performed by Weatherford Laboratories (2009) on 28 cores samples taken from the 1/07 well. The exploration well 1/07 located at 23 m was plugged and abandoned. WAGCoE organized thermal conductivity measurements performed by CSIRO on 15 cores from 1/07 to assist the thermal characterization study. The selection of core samples was driven by the intra-reservoir characterization objective and therefore, most of the measurements were done at the injection/ production depth interval, 300-420 m below ground level.

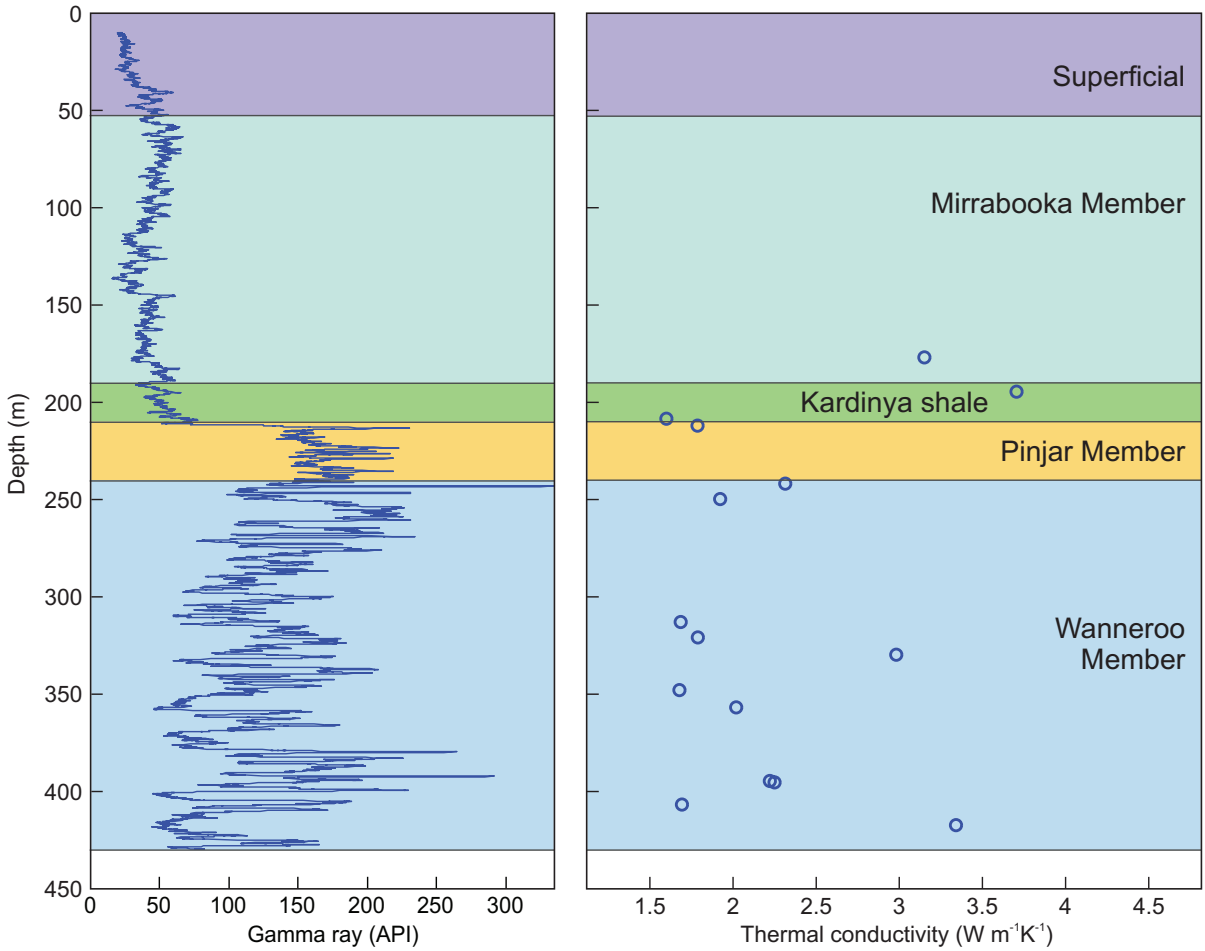

Figure 4.18: Left, gamma ray log at 1/09; right, measured dry thermal conductivity values for each sample taken from 1/07 well overlain on the local lithology.

The measured dry thermal conductivity values vary between 1.6 and 3.7 W m^{-1} K^{-1}. Low thermal conductivity corresponds to shaly layers whereas high thermal conductivity corresponds to sandy layers. The variability thermal conductivity values in the Wanneroo Member reflect the strong vertical heterogeneity within that unit.

The internal lithology of the Wanneroo Member at the depth of the two injection intervals was sub-divided into three facies: Sand, Mix and Shale using two cut-offs on the gamma-ray trace. Average values of porosity, thermal conductivity and hydraulic conductivity for the three facies were determined (Table 4.2) using the core measurements available. The saturated thermal conductivity was calculated using the dry thermal conductivity, the porosity and the thermal conductivity of water using the following formula:

$$\lambda_{wet} = \lambda_{dry} + \phi.\lambda_{water} \qquad 1$$

Facies	Porosity	Tc_{dry} W m^{-1} K^{-1}	Tc_{wet} W m^{-1} K^{-1}
Sand	0.38	3.27	3.5
Mix	0.36	2.10	2.32
Shale	0.31	1.72	1.91

Table 4.2: Facies distinguished for the injection zone at M345 with associated porosity and thermal conductivity estimates.

4.5.2 Time-lapse observations

The ASR trial was composed of independent pumping cycles. Each cycle has three stages: injection, waiting (residence) period and production. The injection and production flow rates varied daily.

Temperature logging measurements at 1/09 and 4/08, respectively 20 and 40 m away from the 2/07 well, were recorded several times during ASR Cycles 1 and 2. All temperature logs lie close upon each other throughout the first 280 m below ground.

A time-lapse study for three time periods over the trial was performed. The detailed stratigraphic breakdown of the Wanneroo Member from the gamma-ray measurement presented earlier was used to guide the time-lapse analysis. In shale layers, fluid flow rates are reduced; therefore heat transfer is more likely to be conduction dominated. In sand layers, fluid flow occurs at higher rates and, depending on the velocity of the fluid, heat transfer may be advection dominated.

4.5.2.1 Time lapse 3

The time lapse 3 (TL3) period examines part of the injection stage of the second Cycle. Temperature logs on 2 August 2010 for 4/08 and on 22 July 2010 for 1/09 provide the temperature baseline measurements. Temperature logging measurements on 9 September 2010 for 4/08 and 1/09 are measurements taken after the completion of the production stage. During this timeframe, the injected water temperature is 23.6 °C, and therefore is cooler than the formation at the screened intervals.

The analysis of TL3 provides information on the reservoir temperature disturbance resulting from injection of water. The temperature disturbance can be seen in the temperature logging measurements (Figure 4.19) at 4/08 and 1/09 located 20 and 40 m away, respectively. Time lapse temperature logs were compared to vertical facies and permeability interpretations. The temperature difference is negative, confirming that the formation is cooled by the water injection. The disturbance is also larger at 4/08 than at 1/09. For both wells the disturbance varies vertically, with temperature disturbance peaks correlated to the lithological facies. Large disturbances occur in the sandy layers and smaller disturbances are observed in the shaly and silty ones. The absolute amplitude of the disturbance at 4/08 is about 1.2 °C while it is 2.3 °C at 1/09. However, at the same depth, the amplitude of temperature disturbance is smaller at 1/09.

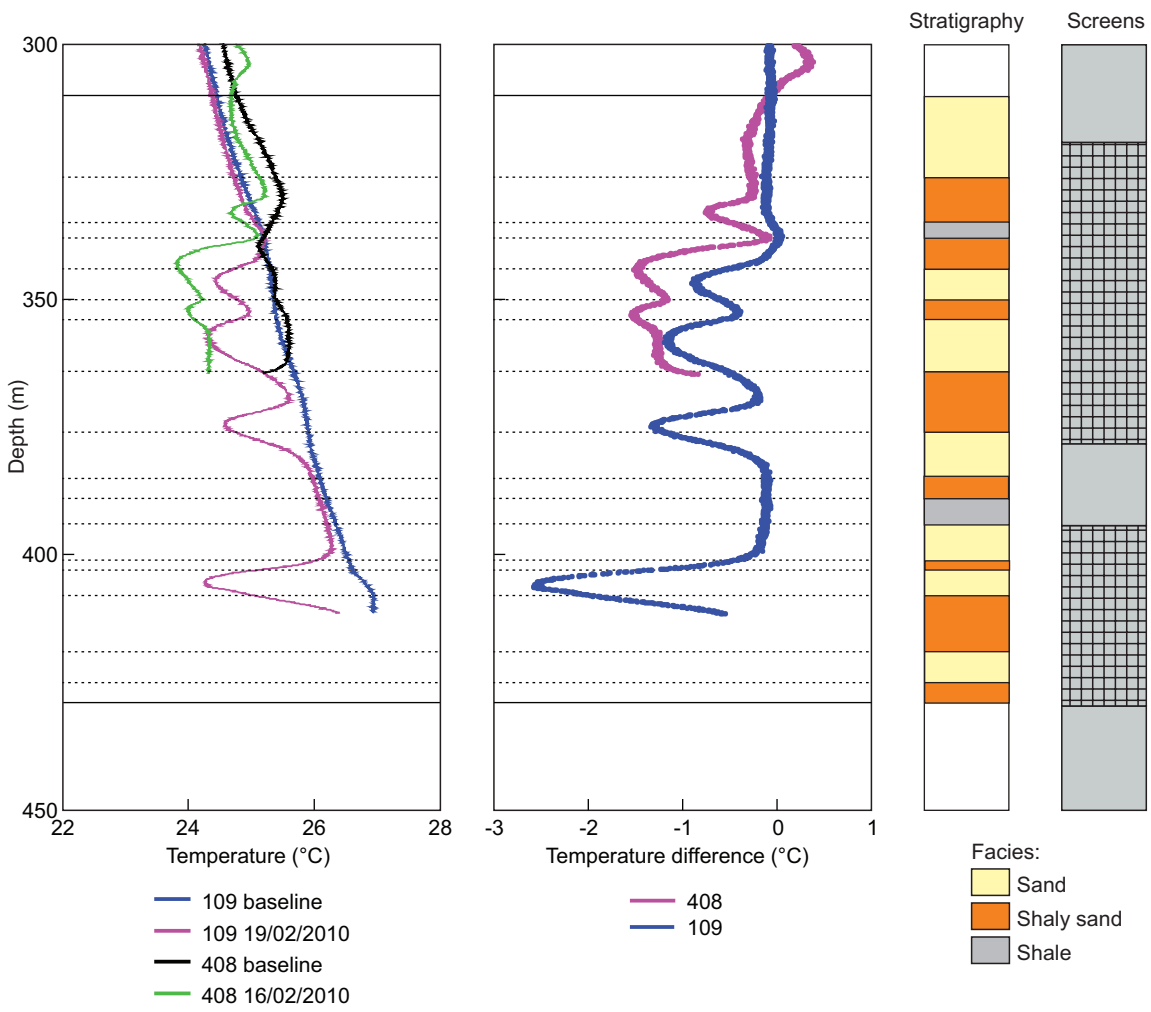

Figure 4.19: Time lapse 3 (TL3): (left) comparison of temperature logs with 4/08 baseline in black, 1/09 baseline in blue, 4/08 temperature log in red and 1/09 temperature log in pink; (b) temperature difference in 4/08 (pink) and 1/09 (blue) with local stratigraphy and injection intervals.

4.5.3 Summary

This section described the thermal characterization of the shallow subsurface at the M345 Aquifer Storage and Recovery trial site. As part of this characterization, 18 new thermal conductivity measurements were acquired to characterise the shallow formations within the Perth Metropolitan Area. These measurements provide the most comprehensive thermal conductivity analysis for the Leederville Formation publicly available. A new thermal conductivity estimate for the Leederville Formation has been generated based on these measurements.

Thermal characterization prior to the ASR trial demonstrated a thermal regime dominated by vertical conduction with a local heat flow of 53 mW m^{-2}. A detailed lithological characterisation was performed based on drill core samples to determine the facies variation within the Wanneroo Member at the M345 ASR trial site.

Time-lapse temperature logs were analysed along with the detailed lithology and the production history. Due to differences between the temperature of the water injected and the formation temperature, the water injection triggered temperature disturbances. The disturbances seem to propagate in relation to the local vertical heterogeneity of the Wanneroo Member. The time-lapse temperature analysis at the M345 ASR confirms the reservoir characterization previously made from gamma-ray measurements. These temperature observations also provide insights on the lateral connectivity between the injector well and two of the monitoring wells. These results showed horizontal fingering of thermal disturbances along sandy intervals in the interbedded sand-shale sequence of the Wanneroo Member. It is likely that heat flow would display this fingering characteristic in many formations of the Perth Basin, especially where gamma-ray variations are noted.

4.6 Thermal conductivity modelling

Geothermal resource estimation requires an understanding of the reservoir temperature distribution. However, temperature measurements are not always available at the target reservoir depth. Therefore, temperature predictions become important. If, as a first approximation, we consider conductive transport as being the dominant heat flow process in a geothermal reservoir, rock and fluid thermal conductivity (TC in W m^{-1} K^{-1}) and specific heat (or heat capacity in J kg^{-1} K^{-1}) are the fundamental parameters to be quantified, either from direct measurements or from theoretical predictions.

Temperature modelling studies to predict temperatures at specific targeted depths or geological units often require rock physical properties data-estimates at the formation scale. Thermal conductivity is a property, which cannot be, measured directly at in-situ reservoir conditions. However, TC can be measured in the laboratory on core samples using various methods (divided-bar, thermistor, optical thermal scanner, hot wire, guarded hot plate, needle thermo-couple). While laboratory measurements are accurate and with high resolution, the drawback is that insufficient samples and measurements are available to support a representative estimate of TC at the formation scale. Furthermore, the in-situ conditions (temperature, pressure, local stress, pore fluid content etc.) are partially, if not fully, lost despite laboratory attempts to recreate in-situ conditions during measurements. Capturing the rock-formation heterogeneities such as faults, cracks, sedimentary features or mineralogy patches which influences the TC at larger scales than the core scale is challenging. To capture vertical heterogeneities, traditional wireline logging measurements during and/or after drilling phase are sought. Several techniques allow the estimation of a TC log using a combination of different well logs, such as the gamma-ray, neutron-density, and electrical resistivity logs. Together, these three logs provide information on clay/sediment ratios, porosity, and water saturation/salinity, respectively. All these techniques are based only on empirical or semi-empirical mixing laws using simple approaches such as Archie's equation (Brigaud et al., 1989; Abdulagatova et al., 2009). Surprisingly, although the sonic velocity is always used in petroleum exploration it is rarely used in geothermal exploration. Recent experimental studies observed an empirical correlation between thermal conductivity and velocity properties of the rock in laboratory (Zamora et al., 1993;

Popov et al., 2004; Ozkahraman et al., 2004) and from neural network analysis from various wells (Goutorbe et al., 2006).

4.6.1 Thermal conductivity estimation

To address the lack of physical approaches to thermal conductivity estimation (as compared to empirical laws), WAGCoE and CSIRO developed a thermal conductivity modelling workflow (Pimienta et al., 2012) based on effective medium theory combining two robust models of effective thermal conductivity (ETC; Giraud et al., 2007) and elastic wave velocities (EWV; Fortin et al., 2007) and relying on a generic rock microstructure (Figure 4.20). This microstructure involves at this stage the use of porosity and supposes monomineralic rock such as sandstone made of only quartz.

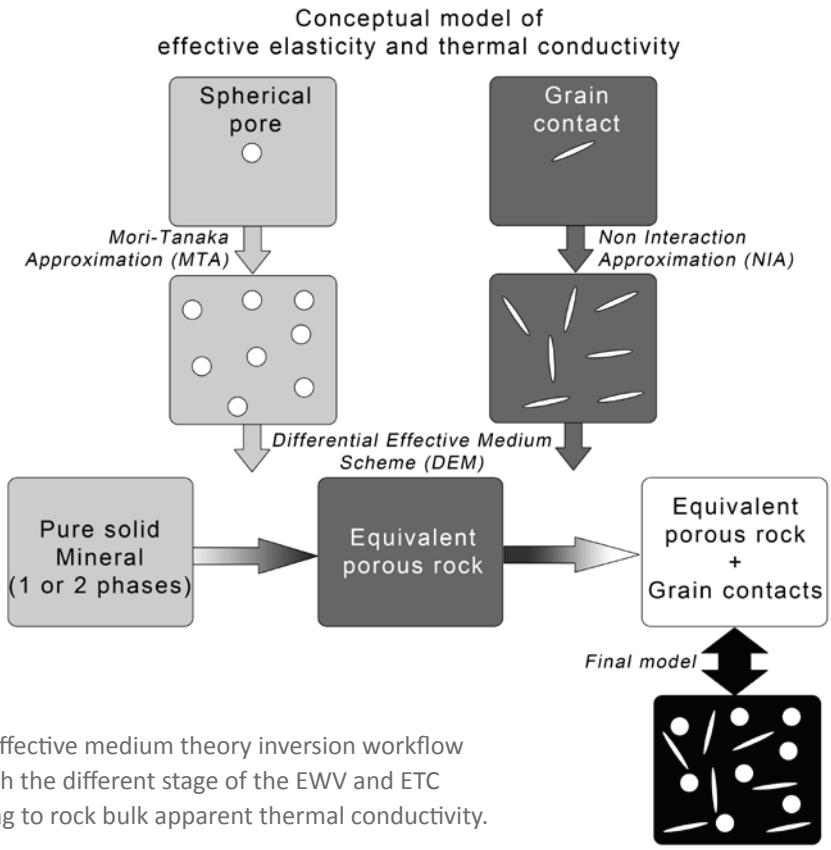

Figure 4.20: Effective medium theory inversion workflow schematic with the different stage of the EWV and ETC models leading to rock bulk apparent thermal conductivity.

Using available seismic data (elastic wave velocities in a given lithology) or ultrasonic measurements from representative core samples in laboratory, the P-waves and S-waves are processed through the EWV model to extract and quantify the grain contact density and their shape ratio characteristics for any lithologies of the geological formation. These new microstructural parameters are then input in the ETC model to predict the thermal conductivity of the targeted lithologies at different intensities of water saturation from dry to fully saturated.

4.6.2 Core measurements and results

Thermal conductivity and elastic wave velocity were measured on rock cores recovered from the Cockburn 1 well, Western Australia. Thermal conductivity was measured on an optical thermal scanner (OTS, Popov et al., 1999) under dry and saturated conditions before being corrected for the porosity in-situ condition and water damage effects due to a small occurrence of clay minerals during laboratory experimentation. The P- and S-waves were acquired on the same samples and conditions using bench-top ultrasonic transducers. A typical outcome of this new workflow and associated micro-physics modelling is exemplified in Figure 4.21. Predictions of thermal conductivity from EWV measurements using the new workflow (green squares) are compared to the direct laboratory measurements of TC (orange discs) and corrected measurements (orange circles) using the presented inversion workflow. The inversion method is also tested with rare dataset available from the literature (Zamora et al., 1993; Revil, 2000; Abdulagatova et al., 2009; Côté and Konrad, 2009; Gomez et al., 2010; Smits et al., 2010). The prediction of thermal conductivity from the literature data gives a reasonable correlation (Figure 4.21). Note how the range of thermal conductivity under dry conditions is much higher than the water saturated conditions. The data acquired from the Cockburn-1 well gave a misfit of 15 to 20% between raw measured and predicted TC. After water damage corrections of the porosity using geometric or arithmetic mean derived equation from Archie's law and recalculation of the thermal conductivity under in-situ stress conditions, the new TC corrected measurements shifted the laboratory data (red circles in Figure 4.21) to almost superimpose the prediction from the model. However, the saturated case still slightly under-estimate the laboratory data by about 5-10% despite the porosity correction, but the overall trends obtained by this predictive method are consistent with the TC measurements (Pimienta et al., 2011a,b).

Apart from the inherent limitations associated with any modelling approach, the discrepancy between the predictions and the direct TC measurements could further be explained by experimental factors associated with the present study: (i) non ideal preservation of the (dry) Cockburn 1 core plugs since underground recovery many years prior to the laboratory measurements of TC; (ii) the EWV were measured on these same plugs but after several cycles of water re-saturation and oven-drying at 65 °C. Such cycles are known to irreversibly modify the rocks microstructure when even small amounts of clay are present, in particular in terms of grain contact characteristics. For instance, EWV are known to artificially decrease with an increasing number of re-saturation/drying cycles, which may lead to the observed under-estimation of the actual TC when such EWV are used for the prediction.

Therefore, the discrepancy between EWV-predicted and directly measured TC is likely to be reduced if a dedicated systematic experimental investigation is carried out. Furthermore, if an optimal dataset is acquired in the laboratory, it is likely that the modelling side of the problem could also be improved to yield better predictions.

The next phase of this model, currently under development, is to solve the inversion model when several types of minerals occur such as quartz with clays. The first results from other geothermal reservoirs (Soultz-sous-Forêts, France) seem to correlate the misfit of data and correlations with the

amount of clays. Therefore, inclusion of a simple gamma-ray log should help to properly calibrate the model to predict more accurately the thermal conductivity.

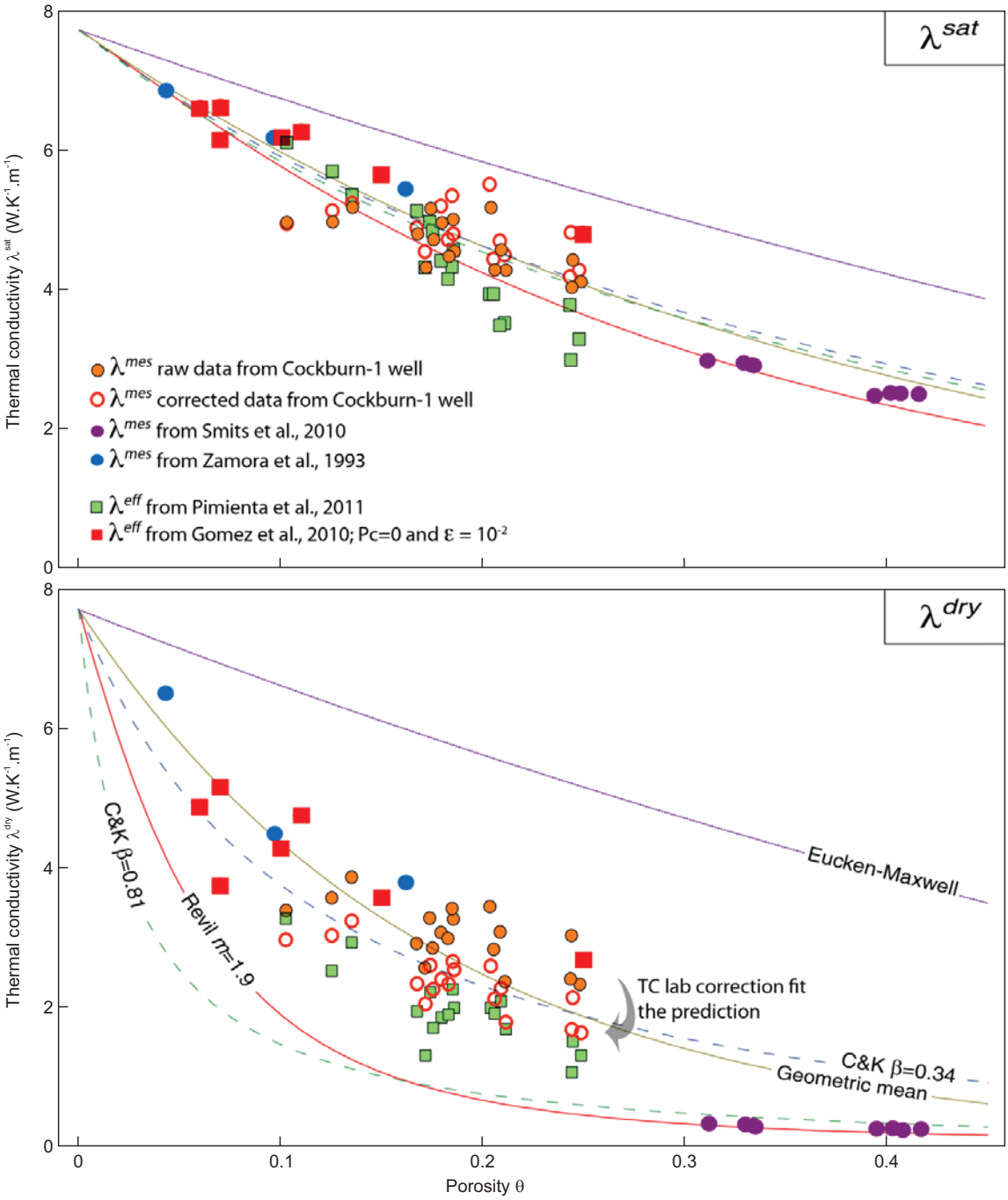

Figure 4.21: Comparison of TC predicted (squares) and directly TC measured (discs) for several rock aggregates: purple, orange, and blue discs denote the TC measurements for an unconsolidated sand, the Cockburn 1 sandstone, and the Fontainebleau sandstone, respectively; green and red squares denote the EWV-predicted TC for the Cockburn 1 and the Fontainebleau sandstones, respectively (Pimienta et al., 2011a,b). λ^{eff} stands for thermal conductivity from the Pimienta model prediction and λ^{mes} stands for laboratory measurements of thermal conductivity.

4.7 Deep temperature predictions in the Perth Metropolitan Area

Core analyses, wireline temperature logging and lithological data provide information on the rock thermal properties at different scales and on the effects of formation heterogeneities. A joint-interpretation of geophysics-petrophysics-rock physics dataset is the best approach for accurate and consistent thermal characterization of the subsurface. A thermal characterization in the vicinity of the Cockburn 1 well site (Perth Metropolitan Area, Figure 4.22) was carried out using GeoTemp™ by taking into account data from shallow monitoring wells (temperature logging), core measurements and by considering a vertically conductive heat transfer model. The results obtained were used to predict temperature estimates at the Cockburn 1 well site and were compared to existing Bottom Hole Temperature (BHT) measurements at the Cockburn 1 well.

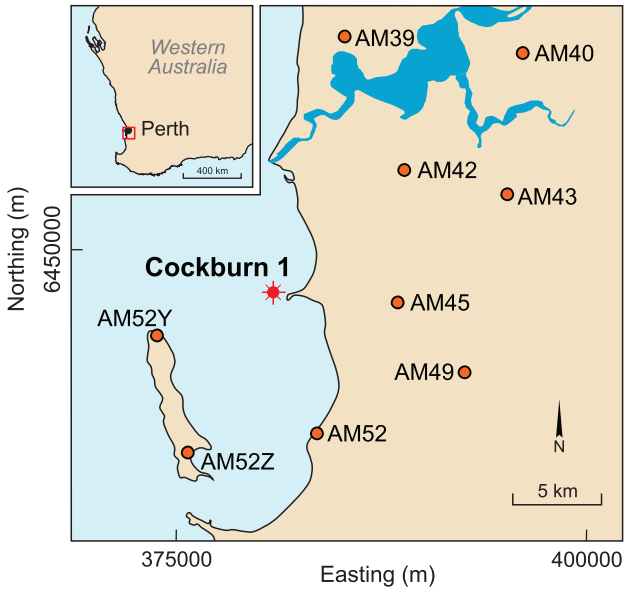

Figure 4.22: Location of the Cockburn 1 well.

4.7.1 Existing Cockburn 1 dataset

At the Cockburn 1 site, existing temperature data consist of:

- a BHT value of 81.1 °C at 3048 m in the Cockburn 1 well obtained during drilling phase.
- wireline temperature logging measurements available at the artesian monitoring wells AM42, AM45A, AM52, AM52Y and AM52Z (Figure 4.22) located in the vicinity of the Cockburn 1 well and carried out in 1980 and 2011 (see Reid et al. (2011) for further details). Temperature wireline data at AM42, AM52, AM52Y and AM52Z were acquired in 1980s while measurements AM45A and AM52Y were obtained in 2010. AM52Y has two temperature measurements.

Thermal conductivities were measured on core samples from the Perth Basin at room conditions in the laboratory (Hot Dry Rocks Pty Ltd, 2008). Additional core measurements were acquired recently (Delle Piane et al., 2012).

The local shallow hydrogeology consists of three main aquifers (Davidson, 1995; Table 4.3): the unconfined Rockingham superficial aquifer, the confined Leederville aquifer and the confined Yarragadee aquifer. Both confined aquifers are widely exploited for domestic use.

Aquifer	Formation
Superficial aquifer	Rockingham Sand
Confining bed	Kings Park Formation
Confining bed	Kardinya Shale Member
Leederville aquifer	Henley Sandstone Member
Leederville aquifer	Pinjar Member
Leederville aquifer	Wanneroo Member
Leederville aquifer	Mariginiup Member
Confining bed	South Perth Shale
Yarragadee aquifer	Gage Formation
Confining bed	Cattamarra Coal Measures

Table 4.3: Local stratigraphic sequence.

4.7.2 Wireline temperature analysis

According to Reid et al. (2011) radiogenic heat production is a minor source of heat within the shallow Perth Metropolitan Area sediments, producing less than 1% of total estimated vertical heat flow. Wireline temperature logging measurements are available in five artesian monitoring wells close to the Cockburn 1 well (Figure 4.23). The analysis of the geothermal gradient (Table 4.4) indicates that the local thermal regime is approximately vertically conductive.

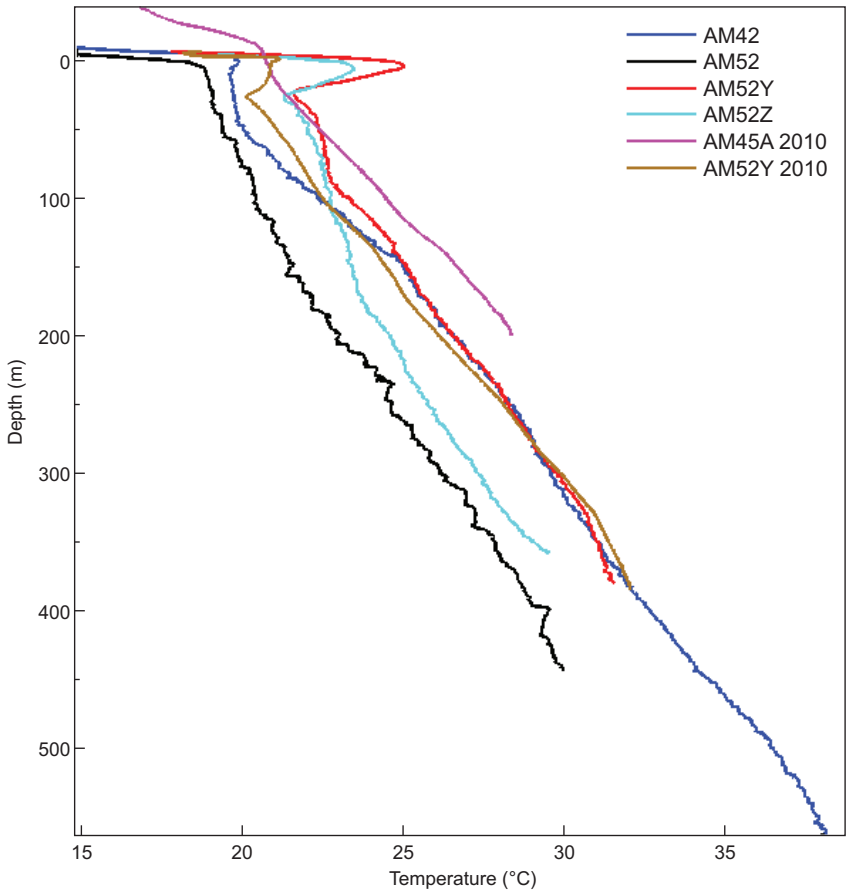

Figure 4.23: Wireline temperature log measurements for AM42, AM45A, AM52, AM52Y, AM52Y and AM52Z, measured at depths below AHD.

Formations	Thermal gradient average	Thermal gradient std dev	Cond. error average	Cond. error std dev
Kardinya Shale Member	34.7	6.7	3.8	1.9
Henley Sandstone Member	23.8	5.3	2.1	0.6
Pinjar Member	33.2	8.0	2.2	1.3
Wanneroo Member	31.0	6.8	2.1	1.2
Mariginiup Member	32.5	4.8	1.4	1.2
South Perth Shale	34.7	3.4	1.9	0.9
Gage Formation	21.8	4.4	1.8	0.8

Table 4.4: Average geothermal gradient by formation for wells AM42, AM45A, AM52, AM52Y, AM52Y 2010 and AM52Z with relative error between linear gradient and real data (from Reid et al., 2011).

4.7.3 Thermal conductivity estimates from temperature logging

Thermal conductivities can be estimated by formation by assuming a vertically conductive heat transport model, by assuming a value for the vertical heat flow in Cockburn 1 (e.g. 76 ± 3.1 mW m^{-2}, Hot Dry Rock Pty Ltd, 2008) and by taking into account the geothermal gradient by formation (Table 4.4). The calculated thermal conductivities can be compared to core measurements available in the literature (Table 4.5). The analysis based on the shallow wireline temperature measurements can only be compared with formation thermal conductivities values available from Hot Dry Rock Pty Ltd (2008). Significant differences are observed for the Rockingham, Kings Park, Kardinya, Henley, and Gage units. These differences can be explained by the non-validity of the vertical heat flow assumption and/or the uncertainty and inaccuracy of core thermal conductivity measurements. The thermal conductivity values by formation were derived from analogous sediments in the Carnarvon Basin (Western Australia) and hence are not necessary representative of the relevant sediments in the Perth Metropolitan Area.

Formations	TC mean	TC std dev	HDRPL mean	HDRPL std dev
Rockingham Sand	3.62	0.15	1.42	0.14
Kings Park Formation	5.35	0.22	1.42	0.14
Kardinya Shale Member	2.26	0.09	1.13	0.08
Henley Sandstone Member	3.34	0.14	1.13	0.08
Pinjar Member	2.45	0.10	2.56	0.18
Wanneroo Member	2.53	0.10	2.56	0.18
Mariginiup Member	2.38	0.10	2.56	0.18
South Perth Shale	2.21	0.09	1.71	0.14
Gage Formation	3.59	0.15	1.93	0.04
Cattamarra Coal Measures	0.67	0.03	3.73	0.2

Table 4.5: Formation thermal conductivities mean and variability within units estimated by Hot Dry Rock Pty Ltd (2008) and by temperature interpretation of wells AM42, AM45A, AM52, AM52Y, AM52Y 2010 and AM52Z.

4.7.4 Thermal conductivity measurements on core samples

Steady-state thermal conductivity measurements were collected by Hot Dry Rock Pty Ltd (2008) for various rock samples of the Perth Basin, using Hot Dry Rock Pty Ltd's portable divided bar thermal conductivity apparatus. Thermal conductivities by formation were estimated from 36 representative core sample measurements. Note that Hot Dry Rock Pty Ltd reported values in the shallow sediments and Osborne Formation were derived from analogous sediments in the Carnarvon Basin of Western Australia. The Gage Formation samples were taken in shaly beds and may not accurately reflect the sandstone portions of this heterogeneous formation.

In 2011, a collection of 225 core samples were collected by CSIRO from 4 deep wells in the Perth Metropolitan Area (Cockburn 1, Pinjarra 1, Gingin 1 and Gingin 2) to provide a better statistical representation of the measured physical properties for each formation. Among this collection, 27 samples from the Cockburn 1 well were used to measure (i) porosity and permeability at 3 confining pressures (500, 1000 and 2000 psi) to re-create the in-situ conditions, (ii) acoustic ultrasonic P- and S- wave velocities Vp-Vs on dry and saturated conditions at room conditions of pressure and temperature, (iii) thermal conductivity and thermal diffusivity using the optical thermal scanner (OTS; Popov et al., (1999)) from the University of Melbourne (Earth Science School). New thermal conductivity values were estimated per formation from these measurements and are presented in Table 4.6.

Formations	Thermal conductivity mean ($W\ m^{-1}\ K^{-1}$)	Thermal conductivity std dev ($W\ m^{-1}\ K^{-1}$)	Nb samples
Yarragadee Formation (HDRPL)	3.31	1.42	2
Yarragadee Formation (CSIRO)	4.2	0.61	16
Cadda Formation (HDRPL)	94.1	0.54	2
Cadda Formation (CSIRO)	74.30	N/A	1
Cattamarra Coal Measures (HDRPL)	3.84	0.90	2
Cattamarra Coal Measures (CSIRO)	4.40	0.60	7

Table 4.6: Thermal conductivities mean and variability within units measured from Hot Dry Rock Pty Ltd (2008) and CSIRO (Esteban et al., in preparation).

4.7.5 Temperature predictions

A vertical heat conduction model was used to predict temperature (Figure 4.24) from surface to 4000 m for well AM42 based on the modelled vertical heat flow, on the new thermal conductivities values and their associated uncertainties (including Hot Dry Rock Pty Ltd (2008) and Delle Piane et al. (2012)) and on the lithological boundaries observed in Cockburn 1. The temperature predictions show an increasing uncertainty as depth increases with a cumulative uncertainty of
± 20 °C at 4000 m (Table 4.7). Depth at a given temperature is a good measure for assessing the potential for direct-use geothermal applications (Table 4.8). For example, the temperature model predicted a temperature of 80 °C at depths between 2200 and 3300 m. The model also predicted temperatures in the range 73-97 °C at 3000 m depth, which can be compared with the single BHT of 81.1 °C at 3048 m measured during the drilling phase

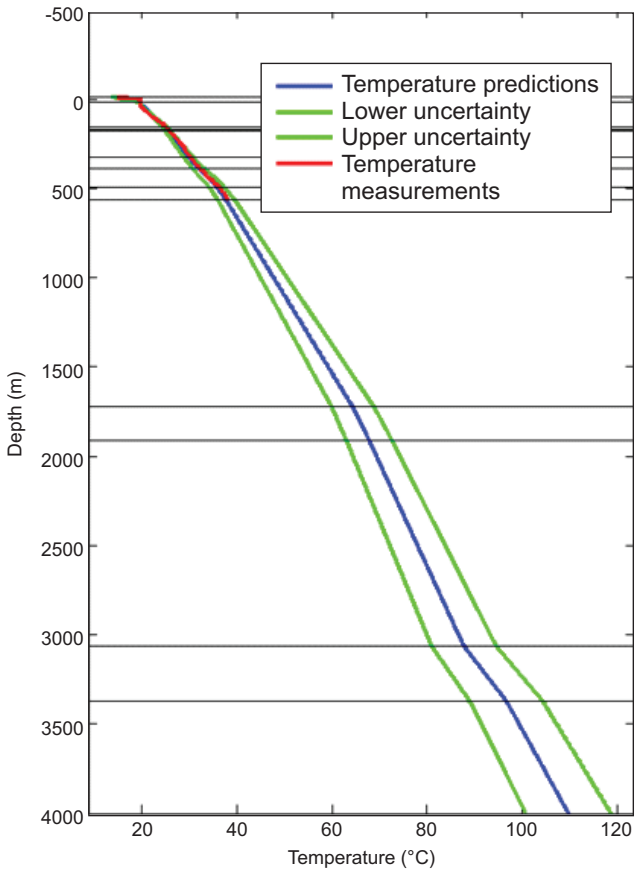

Figure 4.24: Temperature prediction for AM42 using modelled heat flow and thermal conductivities with associated uncertainties.

Depth (m)	Min T (°C)	Mean T (°C)	Max T (°C)
1000	43.76	46.37	49.82
2000	58.59	64.84	73.64
3000	72.80	82.80	97.21
4000	92.90	106.82	126.58

Table 4.7: Temperature estimates at well AM42.

T (°C)	Min depth (m)	Mean depth (m)	Max depth (m)
80	2269	2844.10	3325
100	3094	3684.00	4000
110	3347	> 4000	> 4000

Table 4.8: Depths to 80, 100 and 110 °C temperature at well AM42.

4.7.6 Discussion

New thermal conductivity measurements (27) were performed to complete the limited thermal dataset currently available for Cockburn 1. The combination of thermal conductivity measurements from core laboratory, wireline temperature logs, and heat flow predictions provide a basis for improving the estimation of thermal conductivities by formation. The thermal modelling carried out by using these new values of thermal conductivities (and their associated uncertainties) showed that temperature at greater depths can be predicted from nearby wireline temperature measurements. The results show that temperatures predicted at 3000 m range from 72 to 97 °C and suggest this area has a potential for a wide range of direct-use geothermal applications.

4.8 Conclusions

The working fluid temperature is a key factor for geothermal resource estimation as it determines the range of feasible geothermal surface applications. Therefore, building an understanding of the spatial temperature distribution is critical to the planning and development of geothermal applications.

In this section, we addressed the use of temperature measurements for geothermal exploration in the Perth Basin. Sparse temperature measurements have mostly a low level of reliability. Simple analysis of sparse data can provide a first understanding of the thermal regime at the basin scale. However, the low reliability and poor vertical distribution of sparse thermal data limit the resolution of the analysis at target locations. Temperature logging measurements improve statistical significance and joint geology-geophysics-hydrogeology interpretations have the potential to greatly improve the subsurface understandings.

In our study of the Perth Basin, sparse and deep temperature measurements were analysed in their uncorrected and corrected forms. A shallow thermal characterization of the Perth Metropolitan Area based on the collection and analysis of temperature logging measurements was presented. A low temperature anomaly was investigated and confirmed in the Gnangara Mound, a location where local faulting has been identified (Timms et al., 2012). The effect of fine-scale vertical heterogeneity on the migration of heat in the subsurface was observed and studied in the Leederville aquifer.

Processing and the interpretation of temperature measurements requires quantitative analysis tools combining geology, geophysics and temperature data. The GeoTemp™ software tool assists engineers perform these tasks and to interpolate/extrapolate temperature. Several applications of GeoTemp™ were presented in this section.

5. SESKA PROJECT

Several geothermal projects in the Perth Metropolitan Area have already demonstrated the geothermal potential for aquifers down to 1 km depth. These successful projects provide the benefit of exploration data and reduced risk for new projects planned at the same depth range. The challenges for geothermal exploitation lie at greater depths where higher temperatures and therefore different geothermal applications exist. One of the key deliverables of WAGCoE is to assess the geothermal potential of deeper aquifers within the Perth Basin.

In June 2010, CSIRO was awarded $47.30 million through the Australian Government's Education Investment Fund (EIF) to undertake the Sustainable Energy for SKA (SESKA) Project. The geothermal component of this project proposed the establishment of Australia's largest direct-heat geothermal production system (and deep-earth observatory) at the site of the Pawsey Centre supercomputer and CSIRO's Australian Resources Research Centre (ARRC).

The key objectives of the Geothermal Component of the SESKA Project are to:

- Delineate/define the geothermal resource of the Perth Basin at the ARRC site via a deep exploration well.
- Establish a direct-heat geothermal production system at the ARRC site, informed by critical design parameters (permeability and water temperature/chemistry) to accommodate the heating/cooling requirements of the ARRC facility and with capacity to contribute to the future cooling needs of the Pawsey Centre supercomputer.
- Provide an enduring deep-earth observatory, or research well, for the benefit of the Australian R&D community.

WAGCoE contributed to the SESKA Geothermal project by performing preliminary well proposals and designs to fulfil the exploration objectives and by assessing the potential of the geothermal resources.

5.1 Exploration objectives

As part of the geothermal exploration objectives of the SESKA Geothermal project, an exploration well, identified here as Kensington-1, will be drilled at the ARRC site.

The purpose of Kensington1 is to provide key information on the geothermal resources at depth below the ARRC site. The Perth Metropolitan Area is well served by exploration and water production wells that penetrate the relatively shallow Leederville and Yarragadee aquifers to depths not significantly greater than 1 km. However deeper exploration wells are scarce. Given Perth's average geothermal gradients, which range from 20-30 °C km^{-1}, depths of approximately 3 km will be required to reach temperatures close to 100 °C (the ambient water temperature close to the surface is approximately 20 °C). The nearest logged well that extends to this projected depth is Cockburn1, approximately 21 km south-west of the ARRC site. The lack of proximate offset wells means that knowledge of the deeper strata underlying ARRC is scant, and consequently that uncertainties associated with drilling and geothermal resource estimation are high. The broad motivation

for drilling Kensington1 at the ARRC location is to reduce uncertainties about the existence and characteristics of geothermal resources with temperatures over 70 °C close to the Perth city centre.

5.2 Geodetic and geological information

The Australian Resources Research Centre (ARRC) site is located in the City of South Perth and is part of the Perth Metropolitan Area (Figure 2.3Right under SESKA). The Perth Metropolitan Area covers the central portion of the eastern onshore margin of the Perth Basin and overlies the southern end of the Dandaragan Trough, a major structural subdivision within the basin. Seismic data indicate that the sedimentary sequence in this part of the Perth Basin is up to 12 000 m thick (Crostella and Backhouse, 2000) and separated from the crystalline rocks of the Yilgarn Craton by the Darling Fault.

The Lower Yarragadee Formation comprises the primary objective, while the Cadda Formation and the Cattamarra Coal Measures comprise a secondary objective (Figure 2.4 for stratigraphy information).

The primary target, the Lower Yarragadee Formation, has currently been identified in the Eclipse1 and Rockingham1 petroleum exploration wells in the Central Perth Basin. In Rockingham1, the Lower Yarragadee Formation is 280 m thick, whereas further north, the Lower Yarragadee Formation thickens to 529 m in Eclipse1. The Lower Yarragadee Formation consists of laterally discontinuous interbedded sandstones, siltstones and shales. The formation is a predominantly fluvial deposit, with shales and coals representing minor overbank deposits, parts of the fluvial system, or swamps. Layers of coarse to medium grained unconsolidated sands alternate with finer grained and cemented sands.

The second target, the Cattamarra Coal Measures, consists of coarse grained quartz sandstone interbedded with dark carbonaceous fine-grained clastic rocks and thick coal seams. In the Perth Region, the sandstones are present in units up to 50 m thick, while the siltstones and shales intervals can be up to 30 m thick (Davidson, 1995).

Due to the lack of deep exploration wells available in the Perth Metropolitan area, it is quite difficult to assess the reservoir properties of the two geothermal and hydrogeologic objectives at the target well. The closest deep wells are more than 20 km away for the well location: Cockburn1, 21 km south-west of the target well and Rockingham1, 33.5 km south. Porosities and permeabilities in the Yarragadee Formation are variable. In Rockingham1, the lower Yarragadee Formation porosities range from 16 to 23%. Porosities between 1% and 25% have been estimated in Cockburn1 with measured permeabilities of up to 9869 mD. In Eclipse-1, 62 km north of proposed well, high porosity and permeability sands were reported throughout the Yarragadee Formation but no quantitative measurements are available.

Porosity and permeability of the Cattamarra Coal Measures also appear to be quite variable. Porosities in Rockingham1 range from 18% to 27%. Measurements on Cockburn1 cores show permeability ranging from 1-137 mD. Further south, measurements on Pinjarra1 cores show that the Cattamarra Coal Measures has permeability and porosity ranging from 730-1715 mD and 19-37%, respectively. In Gingin3, further north of the proposed well, permeability and porosities are generally

lower. Depending on the sand units, the permeability ranges from 0.001-190 mD and porosity from 1-17%.

To estimate the depths of formation boundaries in the Perth Metropolitan area, a 3D geological model of the central and southern Perth Basin has been created using GeoModeller and Gocad Mining Suite packages. The model was constrained using deep petroleum wells and depths to basement provided by OzSeebase (PESANews, 2005). Although water wells are available in the Perth Metropolitan area, none extend to the base of the Yarragadee Formation; therefore they could not be used to constrain the model.

The final model fits the data available in the Perth Basin, but because the data is sparse, a high degree of uncertainty in the formation depths exists.

5.3 Geophysics

Limited geophysical data are available at the Kensington1 site. Only 2D seismic lines have been shot in Perth Metropolitan Area with little interpretation of the raw data. The nearest seismic line is located 10 km from the site. Pre-existing gravity and magnetics data are sparse. Gravity, aeromagnetic, bathymetry and digital terrain data for the whole Perth basin (onshore and offshore) are available from Geoscience Australia (GA).

New gravity data were acquired by WAGCoE in 2009 in the Perth Metropolitan area - around UWA in Claremont, Dalkeith, Nedlands, Subiaco and also from Fremantle to Perth Airport, with extra stations around ARRC and Curtin University. More gravity data were acquired in December 2010 and January 2011. These new datasets have been integrated with the GA data and interpreted for the fault network. Further details on this study can be found in Timms et al. (2012).

5.4 Hydrodynamics and temperatures

Because Perth relies upon groundwater for a large portion of potable water supply, the surficial aquifers are well understood (Davidson and Yu, 2008; Davidson, 1995). These studies extend to depths within the Yarragadee Aquifer, which is defined as comprising the Yarragadee Formation, the Cattamarra Coal Measures, and in some regions, the Gage Formation. An extensive series of monitoring bores maintained by the Department of Water taps the top 800 m of the surficial aquifers. Around the ARRC geothermal project site, three of the closest monitoring bores are screened in the Yarragadee Formation, while further south several bores intersect the Cattamarra Coal Measures. However, hydrodynamic pressure information is very scarce in deeper formations below Perth. None of the Cockburn1, Pinjarra1, or Bullsbrook1 petroleum wells performed pressure testing to provide details of subsurface hydrodynamic properties or conditions. The closest petroleum well with pressure information is Gingin3, obtained during DST tests. Within the Cattamarra Coal Measures, the formation waters are slightly overpressured, with freshwater head exceeding hydrostatic values by approximately 20 m at nearly 4000 m depth. Within the Yarragadee Formation, the formation is also slightly overpressured with a freshwater head exceeding hydrostatic values by approximately 48 m at 2000 m depth. These calculations assume a salinity of 2000 mg/L in the Yarragadee

Formation and 10 000 mg/L in the Cattamarra Coal Measures. At Gingin3, the formation pressures within the Cattamarra Coal Measures were consistent with a connected aquifer.

The Western Australian Geothermal Centre of Excellence has performed detailed temperature and gamma ray logging in sixteen DoW artesian monitoring wells. Temperature logs from the 1980s in 55 DoW wells were also digitized. The data was mapped to produce estimates of temperature throughout the shallow Perth Metropolitan Area (PMA) (Reid et al., 2011).

However, deeper conditions in the Perth Metropolitan region are not described by well data. As described above, the deep temperature data is obtained from two plugged and abandoned petroleum exploration wells at Cockburn1 (21 km south west), and Bullsbrook1 (51 km north east). Given an assumed surface temperature of 20 °C, geothermal gradients can be calculated from these shallow and deep wells. For Cockburn1 and Bullsbrook1 (Figure 2.3 for localisation), a report by Hot Dry Rocks Pty Ltd (2008) estimates heat flow at these locations. For the Cockburn1 well, an earlier report by Chopra and Holgate (2007) calculated a gradient of 21.2 °C km^{-1}. Estimated average geothermal gradients can be derived from nearby shallow and more distant deep wells from temperature measurements within the Yarragadee (Jy), Cattamarra Coal Measures (Jc) or shallower Gage Formation (Kwg):

- AM40, Jy, 38.8 °C at 665 m (DoW records, 19/9/1980); gradient 28.3 °C/km^{-1}
- AM42, Kwg, 38.1 °C at 572.5 m (DoW records 17/6/1982); gradient 31.6 °C/km^{-1}
- AM49, Jy, 36.50 °C at 535 m (scanned records 7/10/1982); gradient 30.8 °C/km^{-1}
- Cockburn1, Jc, 81.1 °C BHT at 3109 m, 8+3/4" hole size; uncorrected. Chopra and Holgate suggest 21.18 °C km^{-1} gradient; Hot Dry Rocks Pty Ltd (2008) suggests heat flow of 76 mW m^{-2}.
- Bullsbrook1, Jc, 100 ˚C BHT, 104 ˚C extrapolated TFT at 4253 m; calculated gradient 19.8 °C km^{-1}; Hot Dry Rocks Pty Ltd (2008) suggests heat flow of 68 mW m^{-2}.
- Gingin3, Jc, 103.8 °C BHT at 3294 m; reliable calculated gradient 25.4 °C km^{-1}

5.5 Water quality

Water quality has been assessed by measurements of salinity and water saturation in the following sections.

5.5.1 Background salinity

Salinity information is available from several sources. In an overview sense, (Davidson, 1995) reviews water quality in aquifers down to the Yarragadee Aquifer. Specific information on the Leederville Aquifer is available in a comprehensive study by Leyland (2011). Deeper water quality analyses are available from petroleum wells at Cockburn1, Bullsbrook1, and Gingin3, usually from samples taken during drill-stem tests (DST). These information sources may be summarised as follows:

- Davidson (1995) reports that in the Yarragadee aquifer, salinity ranges from 140 to 10 000 mg L^{-1} Total Dissolved Solids (TDS). Typically, salinity increases with increasing depth and in the direction of groundwater flow (generally towards the Indian Ocean). Of this TDS, the majority ions are sodium chloride. Sulphates are less than 50 mg/L^{-1} and the aquifer generally

contains low dissolved iron.

- Davidson (1995) also reports that Cattamarra Coal Measures contains dissolved iron at concentrations exceeding drinking water guidelines (0.3 mg L^{-1}).
- The Cockburn1 completion report provides salinity estimates of less than 1000 mg L^{-1} sodium chloride equivalent in the Yarragadee Formation and 30 000 mg L^{-1} in the Cattamarra Coal Measures.
- Formation water salinity in Bullsbrook1 is calculated from electrical resistivity logs (mg L^{-1} NaCl equivalent). The upper portion of the Yarragadee Formation is considered freshwater of less than 1700 mg L^{-1} NaCl equivalent, while the deepest part of the Jy, the Cadda Formation and the Cattamarra Coal Measures are considered much more saline, up to 70 000 mg L^{-1} (40 000 mg L^{-1} in the Cadda Formation). The logging suggests a shale-siltstone barrier between 3862 m and 3991 m apparently acting as a barrier and causing a distinct drop in salinity occurring below this section.
- At Gingin3, water samples were collected during drill stem tests, all from the Cattamarra Coal Measures. Chloride concentrations ranged from 1400 mg L^{-1} to 13 000 mg L^{-1}.

5.5.2 Background water saturation

The deep petroleum wells in the Perth Basin were drilled as exploration wells. Significant hydrocarbons were not encountered in any of the formations intersected in Rockingham1 and Cockburn1. However, some gas was recorded in Eclipse1, 62 km north of Perth, within the Yarragadee Formation. Gas levels were in between 0.01% to 0.95%. Four commercial discoveries in the Dandaragan Trough have produced both oil and gas from multiple sands within the Cattamarra Coal Measures. The Gingin1 well, 89 km north of Perth, encountered two petroleum bearing units within the Cockleshell Gully Formation (now named the Cattamarra Coal Measures) near depths of 3661 m and 3745 m below sea level (Cadman et al., 1994).

The Cockburn1 and Bullsbrook1 wells were plugged and abandoned after exploratory drilling due to lack of significant prospectivity. At Gingin3, the well was drilled to further explore a gas field producing from the Cattamarra Coal Measures; the well is currently suspended but not abandoned. Within these petroleum wells, electrical wireline logs permit the estimation of the water saturation within the formations. Water saturations less than 1.0 (100%) indicate the presumed presence of gas or oil in the formation. Salient items are:

- Cockburn1 lists no water saturation percentages.
- Rockingham1 shows that both the Yarragadee Formation and the Cattamarra Coal Measures are fully water saturated.
- Bullsbrook1 wireline logs showed minor gas saturations in the Cattamarra Coal Measures, and a few intervals of less than 5 m containing decreased water saturations between 34 to 80%.

The Gingin3 completion report lists water saturation close to 1.0 in most intervals within the Cattamarra Coal Measures. Exceptions with water saturation less than 95% include six intervals of less than 25 m with average water saturation ranging between 37 and 92%.

5.6 Reservoir targets

As part of the exploration plan, the characterization of the following targets is proposed.

Targets: Formations with sufficient permeability and storage capacity to sustain high flow rates (> 50 kg s^{-1}) at a minimum water temperature of over 70 °C.

Primary Target: Lower Yarragadee Formation at approximately 1900 to 2200 m TVD.

Secondary Targets: Cadda Formation predicted at approximately 2200 m to 2300 m TVD, Cattamarra Coal Measures predicted approximately below 2300 m TVD.

Tertiary Target: Eneabba Formation predicted at greater than 3300 m TVD,

These targets have been identified considering the available subsurface background information and the geothermal production requirements (not discussed in this document). A suitable target for geothermal direct heat use should demonstrate sufficient permeability, storage capacity to sustain high flow rate (> 50 kg s^{-1}) at a minimum water temperature of over 70 °C.

Exploration data acquired from this proposed well would be used to determine the geothermal production potential from the Lower Yarragadee Formation, the Cadda Formation and the Cattamarra Coal Measures for the SESKA Geothermal project.

The currently available data do not allow a reliable assessment of the geothermal reservoir productivity. As part of the exploration risk mitigation, the exploration well design will address the lack of data by incorporating suitable data acquisition activities. A suggested data acquisition program can be found in Ricard et al. (2011b).

5.7 Conclusions

The shallow geothermal potential of the Perth Basin has been confirmed over the past fifteen years and now with the risks of exploration and exploitation well understood the development of new shallow (up to 1000 m depth) projects is almost routine. The challenges for new geothermal development in the Perth Metropolitan Area lie in exploiting deeper, hotter resources. In this section, WAGCoE assisted with the development of a new deep demonstration project for the Perth Metropolitan Area, funded by the Commonwealth Government. Further relevant research, focusing on shallow heat rejection dynamics with applications to the ARRC/ Pawsey Project, is presented in sections 6.2 and 6.4.

6. ADVANCES IN RESERVOIR MANAGEMENT

6.1 Introduction

Conventional methods of utilizing thermal resources of geothermal reservoirs are similar to methods used in water supply and petroleum/gas industries. The essential technological step is to drill bores into the reservoir of interest and then to extract and/or inject fluids, exchanging heat with the reservoir matrix. If the amount of heat exchanged is large enough, the thermal state of the reservoir can be altered, which in turn affects the performance of the heat exchange scheme. If thermal alterations are sufficiently large and long-lasting, the heat exchange performance of the system can degrade to such an extent that the original scheme becomes uneconomic or even thermally unfeasible. In any geothermal application, the sustainability of the application is critical.

In most geothermal applications, sustainability considerations form part of the economic justification. Typically, geothermal infrastructure is designed to operate for a minimum lifespan in order to repay capital investment and recurring maintenance costs. The selection of minimum lifespan is informed by plant depreciation schedules and also by the sustainability of the geothermal resource. Clever reservoir management can significantly boost the economic feasibility of geothermal projects by extending the useful lifetime of the geothermal resource. Efficient reservoir management seeks to exchange the maximum amount of heat with the reservoir whilst maintaining the necessary thermal characteristics for the above-ground application for the maximum period possible. This optimisation problem requires a good understanding of the geothermal resource, and a management protocol capable of achieving high efficiencies of heat exchange.

In the following three subsections we describe the results of published WAGCoE research into (i) a new method of heat exchange with geothermal reservoirs that promises a step change in subsurface engineering technology (subsurface stirring); (ii) a new method of reservoir characterisation that achieves estimation of reservoir permeability structure based on space-time observations of fluid pressure oscillations (stochastic spectral method); and (iii) a new multidisciplinary protocol for assessing the potential biogeochemical impacts of thermal perturbations to groundwater systems, together with an example application of the protocol to a proposed shallow heat rejection system in the Perth metropolitan area.

6.2 Subsurface Stirring

Reservoir production methods usually employ bores emplaced to extract/inject fluids, often with steady pumping schedules. The induced fluid flows can be characterized by dipole potential flows, which have the characteristic of high flow speeds between paired injection and extraction wells, but with progressively lower flow speeds for locations further off the dipole axis. Over time, this generates an uneven spatial distribution of heat exchange in the reservoir, thus the maximum potential heat exchange is not reached and the effective operating lifespan of the reservoir is reduced. WAGCoE researchers have been studying the use of innovative dynamical techniques to optimize geothermal reservoir productivity. One such technique is subsurface stirring, a CSIRO

technique for controlling and manipulating subsurface heat distributions via dynamical flow phenomena, e.g. chaotic mixing and kinematic confinement. In following text we will introduce the basic dynamical concepts of subsurface stirring and give examples of how this may be used to benefit shallow geothermal activities, i.e. situations where the capital costs of bore drilling and completion are not so large as to preclude extra investment in bore infrastructure.

6.2.1 Chaotic processes in porous systems

Chaotic advection is a concept that is relatively new to hydrology and that holds the potential for manipulating distributions of scalar quantities (e.g. dissolved phase concentrations or heat) in flows within the terrestrial subsurface. Whilst much has already been learnt about chaotic dynamics in reactive fluid systems (see Tel et al., 2005), only a small, but growing, body of work exists on the mathematical basis of chaotic advection and its application to non-turbulent flows within porous media (Sposito, 1994; Metcalfe et al., 2007; Lester et al., 2009; Zhang et al., 2009; Metcalfe et al., 2010a,b; Trefry et al., 2010; Lester et al., 2010).

In the 1990s, the internal mixing state of solute plumes became of interest. Based on entropic considerations, Kitanidis (1994) defined a dilution index which compared internal plume structure to an idealized Gaussian limit. Trefry et al. (2003) showed that non-Gaussian behaviour was persistent in two-dimensional plumes advecting in steady heterogeneous flow fields, i.e. the progress to a well-mixed plume was slow. Weeks and Sposito (1998) pointed out that mixing efficiency is promoted by physical heterogeneity of the porous medium, but that high mixing efficiency is best achieved by chaotic flow regimes, such as may be induced by periodic reorientations (Ottino, 1990). Trefry et al. (2012) note that chaotic processes occur at many scales within porous media, including pore scales at which Stokesian flow phenomena dominate, and at larger (Darcian) scales determined by the correlation structure of the porous matrix.

6.2.1.1 Engineered flows

The ability to engineer macroscopic Darcy flows with high mixing efficiency is important in promoting dilution of scalars advecting with the groundwater flow (e.g. heat or concentration). This was recently demonstrated by Zhang et al. (2009) in a series of experiments on the mixing and reaction of plumes advecting in oscillatory flow fields. In these experiments, it was shown how oscillating velocity vectors enhanced reaction by a factor of two for homogeneous sand and a factor of three for layered sand. The enhancement was interpreted to be caused by an effective increase of the contact interface area swept by the local velocity vector. In a geothermal sense, mixing can be used to reject excess heat in an enhanced fashion by maximizing the contact of hot fluids with cool sediments: mixing a volume of groundwater will act to equalize temperatures and may reduce or avoid heat rejection inefficiencies associated with persistent hot spots in the subsurface.

Recovery of dissolved contaminants is another potential application for enhanced mixing technologies in groundwater systems. Luo et al. (2007) describe a nested pumping scheme for introducing biological amendments to a target zone in order to stimulate bioremediation of uranium contaminated groundwater and sediments. They note that various factors can make it difficult to

employ conventional methods to predict and interpret tracer dynamics in such systems, including non-uniform flow fields, transient effects, heterogeneity and recirculation of fluid through injection and extraction wells. Alcolea et al. (2009) show how a conventional inverse stochastic modelling approach, which identified optimal placement of steady pumping bores within a heterogeneous aquifer, may boost the efficiency of saline recovery schemes. The improvement in recovery due to optimal design of the steady pumping bore layout was estimated by Alcolea et al. (2009) to be 10% of total cost (capital and operating costs) when compared to a traditional pumping layout. Despite the sophisticated optimization procedure, this improvement is modest in comparison to the doubled mixing enhancement observed by Zhang et al. (2009) for homogeneous systems where the flow field was allowed to oscillate.

6.2.1.2 Engineering chaos

Chaos may be the ideal mechanism for maximizing mixing in the subsurface. It is known that steady chaotic flow may occur in three dimensions (Arnol'd, 1965), but that time dependence is necessary for chaotic flows in two dimensions (Aref, 2002). Metcalfe et al. (2010b) showed that periodic re-orientation of two-dimensional Darcy flow is sufficient to induce chaotic advection over large ranges of the re-orientation parameter space. Despite the apparent simplicity of two dimensional oscillating Darcy flow in a homogeneous domain, the resulting chaotic dynamics are rich (Lester et al., 2009) with a wide range of fluid stirring behaviours able to be accessed by judicious choice of reorientation angles and induced flow rates. Even so, the chaotic mixing process induced by periodic re-orientation may not significantly increase pumping recovery rates of scalar quantities distributed in homogeneous regions, unless the flow Peclet number is large ($Pe=LV/D$, where L, V are characteristic length and velocity scales, and D is the dispersion coefficient). As noted by Weeks and Sposito (1998) and demonstrated by Bauer et al. (2009), Rolle et al. (2009) and Zhang et al. (2009), mixing is also enhanced where permeability contrasts are large (see also Phillips, 1991), therefore it is natural to consider how mixing may be governed by the combination of chaotic advection with structural heterogeneity.

Just as efficient mixing dynamics in porous media flows are created by judicious "programming" of stirring protocols, similarly non-mixing flows may also be programmed by different forcing protocols. Such flows possess the ability to encapsulate fluid regions so that they are confined apart from the rest of the background flow field. Such behaviour gives rise to a number of possible groundwater engineering applications including localization of pollutants for in-situ remediation and recovery, confinement of lixiviant and pregnant liquors in in-situ mining operations, and trapping of heated fluids in geothermal applications. Flow confinement is achieved by creating a so-called "kinematic barrier" between the encapsulated region and the bulk flow, and identical pumping infrastructure to that which generates efficient mixing can also engender confinement, albeit using a different pumping protocol.

Clearly there is rich potential for programmed manipulation of flows in the subsurface, with chaotic advection representing a novel groundwater engineering concept capable of engendering both efficient mixing and flow confinement. In the remainder of this section we investigate the application

of chaos theory to linear (confined) groundwater systems, with the kinematic and mixing properties given particular attention.

6.2.2 Fundamentals of subsurface stirring in porous media

For shallow geothermal reservoirs, the dynamics of Darcy flows are of prime interest. In steady Darcy flows orbits (motions of elemental parcels of fluid) can neither wander and fill the domain (mix), nor close on themselves (confine). Time dependent Darcy flows generically create both chaotic and closed orbits in both two and three dimensions by the crossing of streamlines in time (Lester et al., 2009). By this we imagine that in some region of the porous medium a first Darcy flow, e.g. the dipole flow between one injection and one extraction well, operates for a given duration of time, then the first flow is switched off and a second, independent flow is switched on in the same region. This second flow can be similar to or different from the first flow. The important thing is that when the streamlines of both flows are drawn and superposed, the streamlines of the two flows cross. What this sequence of flows does is to stretch fluid parcels into lines along the streamlines of the first flow, then the next flow folds those lines and stretches them again. By repeating the flow time dependence to repeatedly stretch and fold the fluid, the fluid pathlines diverge from the flow streamlines, even when no such stretching and folding motion exists in the streamlines of the velocity field. The reader probably sees intuitively that repeated stretching and folding is the essence of mixing.

This kind of mixing is called chaotic advection, and a generic chaotic flow has regions of both well-mixed flows and regular regions where fluid is confined. This chaotic mixing is not to be confused with turbulent fluid flow; the flows remain laminar. Figure 6.1 shows an industrial example of using chaotic flow in the manner described to mix two fluid streams in an empty pipe. Using the tools of chaotic advection, the job of the geothermal hydrologist is to design a suitable intervention, i.e. a sequence of flows through a given geothermal reservoir with particular physical properties that will maximize mixing (minimize regular regions) or maximize confined regions (minimize mixing) or obtain an optimal combination of each to accomplish any particular objective. Below we describe a chaotic Darcy flow that utilizes only dipole pumping pairs to mix and confine. And while our example flow may seem abstract, our aim is to use it to illustrate principles and examples in order to motivate the further study required to reliably use chaotic advection for geothermal reservoir engineering.

6.2.2.1 RPM Flows

An example of a programming dynamical flow system is Rotated Potential Mixing (RPM) flow. RPM flow is generated by assemblies of dipole pumping pairs (Metcalfe et al., 2010a,b) operating in a plane. Such an arrangement is analogous to a two-dimensional confined groundwater flow problem in plan view. In Metcalfe et al. (2010a,b) the conductivity was assumed to be spatially homogeneous and the theoretical predictions were confirmed in a series of experiments with a Hele-Shaw cell; we address questions of heterogeneity in later text. A simple RPM flow sequence is illustrated in Figure 6.2. An injection-extraction pair generates the dipole flow with streamlines in red. At a later time the first flow switches off and a reoriented copy of the first flow switches on with streamlines in blue. Re-orientation of the flow is parameterized by the jump angle Θ and the activation time τ which is normalized by the domain emptying time t_b.

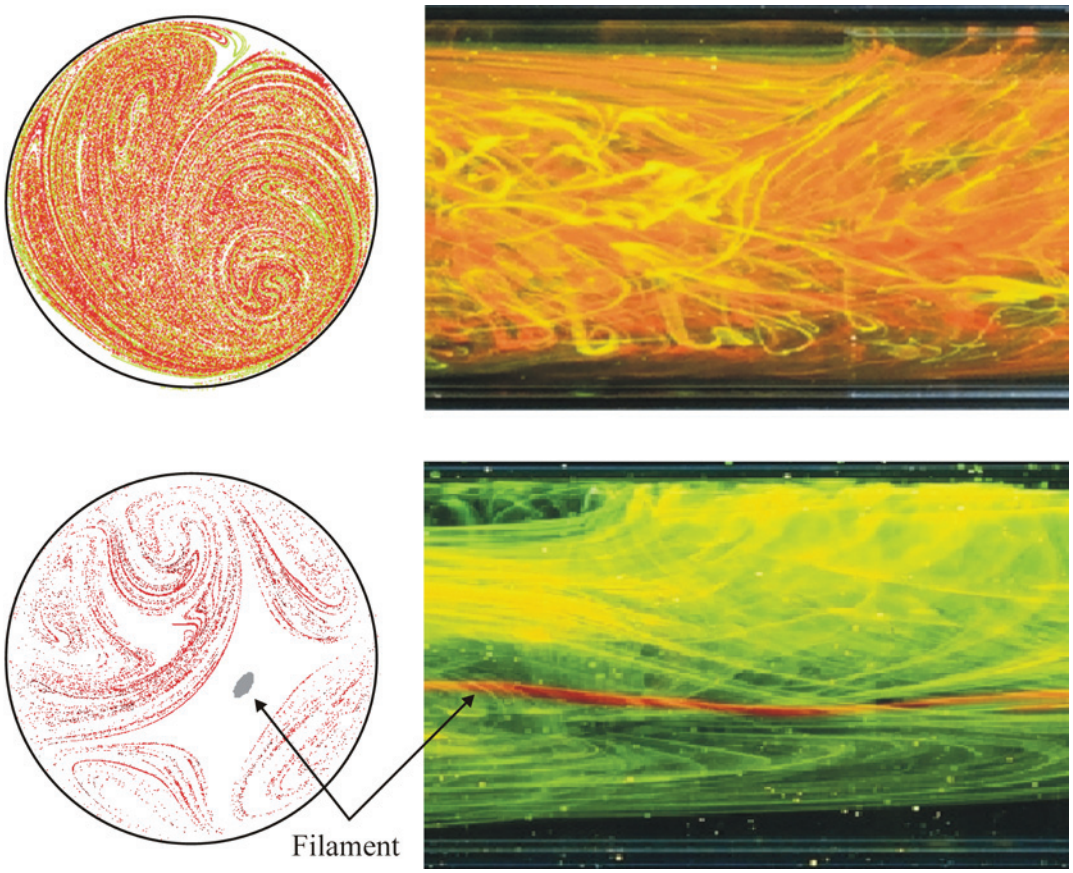

Figure 6.1: Selective chaotic mixing and kinematic confinement in high-Peclet number pipe flows (from Trefry et al., 2012).

Implicit in drawing the circular boundary in Figure 6.2 is the assumption that trajectories that lie outside the circular boundary defined by the dipole separation distance are not relevant to the long-term RPM chaotic processes within the boundary. External streamlines are hence neglected in establishing the characteristics of RPM flow. Furthermore, any fluid exiting the domain through the extraction well is immediately re-injected at the injection well, i.e. the flow system is closed.

Another key assumption of the RPM flow is that the flow is piecewise steady, such that each dipole switches instantaneously to the new configuration without transitory effects. It has been established elsewhere (Lester et al., 2009) that the response time of the Stokes flow is negligible with regard to the time-scale of the flow. However, it is well known in groundwater hydrology that the pumping response in aquifers, even in confined aquifers, is strongly time-dependent due to elastic properties of the formation. Nevertheless, as shown by Trefry et al. (2012), for many sedimentary reservoirs the hydrogeological response times are small compared to the basin emptying time t_b and hence the RPM ansatz is a useful approach for modelling dynamical response in geothermal reservoirs.

The redistribution of fluid generated by RPM flow is illustrated by a numerical dye trace evolution supplied in Figure 6.3, which shows the mixing (viewed from above) of an initially half-grey half-white coloured fluid as it flows between a set of 9 injection/extraction well pairs situated around

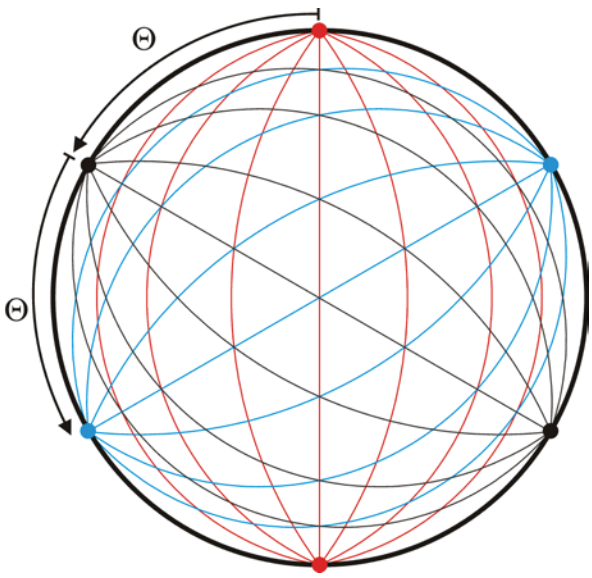

Figure 6.2: Example programmed dipole sequence for RPM flow. The red streamlines show the flow regime induced by one well dipole, then, after some programmed duration τ, this dipole is deactivated and another dipole at jump angle Θ is activated (black streamlines), then deactivated at time 2τ and a third dipole is immediately activated (blue streamlines), and so on (from Trefry et al., 2012).

the perimeter of a circular domain (defined by unit disk streamlines). These wells are shown as circles in the first subfigure (t=0), where the injection wells are coloured red, extraction wells blue, and inactive wells green. The dipole flow through the porous medium between active well pairs is shown by the blue streamlines. At a specific time $\tau = 1.7\ t_b$, the active wells switch off, and another pair offset by 100° switches on for duration τ, and the cycle continues. The initially thick regions of grey and white fluid rapidly stretch along streamlines to form thin interwoven striations which eventually become a uniform light-grey well-mixed fluid.

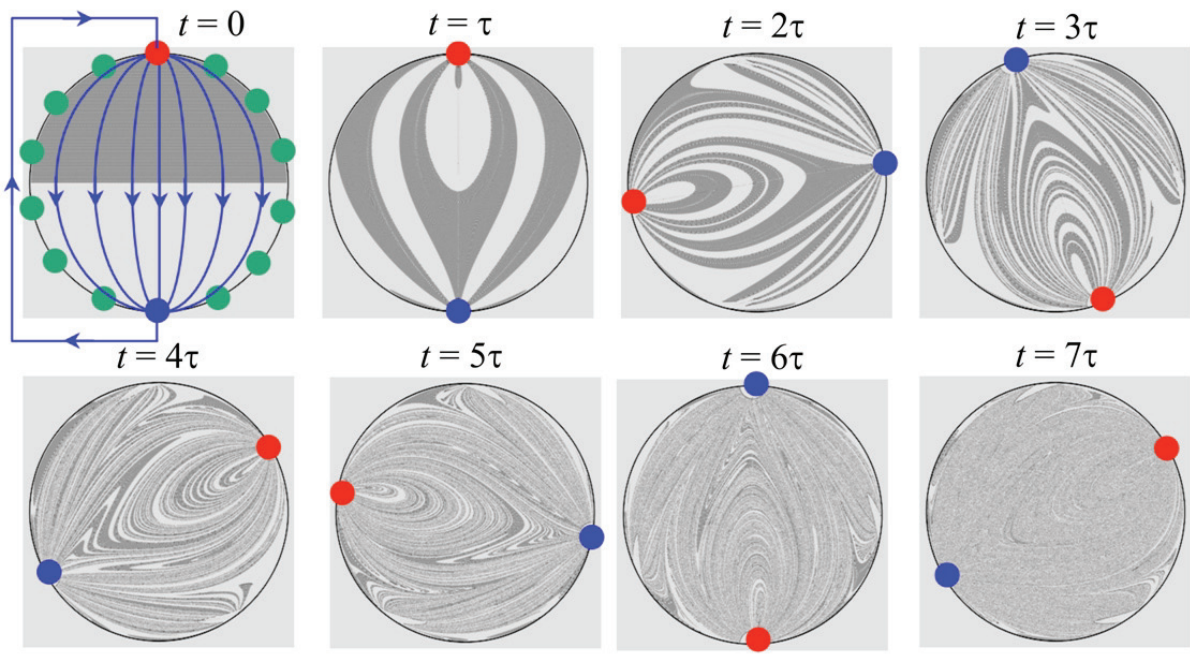

Figure 6.3: Rapid, complete mixing in a simulated RPM flow, driven by reorientation of the injection (red) and extraction (blue) wells. In this case the RPM is operated in closed mode, where material exiting via an extraction well is instantaneously re-injected at the injection well along the same streamline. Green dots indicate well locations for this RPM system (from Trefry et al., 2012).

6.2.2.2 Kinematic confinement

As we have seen, the RPM flow is characterized by choice of re-orientation angle Θ and activation time τ. This two-dimensional parameter space admits rich structure, with the resulting flows ranging from the rapid mixing of Figure 6.3 to complex maps of Lyapunov exponent and bifurcation behaviour (Lester et al., 2009). An informative picture of the RPM flow characteristic is provided by the Poincaré section, which can be calculated for any (Θ,τ) coordinate by releasing particles into the RPM flow and tracking their positions at multiples of the RPM period until structure emerges.

As shown by Lester et al. (2009), the Poincaré sections for the RPM flows clearly show two broad phenomena. First, for some values of (Θ,τ), fully chaotic flows are established by repeated application of the RPM cycles. These are indicated by random distributions of points on the Poincaré section. For other values of (Θ,τ), the Poincaré sections show well-defined, continuous orbits in one or more sub-regions of the disk. For dispersion-free scalar transport, these regular orbits are bounded kinematically, i.e. flows do not cross the boundaries of the orbit regions. Figure 6.4 shows example Poincaré sections for three RPM flows, highlighting zones of rapid chaotic mixing and kinematic orbits and boundaries. Conceptually, the kinematic boundaries separate zones of chaotic disorder from zones in which fluid may be confined indefinitely in regular orbits by the intrinsic RPM flow dynamics. Kinematic boundaries are described by the outermost (bounding) kinematic orbit neighbouring a (chaotic) zone of enhanced mixing. However, scalar transport in realistic porous media always experiences dispersion, so in practical cases confinement of fluid scalars will eventually deteriorate through dispersive leakage across the kinematic boundary.

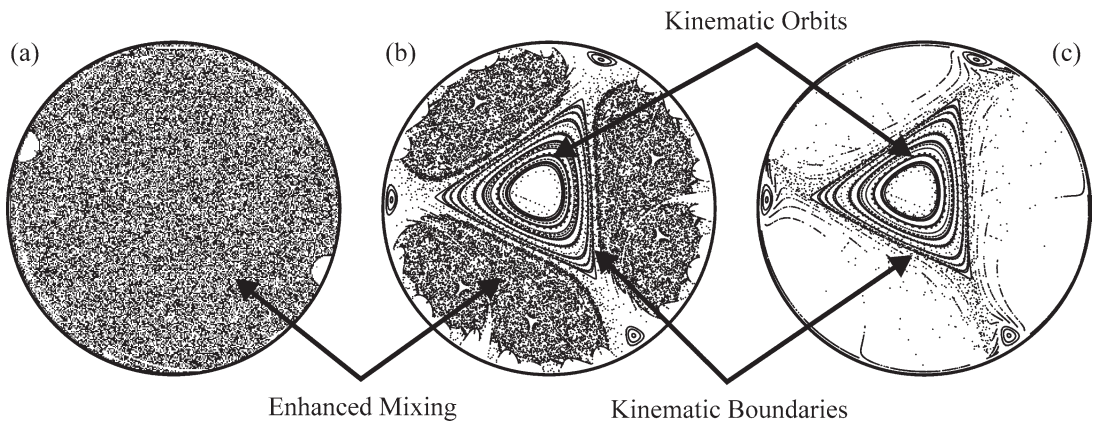

Figure 6.4: Poincaré sections of RPM flows, showing enhanced mixing zones and kinematic stability. (a): Θ = 5π/8 and τ = 5.1 t_b with unmixed re-injection; (b): Θ = 5π/8, τ = 0.2 t_b with unmixed re-injection; (c): Θ = 5π/8 and τ = 0.2 t_b with mixed re-injection (from Trefry et al., 2012).

Figure 6.4 also shows the impact of the unmixed pumping manifold feature introduced in the previous section. With unmixed reinjection (Figure 6.4(b)), kinematic boundaries form for some RPM programs, and significant coherence outside these boundaries can remain (see also Lester et al. 2009). However, for the more realistic case where communication between the extraction and injection wells engenders mixing (Figure 6.4(c)), zones outside the kinematic boundaries lose coherence and do not appear in the Poincaré section.

6.2.2.3 Accelerated mixing

Zones outside the kinematic boundaries are referred to as the "chaotic sea"; these correspond to parts of the RPM flow system that experience enhanced mixing. By employing a Floquet analysis to identify leading temporal eigenmodes for a standard transport problem, Lester et al. (2010) show that such chaotic zones mix scalars at a rate significantly greater than accounted for by advective-dispersive processes alone, even in homogeneous conductivity fields. For high Peclet number transport (Pe ~ 104), the chaotic mixing acceleration (defined as the ratio of the rate of asymptotic scalar decay toward homogeneity as compared to dispersion in a non-chaotic flow) from RPM flow was quantified to be up to 150 times greater than steady advection-dispersion. For moderate to low values of the Peclet number, i.e. systems where dispersion dominates advective velocity, the RPM mixing effect is of the same order as dispersion (Lester et al., 2010).

Figure 6.5 shows how a dispersive RPM system starts with a radially symmetric scalar distribution, and converges with time to the dominant Floquet eigenmode, which displays the gross symmetry of the Poincaré section in Figure 6.4. For this kind of initial value problem, the rapidity at which the scalar distribution approaches the dominant eigenmode depends on the separation of the eigenvalue spectrum (Lester et al., 2010). This approach is valid for any Peclet numbers. Thus, for geothermal applications, we can have confidence that the dispersing heat plumes will evolve to shapes that conform to the kinematic boundaries identified through the (infinite Peclet number) analysis of

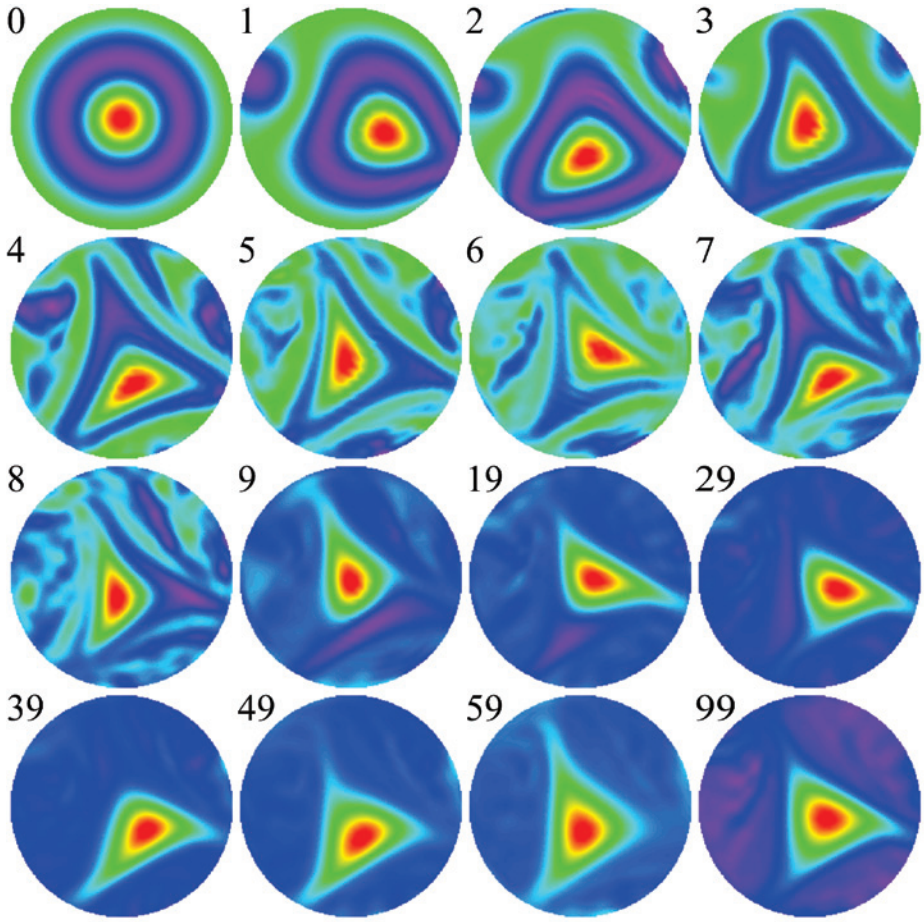

Figure 6.5: Convergence of dispersing RPM flow to the dominant eigenmode, for the RPM case $\Theta = 5\pi/8$, $\tau = 0.2\ t_b$. The reorientation number is provided for each snapshot, and the colour scale refers to scalar concentration, with red maximum and purple minimum (from Trefry et al., 2012).

Poincaré sections discussed earlier. At larger time scales, dispersion will lead to transport of the heat across kinematic boundaries within the circular domain and even across the domain boundary, leading to net loss of heat from the system. Engineering the relative rates of these dispersive losses is an important aspect of practical RPM design for geothermal reservoirs.

6.2.3 Physical phenomena and robustness

In practice, geothermal reservoirs possess a number of characteristics which influence the transport of heat to depart from the simple potential flows considered above. Characteristics of practical reservoirs with major impacts upon heat transport include heterogeneities in the rock property field, regional flow gradients, hydrodynamic dispersion, and three-dimensional flow. These characteristics must be taken into consideration when implementing enhanced intervention methods using chaotic advection. Although a detailed quantitative study of the impact of these characteristics is beyond the scope of this report, in this section we shall outline the nature of these characteristics and consider the impacts upon the primary features of chaotic advection in groundwater flow, namely confinement and enhanced mixing.

6.2.3.1 Heterogeneity

Heterogeneities in the rock property fields (e.g. permeability, porosity, thermal conductivity, heat capacity) occur in all reservoir systems; the length scale of such heterogeneities can range from the pore scale to hundreds of kilometres, and can significantly alter the flow field from the homogeneous case. Let us consider the case of permeability heterogeneity. Studies have shown that enhanced mixing via chaotic advection does indeed persist in systems with heterogeneous permeability, however low permeability regions do result in locally retarded mixing dynamics within these regions. Toward the limit of infinite log-permeability variance, such regions approximate impermeable boundaries to the flow domain and efficient mixing may still be achieved in the permeable regions. Conversely, an increase in permeability variance does reduce the effectiveness of confining flows as will be demonstrated in later text. This occurs due to advection of particles toward the separating streamline for the homogeneous dipole flow, which is more difficult to control for statistically defined log-permeability fields. In this sense, indefinite confinement is not possible in heterogeneous systems; however the confinement time is long enough to permit localised interventions (e.g. treatment and/or recovery of contaminants) even for very high log-permeability variances. We shall return to this point later in this and the following sections.

6.2.3.2 Regional flow gradients

Regional flow gradients occur in all natural reservoirs, and act to advect scalar quantities (desirable or undesirable) out of the flow control region, leading to downstream impacts. Bias in pumping rates or well heads across dipole pairs (given orientation of the dipole flow with respect to the regional gradients) can be used to effectively contain scalar quantities, as demonstrated in later text. As mentioned above, containment in the presence of regional flow becomes less effective with increasing conductivity variance, however the results herein suggest such an approach provides

significant scope for optimization. Such an approach also persists for enhanced mixing, as it is the dipole bias which in essence balances out the regional gradient, irrespective of the flow kinematics (chaotic or otherwise) within the dipole pairs.

6.2.3.3 Hydrodynamic dispersion

Hydrodynamic dispersion arises through combined micro-mixing and molecular diffusion, where the former is driven by (potentially chaotic) three-dimensional Stokes flow through the subsurface pore space, and acts to accelerate dispersion significantly above that of diffusion alone. With respect to mixing and accelerated scalar transport, combined chaotic advection and dispersion acts to increase the rate of global scalar transport significantly, in the same fashion that micro-mixing at the pore scale acts to accelerate molecular diffusion to generate accelerated hydrodynamic dispersion. For homogeneous systems, very significant accelerations are possible at high (order 104) Peclet number. These accelerations scale roughly as , and so the relative effect of scalar advective transport reduces with increasing dispersion.

With respect to flow confinement, dispersion of any magnitude acts to eventually disperse scalar quantities out of the dipole flow domain over time. As such, indefinite flow confinement is impossible. However, if intervention activities can be performed in conjunction with confining flows, it may be possible to ensure untreated zones are not swept outside of the kinematic boundary. For example, consider the case where a heat pulse is injected inside the kinematic boundary with a background temperature in the groundwater. As dispersion also acts to accelerate mixing, it may be possible to design pumping protocols which ensure mixing and equilibration of the thermal distributions prior to escape. This may be achieved by using the protocols outlined in Section 4, or it is also possible to design a nested set of RPM dipole circles, where the outer circle is programmed to promote confinement of heat, and the inner circle is programmed to promote mixing between the disparate heat distributions, i.e. homogenization within the inner circle.

6.2.3.4 Three-dimensionality

Physical groundwater flows are generally three-dimensional in nature, as permeability variations extend in all spatial dimensions. In such flows the question arises as to whether flow confinement or fluid mixing is desirable in two or three dimensions. In the former case, the RPM mixing protocol (albeit extruded in the third spatial dimension, e.g. by employing long pumping screens) can establish mixing or confining flows, with flow perturbations generated in the third spatial dimension by variations in permeability. It is thought that these variations act to alter the mixing or confinement dynamics in a fashion similar to that of two-dimensional heterogeneity discussed above. To establish truly three-dimensional mixing or confinement, it may be sufficient to implement a spherical equivalent of the RPM flow, where a set of three-dimensional reoriented dipole flows are generated by dipole pairs distributed over a spherical surface, e.g. by emplacing multiple wells distributed spatially and with pumping screens emplaced at different depths to approximate the desired geometry (it should be noted that a circular/spherical dipole arrangement is not a practical prerequisite for chaotic advection). At a fundamental level, the dynamics of this system is unchanged

from the equivalent two-dimensional system, aside from the distinction that there exists an extra spatial degree of freedom in both the flow domain and reorientation angles (say Θ_1, Θ_2). Hence, extension of these results to three-dimensional reservoir systems does not represent any significant changes at the conceptual level, and it is believed that enhanced mixing or flow confinement may still be achieved operationally.

6.2.4 Example Application – Control of Emplaced Heat Plume

Control of groundwater flows via specific programmed transient switching of pumping rate or pressures at well heads, such as is achieved in the RPM flow, can be used to achieve two distinct fundamental transport processes: flow confinement and enhanced mixing. These dynamics represent polar opposites of flow dynamics; in the first case, particle trajectories act as kinematic barriers to transport, leading to confinement of fluid regions; whereas in the latter case, particle trajectories form a chaotic tangle, significantly promoting mixing and scalar transport. We demonstrate how the principles of flow confinement may be applied to localization of a heat plume in the presence of a regional flow gradient and of heterogeneous hydraulic conductivity. In the following subsections we specifically exclude representation of hydrodynamic dispersion or diffusion, i.e. we consider flows with infinite Peclet number (D = 0). The reason for this is that we wish to disentangle and examine the key processes that control the performance of confinement and mixing. As we shall see, regional gradients and spatial heterogeneity in K each provide perturbations to, but do not remove, the underlying RPM flow topologies. In this case, it is likely that the inclusion of dispersive processes, which are flow-controlled, will not lead to drastic departures from RPM topologies either.

6.2.4.1 Homogeneous case with regional gradient

Consider a finite heat plume advecting in regional groundwater flow of unit velocity from left to right, as depicted in Figure 6.6 (left). By placing a surrounding circular network of wells, configured such that only two diametrically opposed wells are active at any time (one injecting and one extracting, forming a dipole), a confining flow within this circular network can be programmed via judicious switching of the dipole flows. To ensure balancing against the regional flow gradient, the dipole flows are weighted (biased) as $S(\theta) = 1 - 0.2 \cos(\theta)$, where θ is the angle of the injection well from the positive x-axis (running left to right), and the unweighted dipole flow is of velocity 20 (relative to the regional flow) at the circle centre. This cosine weighting ensures that the regional gradient does not sweep the RPM flow regime out of the disk. Streamlines of the combined regional and dipole flows are shown for $\theta = \pi$, $\theta = \pi/4$ respectively in Figure 6.6 (a),(b). As depicted by the streamlines, there is no exchange of fluid between the dipole and regional flows for $\theta = \pi$, however, exchange does occur for $\theta = \pi/4$, and so a plume within the circular domain would eventually be swept downstream for this flow.

In this idealized, homogeneous and zero-dispersion case, and for $\Theta = 5\pi/8$ and $\tau = 0.2\ t_b$, indefinite confinement is possible, as depicted by evolution of the square plume marked 0 at time t = 0 in Figure 6.6(d). The plume location at $t = 16n\tau$, i.e. after 16n reorientation events, is marked n in Figure 6.6(d) and is periodic over 224 reorientation events. For the chosen plume location, the

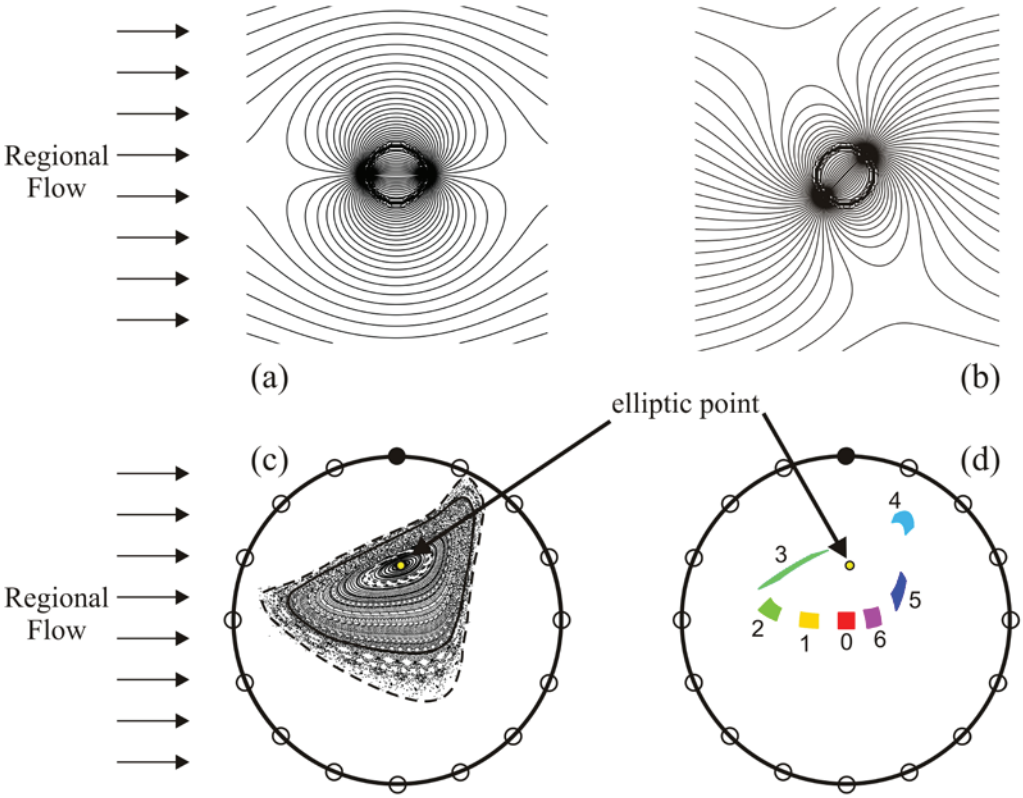

Figure 6.6: Effect of regional gradient on RPM dynamics of Figure 6.4(b). Top row: regional streamlines for combined regional and dipole flow; (a) Θ = π, (b) Θ = π/4. (c) Poincaré section for RPM system perturbed by regional flow. (d) Confined orbit of an idealized square plume in RPM flow (16n-cycle number shown). The plume is drawn in different colours according to the RPM 16n-cycle number (see text) (from Trefry et al., 2012).

plume orbits around the elliptic point marked. As such, this plume can be contained indefinitely within the circular RPM domain, despite the regional flow gradient running left to right and despite the fact that most superposed dipole and regional flows (e.g. θ = π/4, Figure 4.2.6(b)) exchange fluid through the injection and extraction wells. Note that although the plume is advected by the influence of the dipoles, it is not advected through the wells themselves. This long-term localization/confinement of the plume ensures that natural attenuation can be promoted without the usual risk of downstream impacts from the migrating plume. Treatment amendments may also be introduced into the confinement zone to reduce plume concentration during confinement, but mixing within the confinement zone is minimal for homogeneous conductivity fields.

The key issue here is the selection of an RPM arrangement such that the plume is located within the confinement zone. This placement process is complicated by the presence of the regional flow gradient, which generates dynamical leakage. In Figure 6.6(c) two closed curves are superimposed on the Poincaré section. The outer curve (dashed) shows the envelope of points on the section. In the RPM dynamics this curve divides zones of the flow that are retained within the RPM space (inside the curve) from those that rapidly exit the domain. The inner curve (solid) divides zones

within the section that display coherent orbits (inside, yielding confined orbits) from zones that display incoherence (between the solid and dashed curves). Fluid particles on the incoherent orbits eventually leak to the outer zone and are swept outside the RPM domain. The leakage time scales vary greatly for different points within the incoherent domain. It is important to recognize that the incoherence and leakage phenomena are purely dynamical: they occur for homogeneous RPM systems perturbed by a background flow. In such cases, leakage can be minimized by locating the plume within the coherent orbit zone.

6.2.4.2 Heterogeneous case with regional gradient

Clearly hydrodynamic dispersion and heterogeneous hydraulic conductivity may act to transport the plume outside of the circular RPM domain and hence downstream. However the preliminary results for a simple model system (in the previous sections) demonstrate the capacity for programmed dipole flows to retard plume transport in homogeneous systems which can significantly aid groundwater treatment and remediation. To investigate the impact of Darcy flow in heterogeneous media, we consider the persistence of this behaviour in heterogeneous media over a range of hydraulic conductivity (K) contrasts. We consider a heterogeneous log-conductivity field, generated by the Hydro-gen package (Bellin and Rubin, 1996) with a Gaussian correlation spectrum. The integral scale was chosen to be 1% of the dipole distance as such a domain length fraction is (i) sufficiently small to allow RPM advective processes to sample large numbers of conductivity scales without undue homogenization that would occur for heterogeneity expressed at smaller length fractions, and (ii) large enough to still provide appreciable spatial anomalies in the conductivity structure without undue perturbation and bias that would arise from a single realization with greater length fraction The focus here is to study how the deterministic (homogeneous) measures of RPM flows may be perturbed by model heterogeneity – a full survey of the parameter space of heterogeneity is beyond the scope of this paper. The dipole arrangement and log-K field are illustrated in Figure 6.7.

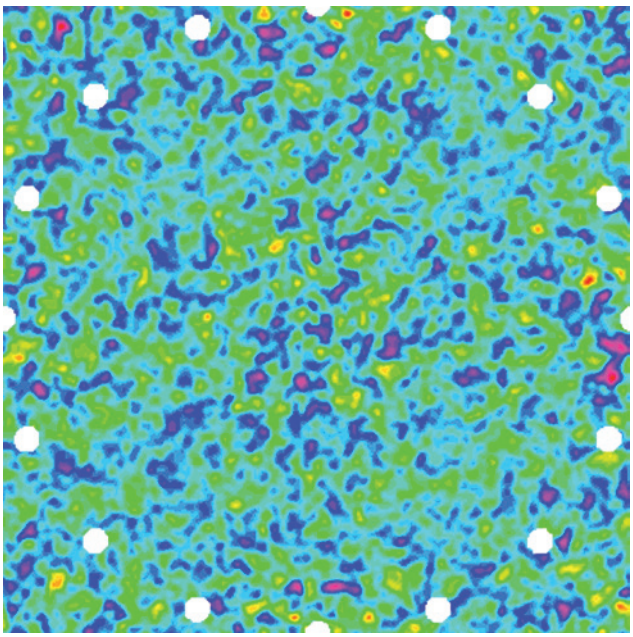

Figure 6.7: Contour plot of the Gaussian log-conductivity field, with unit variance and correlation scale set to 1% of the dipole distance. The white dots show the locations of the dipole wells (from Trefry et al. 2012).

This field, denoted f0(r), where r is the spatial coordinate has mean of zero and unit variance, and so the hydraulic conductivity K(r) is K(r) = exp(σ f0(r)), where σ^2 is the variance of the log-conductivity field. We consider flow confinement over four values of σ^2: 0 (homogeneous, as in the previous section, shown in Figure 6.6), 1/4, 1, and 4, and the streamlines for the combined dipole and regional flows for σ^2 = 1/4,1,4 are shown in Figure 6.8, which may be compared with Figure 6.6(b). The gross flow structure is preserved in all of these cases, with the heterogeneity acting to induce small local perturbations in the streamlines. Note that, as per the theory of Arnol'd discussed earlier, the broad topology of these flows is unchanged by the presence of such heterogeneities.

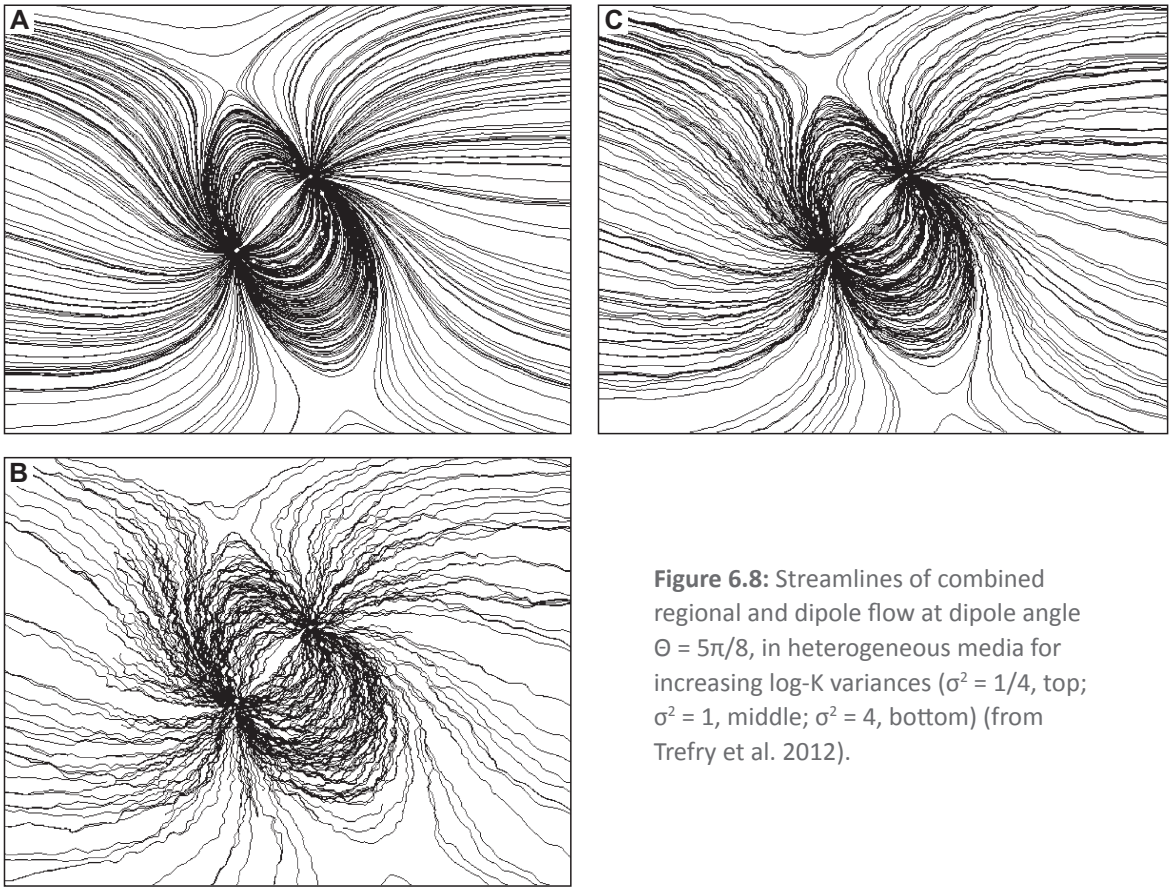

Figure 6.8: Streamlines of combined regional and dipole flow at dipole angle Θ = 5π/8, in heterogeneous media for increasing log-K variances (σ^2 = 1/4, top; σ^2 = 1, middle; σ^2 = 4, bottom) (from Trefry et al. 2012).

To study the impact of such heterogeneities upon flow confinement, we advect a square plume using the dipole flow protocol of Figure 6.6 over a period of P = 224τ and measure the flow confinement performance. The results are illustrated in Figure 6.9, which depicts the location of points initially located within the plume over time with red corresponding to t = 0 and to t = P for σ^2 = 0, 1/4, 1, 4. As seen in Figure 6.6 for the homogeneous case, this protocol generates periodic and hence indefinite confinement in the coherent orbit zone. However, for heterogeneous media with finite σ^2, the plume can leak and eventually escape from the circular RPM domain, even if the plume initially lies within the coherent orbit zone. This is due to the fact that variations in the flow velocity field for heterogeneous media allow particles to be advected onto streamlines which are no longer

encapsulated by the dipole flow, and furthermore the separating streamlines which demarcate encapsulating and non-encapsulating regions are perturbed by heterogeneities in the conductivity field. Heterogeneity in the porous medium stimulates the decay of coherent orbits predicted by Poincaré sections for homogeneous systems.

A. Plume located at disk centre

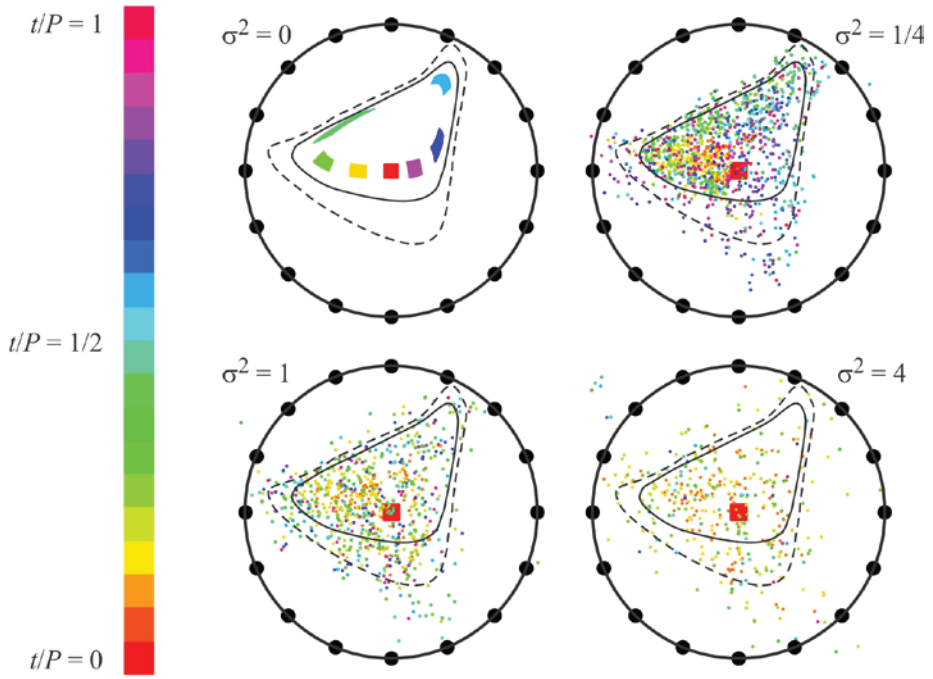

Figure 6.9: Effect of log-K variance on an idealized heat plume subject to RPM confinement in a regional flow gradient to the right, for log-K variances $\sigma^2 = 0$, 1/4, 1, 4. The legend shows colour-coding of plume points at times spaced throughout a complete RPM cycle of period P. The curves indicate the locations of the coherence boundaries for the homogeneous case $\sigma^2 = 0$ (see Figure 6.6) (from Trefry et al. 2012).

B. Plume located at elliptic point

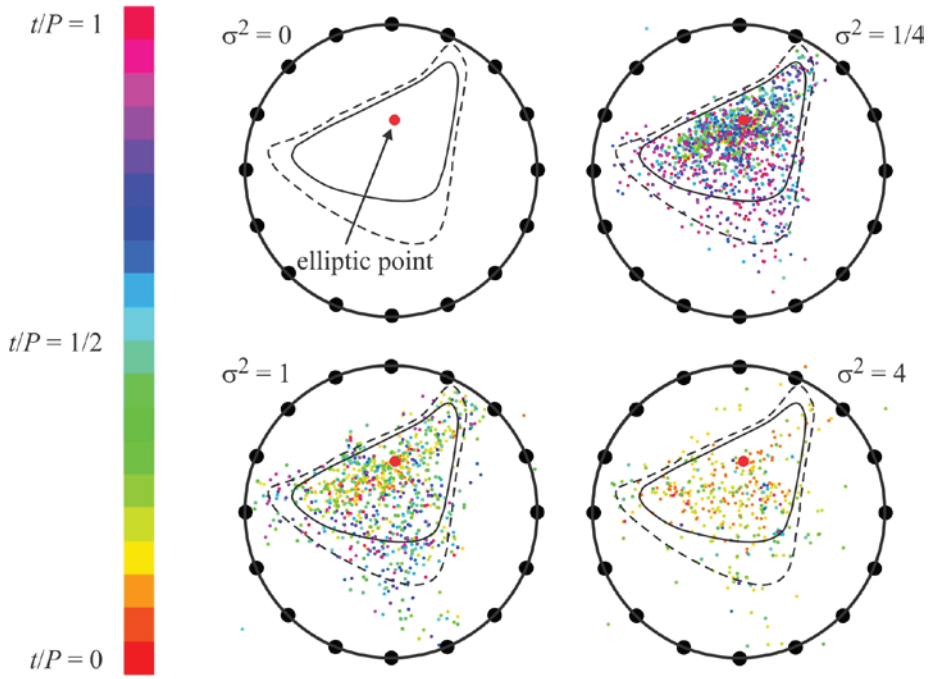

With increasing σ^2, the rate of escape of points on the perimeter of the initial plume increases, as depicted in Figure 6.10 which shows the percentage of confined points as a function of the flow reorientation events for various σ^2. For $\sigma^2 < 4$, flow confinement can be achieved for some finite time t_c, before particles begin to escape downstream, except for the homogeneous flow case. The behaviour of the dipole flow can vary significantly over the control parameter space $\Theta \times \tau$, and so there exists scope for improvement of these results via optimization of the RPM protocol to achieve confinement, especially in light of heterogeneous hydraulic conductivity.

Figure 6.10 also shows the relationship of confinement performance with initial placement of the plume. Placement of the plume near the elliptic point of the confinement zone can markedly increase confinement performance for systems displaying low to moderate heterogeneity. The benefit decays rapidly with increasing σ^2, so that by $\sigma^2 = 4$, no residual confinement benefit remains from locating the plume at the elliptic point. It is worth restating that all the above heterogeneous simulations were performed for the single case where the correlation scale of the heterogeneity was 1% of the RPM dipole distance. Many practical settings are likely to have different correlation scale ratios, smaller or larger, or even more complex spatial correlation structures. In such circumstances we would advise that site-specific engineering analysis of desired RPM protocols be performed, rather than relying on the theoretical results for idealized scenarios presented herein.

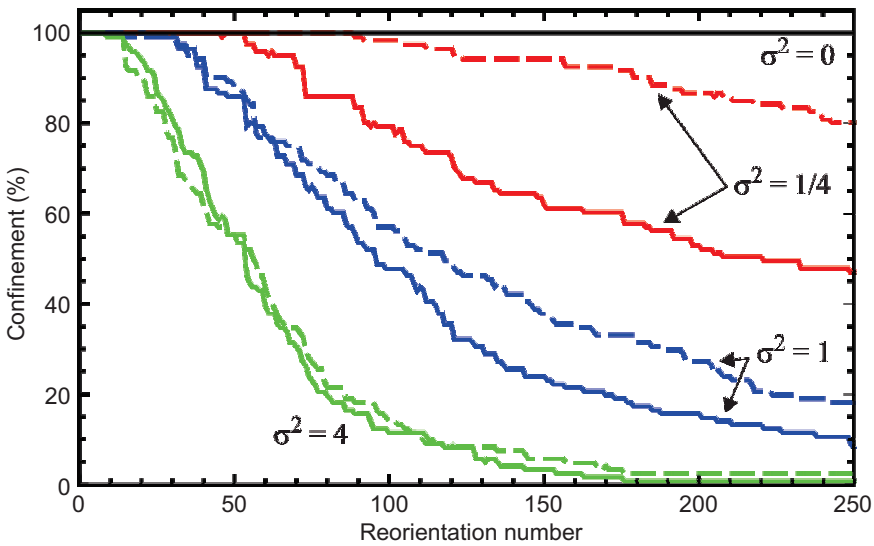

Figure 6.10: Plume confinement percentage as a function of reorientation number for various values of log-K variance for the RPM flows of Figure 6.9. The solid traces are for a plume initially located at the disk centre, and the dashed traces are for initial location at the elliptic point (from Trefry et al. 2012).

6.2.5 Example Application – Homogenization in Heat Rejection

Consider a shallow geothermal reservoir into which waste heat is to be rejected and stored, as may be of interest in the cooling of industrial infrastructure where water loss is to be avoided and hence conventional cooling tower technology is neglected. In this case we have some finite volume V of geothermal reservoir which we want to reject heat into at some fixed energy rate H over time. Our task is to maximize the operating time until we can no longer reject heat at rate H (i.e. we run out of reservoir heat exchange capacity by the increase of reservoir temperature). Furthermore, we want to confine the rejected heat to this reservoir volume V as much as possible and hence minimize "thermal leakage" to the surrounding formations. These two constraints can be translated into operational objectives as

- Maximize mixing within the volume V (so to homogenize the temperature field and delay thermal breakthrough as much as possible)
- Minimize heat losses outside of volume V

To proceed with the example, we consider the volume V to be defined by a two-dimensional circle of unit dimensionless radius 1 within which any well arrangement can be placed. We disregard the possibility of locating wells outside V as heat flowing outside the reservoir of interest is to be avoided. We compare a conventional steady dipole flow (with unit dipole distance) centered in V with a 6-spot pattern of the same inter-well diameter also centered in V.

We non-dimensionalize the heat flow dynamics and include dispersion, conduction and advection, with instantaneous heat transfer assumed between solid (grain) and liquid phases, which reduces the problem to a single phase problem with a retarded advection arising from a weighted average of phase heat capacities. This is an assumption is not physically based since grains conduct heat from grain surfaces to grain interiors at finite rates, so changes in fluid temperature in the pore space will take time to equilibrate with contiguous grain boundary temperatures. The aquifer initial temperature and injected waste heat fluid temperature are non-dimensionalized to be 0 and 1, respectively. The steady dipole consists of variable speed flow (such that constant heat flux is achieved) with all fluid going to/from the above ground heat exchanger. This single-phase dimensionless problem only has two important parameters, the Peclet number (which is assumed to be 100) and the temperature difference at unit flow rate to achieve energy rate H, assumed to be 0.05 in non-dimensional units.

Simulations were run using the COMSOL/Multiphysics simulation platform. Simulations included a conventional doublet heat rejection scheme and a scheme employing subsurface stirring to boost homogenization of the reservoir temperature field and hence increase the useful lifespan of the reservoir. The stirred case consists of a closed periodically reoriented dipole flow at unit flow rate such that all extracted fluid is re-injected except for some fraction which is exchanged with the surface and this fraction changes with time to achieve the same constant heat flux as the steady case.

Figure 6.11 and Figure 6.12 show the temperature distributions calculated for the conventional dipole and subsurface stirring schemes, respectively. The subsurface stirring distributions are rotated periodically, causing the emplaced heat to sample all of the target volume V, whereas the conventional steady dipole induces a temperature distribution that increases in size beyond the boundary of V.

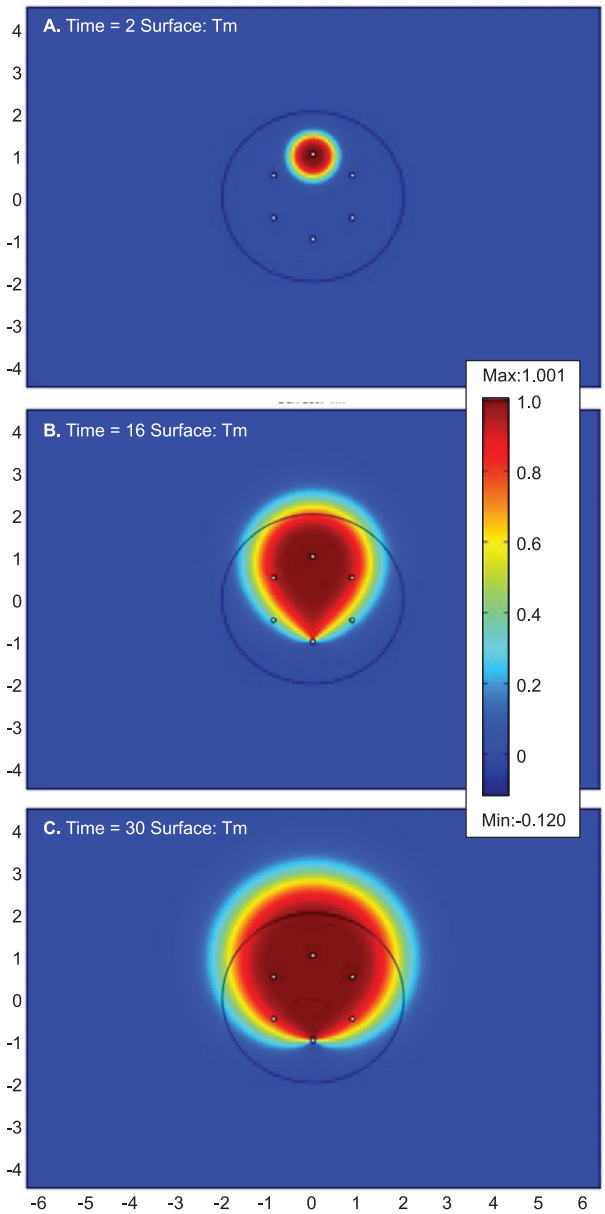

Figure 6.11: Temperature distribution snapshots for a conventional dipole scheme (aligned top to bottom, extraction at the bottom end) emplaced within a circular domain V. Four other wells used for subsurface stirring are also shown for reference. Snapshots are shown shortly after commencement of the pumping (Time=2), and at two subsequent times (Time=16 and 30).

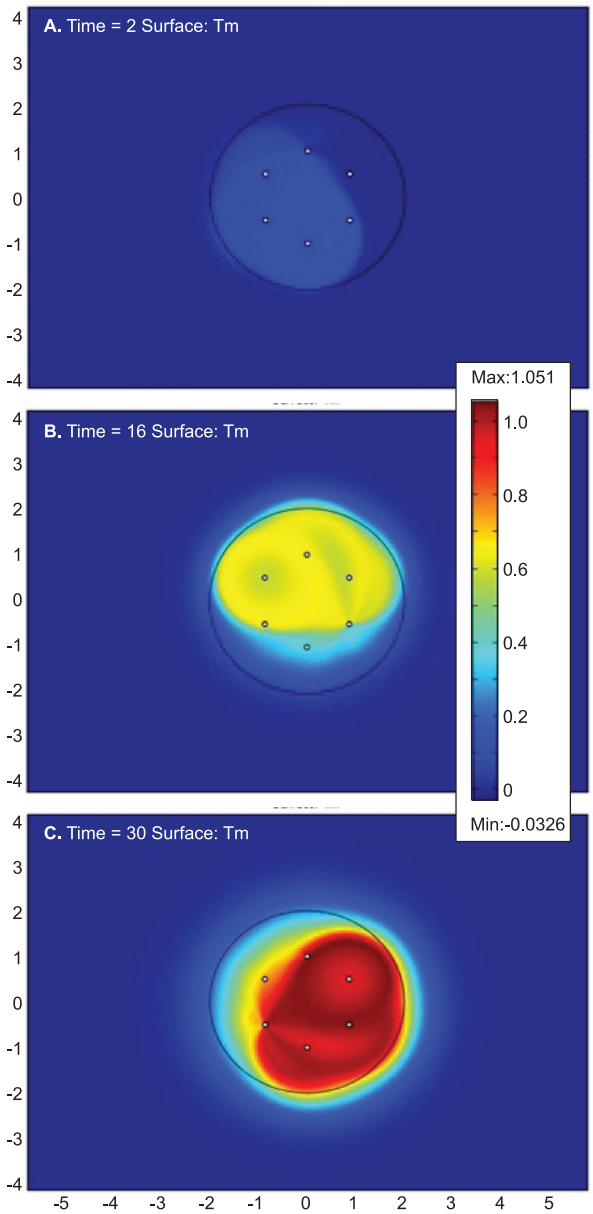

Figure 6.12: Temperature distribution snapshots for a six-well subsurface stirring scheme emplaced within a circular domain V. Snapshots are shown shortly after commencement of the stirring (Time=2), and at two subsequent times (Time=16 and 30).

Figure 6.13 shows that the stirred case outperforms the conventional doublet in terms of heat confinement within V, i.e. the stirring protocol is less likely to lose heat through the boundaries of V. Conversely, the outlet temperature is significantly worse for the stirred case, where the extracted fluid non-dimensional temperature T out exceeds 0.8 after 30 time units. As T out approaches 1, thermal breakthrough is approached.

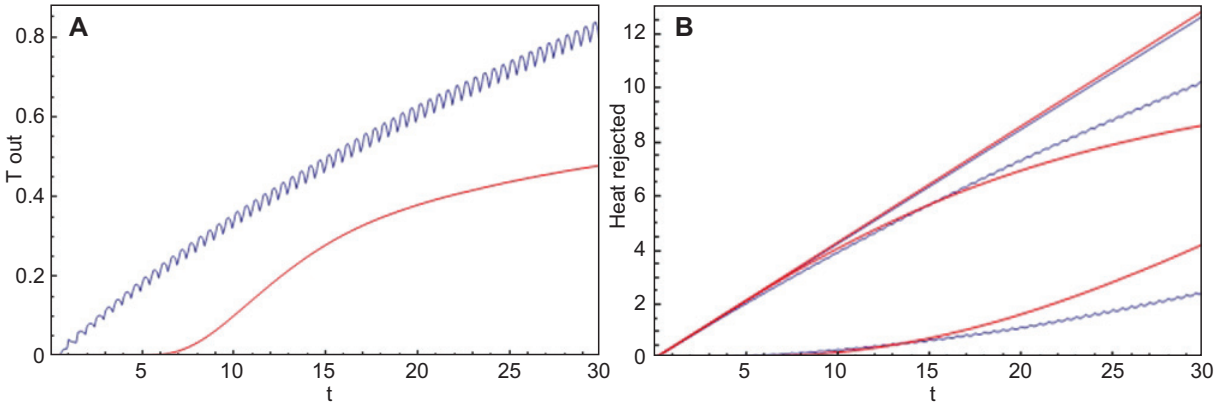

Figure 6.13: Thermal breakthrough (left) and heat rejection performance for a conventional dipole scheme (red curves) and a stirring scheme (blue curves). The 3 curves on the heat rejection plot (right) are for the total heat rejected (top lines), heat rejected into volume V (middle lines) and heat leaked outside of V (bottom lines).

What is the cause of this poor breakthrough performance? Essentially the key criteria here are scale dependence and the physics model. The dipole distance was chosen in such a way that the dipole thermal breakthrough time was maximized (Figure 6.13 left) at the expense of thermal leakage performance (Figure 6.13 right). If the dipole distance was reduced to minimize thermal leakage beyond the boundary of V, then the thermal breakthrough performance would decline rapidly. In terms of the physics, for the single-phase problem the conventional dipole is actually fairly efficient at keeping T out low and confining heat to the neighbourhood of the dipole.

However, if we relax the assumption of instantaneous heat transfer, the problem changes completely as stirring should act to homogenize the fluid temperature field in V, accelerating the net rate of heat transfer to the solid phase within V. Conversely, steady flow acts to “short-circuit” hot fluid to the extraction well. Research on quantifying interphase heat transfer coefficients for shallow geothermal reservoirs (e.g. sedimentary reservoirs) is continuing.

6.3 Stochastic spectral characterization of reservoirs

The use of time-periodic pumping methods to enhance reservoir productivity and lifespan also raises the possibility of using frequency domain techniques to characterize reservoir properties, e.g. permeability. In fact, a wide range of natural and anthropogenic processes can induce periodic responses in geological systems, with periods ranging over many orders of magnitude. In this section we consider how forcing modes with periods of the order of days may influence saturated porous

geothermal systems and how observations of the periodic responses in situ may be use to estimate reservoir structural properties. In this way we show how a valuable and independent estimate of reservoir properties can be gained from inexpensive monitoring of fluid pressures.

In the proceeding analysis we make use of a filtration equation to simulate the fluid dynamic effects of high temperature and high pressure of viscoelastic behaviour, so that the analysis has sufficient generality to describe aspects of high-temperature hydrothermal flow. Typically, spatial data on the properties of the reservoir porous medium are scarce, which limits the ability to build comprehensive geofluid models. Spectral techniques are common means of correlating patterns at like scales and are thus useful in inferring structure between correlated signals where data coverage is uneven. Here a stochastic spatial structure is employed for the properties of the porous medium and a perturbation approach is used to derive a relationship between the spatial spectra of the porous medium properties and the fluid dependent variable.

6.3.1 Generalized viscoelastic dynamics

Consider a non-turbulent fluid undergoing oscillating motion within a porous medium. We seek to generalize the fluid constitutive relation in order to capture a range of phenomena that may potentially apply in geofluid systems. In the simplest limit, the Darcy equation (Darcy 1859; Freeze 1994) relates the fluid flux vector, $\underline{J}$, with the local pressure gradient, ∇P :

$$\underline{J} = -\frac{\kappa}{\eta}\nabla P \qquad (6.3.1)$$

that is, the flow is laminar and the fluid flux is proportional to the fluid pressure gradient. We refer to κ simply as the permeability and η as viscosity. The linear continuity equation (6.3.2) applies (λ is an elastic capacity coefficient)

$$\lambda\frac{\partial u}{\partial t} = -\nabla.\underline{J} \qquad (6.3.2)$$

Extensions to the linear constitutive relation (6.3.1) are common. Brinkman (1947) proposed the addition of a viscous drag term to model frictional forces acting on a steady fluid at grain boundaries:

$$\underline{J} = -\frac{\kappa}{\eta}\nabla u + \beta^2\kappa\nabla^2\underline{J} \qquad (6.3.3)$$

Here the non-negative quantity β is defined by $\beta^2 \equiv \eta'/\eta$, the ratio of the effective viscosity averaged over the local flow within the pore space (η') to the bulk fluid viscosity. In the absence of further information regarding grain boundary friction averaging, β^2 is often assumed to be unity, although Brinkman (1947) provides other possible estimates. As discussed by Capuani et al. (2003), this term is only justified for media with porosity close to unity but has been shown to be useful for describing steady viscous flows in inhomogeneous systems, including biological tissues (Khaled and Vafai 2003). As discussed by Trefry et al. (2010), time-dependent relaxation and retardation phenomena have also been modelled by the inclusion of linear terms in the constitutive relation, motivating by analogy with the behaviour of Oldroyd fluids. We pursue a simplified filtration model of viscoelastic flow in

porous media, and propose the following generalized relationship for a single fluid state variable u subject to Brinkman viscous drag (enhanced dissipation) and dual temporal relaxation (τ) -retardation (ε) phenomena:

$$\left(1+\tau\frac{\partial}{\partial t}-\beta^2\kappa\nabla^2\right)\underline{J}=-\kappa\left(1+\varepsilon\frac{\partial}{\partial t}\right)\nabla u \qquad (6.3.4)$$

Here we have absorbed viscosity η into the definition of κ. Chief among the limiting assumptions is the neglect of any explicit constitutive relation between the fluid stress and strain tensors, i.e. the filtration approximation. In justifying this assumption we appeal to the limit of laminar Darcy flow, that is where the effects of stress-strain relationships are small and can be modelled through a simple momentum law such as equation (6.3.4). In making this assumption, we expressly rule out turbulent effects associated with high-velocity flow through large voids. For broader application it is understood that the general scalar state variable u may variously be associated with fluid pressure, concentration or temperature, according to practical context.

As shown by Trefry et al. (2010), assuming that Brinkman drag can be represented by a homogeneous term the governing equation for the propagation of frequency mode ω = 2πf is given by

$$\nabla.(\kappa\nabla\hat{u})+\left(\frac{\omega\kappa}{i-\omega\tau}\nabla\tau+\frac{i\omega\kappa}{1+i\varepsilon\omega+i\beta^2\lambda\omega}\nabla\varepsilon\right).\nabla\hat{u}-\frac{\lambda\omega(i-\omega\tau)}{1+i\varepsilon\omega+i\beta^2\lambda\omega}\hat{u}=0 \qquad (6.3.5)$$

This hyperbolic equation describes how the Fourier coefficient of u for mode ω varies spatially within the reservoir porous medium in response to spatial variations in κ, τ and ε. The governing equation (6.3.5) may be integrated analytically for special classes of the spatial variations of κ, τ and ε and is amenable to numerical solution by standard finite difference techniques (Trefry et al., 2010).

6.3.2 Effects of spatial correlation in reservoir structure

We seek to derive from first principles a statistical correlation between the input and output fields of (6.3.5) that is independent of the internal correlative structures of the input fields. In order to do so, we will have to make a range of assumptions regarding the strength of the relaxation/retardation and dissipative terms in (6.3.5). We commence by regarding κ, τ, ε and ŭ as spatially random fields that are stationary, that is their means are well defined over the domain of interest with no drift terms. In particular, we introduce the concept of weakly hyperbolic dynamics, that is where ωτ<<1 (weak temporal relaxation) and where both ωε<<1 and $\beta^2\lambda\omega$<<1 (weak temporal retardation and weak Brinkman dissipation, respectively). In these domains, the denominators of (6.3.5) can be expanded to first order, yielding the weakly hyperbolic form:

$$\begin{aligned}&\nabla.(\kappa\nabla\hat{u})+\omega\kappa\left((-i-\omega\tau)\nabla\tau+(i+\varepsilon\omega+\beta^2\lambda\omega)\nabla\varepsilon\right).\nabla\hat{u}\\&-\lambda\omega(i-\omega\tau)\left(1-i\varepsilon\omega-\beta^2\lambda\omega\right)\hat{u}=0\end{aligned} \qquad (6.3.6)$$

Expanding κ, τ, ŭ and about their means (denoted by the expectation operator <•>) and integrating by parts yields

$$-i\alpha\,\lambda\,\omega\left(-i+\omega\tau_G\right)\delta\hat{u}+\kappa_G\,\nabla^2\delta\hat{u}+\kappa_G\,\delta F\,\nabla^2\langle\hat{u}\rangle+ \\ \kappa_G\,\nabla\langle\hat{u}\rangle\left(\nabla\delta F-\omega\,\tau_G\left(i+\omega\tau_G\right)\nabla\delta V+\alpha\,\omega\,\varepsilon_G\,\nabla\delta W\right)\approx 0 \qquad (6.3.7)$$

The δ prefix denotes the spatial fluctuation of a signal, i.e. the signal with its mean subtracted. To circumvent a non-stationary analysis we make the proximity assumption $\nabla\langle\hat{u}(\underline{x})\rangle\approx\nabla\hat{u}_0$, i.e. constant slope of the response near a forcing boundary, which ultimately provides the result obtained by Trefry et al. (2010) that relates the spatial spectral density S of the modal fluctuation ŭ in terms of the spatial cross-spectral densities of the property fields κ, τ and ε.

$$\mathbf{S}_{\delta\hat{u}\,\delta\hat{u}}\approx\frac{\kappa_G^2\left|\nabla\hat{u}_0\right|^2\underline{k}^2}{\underline{k}^4\,\kappa_G^2+\lambda\,\omega^2\left(\lambda+2\,\underline{k}^2\,\kappa_G\,(\varsigma-\tau_G)\right)+\lambda^2\,\omega^4\left(\omega^2\,\tau_G^2\,\varsigma^2+\varsigma^2+\tau_G^2\right)}\times \\ \left(\begin{array}{c}\mathbf{S}_{\delta F\,\delta F}+\\ \omega^2\left[\begin{array}{c}\varepsilon_G^2\,\mathbf{S}_{\delta W\,\delta W}-\varepsilon_G\,\varsigma\,\mathbf{S}_{\delta W\,\delta F}+\tau_G\left(-\varepsilon_G\,\mathbf{S}_{\delta W\,\delta V}+\tau_G\,\mathbf{S}_{\delta V\,\delta V}+\tau_G\left(\mathbf{S}_{\delta V\,\delta F}+\mathbf{S}_{\delta F\,\delta V}\right)\right)-\\ \varepsilon_G\left(\varsigma\,\mathbf{S}_{\delta F\,\delta W}+\tau_G\,\mathbf{S}_{\delta V\,\delta W}\right)+i\,\omega\,\varepsilon_G\,\tau_G\left(\varsigma-\tau_G\right)\left(\mathbf{S}_{\delta W\,\delta V}-\mathbf{S}_{\delta V\,\delta W}\right)\end{array}\right]+\\ \omega^4\left[\tau_G^4\,\mathbf{S}_{\delta V\,\delta V}+\varepsilon_G^2\,\varsigma^2\,\mathbf{S}_{\delta W\,\delta W}-\varepsilon_G\,\tau_G^2\,\varsigma\left(\mathbf{S}_{\delta W\,\delta V}+\mathbf{S}_{\delta V\,\delta W}\right)\right]+\\ i\,\omega\left[\varepsilon_G\left(\mathbf{S}_{\delta F\,\delta W}-\mathbf{S}_{\delta W\,\delta F}\right)+\tau_G\left(\mathbf{S}_{\delta V\,\delta F}-\mathbf{S}_{\delta F\,\delta V}\right)\right]\end{array}\right) \qquad (6.3.8)$$

where $\zeta = \beta^2\lambda + \langle\varepsilon\rangle$. Thus, through (6.3.8), knowledge of the spatial correlation structure of the property fields κ, τ, ε will provide quantitative information on the spatial structure of the scalar state variable u. Or, inversely, observations of the frequency-dependent spatial structure of u will provide quantitative information on the spatial structure of the reservoir property fields κ, τ, ε.

In low-temperature geothermal reservoirs, e.g. hot sedimentary aquifers, the pressure-temperature conditions are likely to permit conventional porous media geofluid dynamics, e.g. Darcian (laminar) flows or Fourier heat conduction. These simple geofluid flow phenomena can be recovered in the limit $\varepsilon_G = \tau_G = \beta^2 = 0$:

$$\mathbf{S}_{\delta\hat{u}\,\delta\hat{u}}\approx\frac{\kappa_G^2\left|\nabla\hat{u}_0\right|^2\underline{k}^2\,\mathbf{S}_{\delta F\,\delta F}}{\underline{k}^4\,\kappa_G^2+\lambda^2\,\omega^2} \qquad (6.3.9)$$

Interpreted for the Darcy flow case, (6.3.9) provides a direct relationship between permeability spatial structure and the spatial structure of the fluid pressure distribution driven by frequency mode ω.

6.3.3 Robustness and invertibility

Trefry et al. (2010) demonstrated the sensitivity of the spectral estimator (6.3.9) to the proximity assumption. As demonstrated by Figure 6.14, small changes in the assumed mean gradient term provide small corrections to the spectral estimator (6.3.9), i.e. the estimator appears robust to the proximity assumption. This conclusion was strengthened in further work by Trefry et al. (2011) who demonstrated the use of the spectral estimator in Darcian reservoirs to deduce statistical parameters of reservoir permeability distributions from observations of head oscillations in finite sets of observation wells. The convergence of the estimates of statistical properties (variance and integral scale) with respect to the number of observation wells was quantified for one- and two-dimensional reservoirs, and a set of analytical scaling forms were derived to relate specific statistical correlation models of permeability to induced head correlations (Trefry et al., 2011).

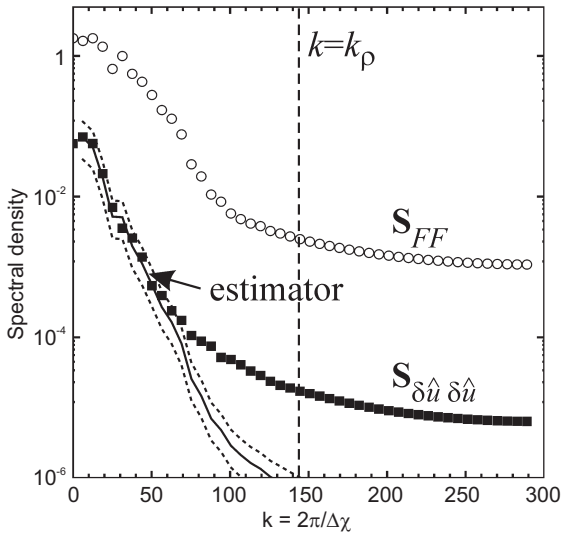

Figure 6.14: Performance of the forward spectral estimator (6.3.9, solid curve) for sample Darcian solutions (Trefry et al., 2010). The dotted curves show the estimators evaluated with 30% increase and decrease in the mean gradient constant. k_ρ is the wavenumber associated with the integral scale of k.

6.4 Biogeochemical assessment for in situ heat rejection

There is a need to explore efficient and sustainable technologies to manage the waste heat budget of the Pawsey Supercomputer Centre, now under construction to support Australia's bid for the Square Kilometre Array (SKA) radiotelescope (iVEC, 2010). The Pawsey Centre will house a petascale supercomputing system with an anticipated heat load of 2.4 MW_{th}. Critically, heat disposal options are constrained by the location of the supercomputer within an existing urban environment in addition to that of the proposed supercomputer research facility. Application of conventional cooling towers to directly cool the computer in-rack cooling system would result in a projected water loss of ca. 28-36.5 ML/annum.

Within the geothermal industry, surplus hot water previously abstracted and utilised in power generation or in heat exchange applications is often disposed by re-injection to local aquifers (Horne, 1982; Panichi, 2004). An alternative option for cooling the supercomputer is the use of local groundwater abstracted from the underlying Mullaloo Aquifer, to be passed through a plate heat

exchanger in a closed loop with the heated groundwater and re-injected into the aquifer, resulting in minimal net loss of groundwater. The Mullaloo Aquifer has a relatively uniform thermal profile, ranging between 20.3 °C and 20.7 °C over its thickness at the Pawsey site.

Sustainability of geothermal systems is an important factor in the economic and engineering feasibility of geothermal applications. Assessments of sustainability must integrate diverse disciplines. The return of heated water to the aquifer may potentially impact the biogeochemistry of the local formation, and hence affect the performance and sustainability of the heat rejection system. To further investigate the suitability and long-term environmental sustainability of the local groundwater abstraction/heat exchange/re-injection option, we have developed and applied a rapid biogeochemical assessment protocol for the Mullaloo Aquifer. In this section, we document the petrography, mineralogy and geochemistry of the Mullaloo Aquifer. These data form part of a larger study in which the major biogeochemical elements of the Mullaloo groundwater/aquifer system, specifically the prevailing groundwater and sediment composition and the microbial population, have been studied using a rapid assessment protocol to discern possible environmental effects, if any, of sustained re-injection of groundwater at higher than ambient temperatures (Douglas et al., 2012). An additional benefit of the assessment protocol is rapid identification of knowledge gaps that subsequent studies can focus on to improve project monitoring and management plans and hence reduce overall geothermal implementation risks.

Critically, groundwater-dependent ecosystems such as wetlands and native vegetation are directly linked to and partially dependent on the superficial aquifer situated immediately above the Mullaloo Aquifer and thus, an increased temperature has the potential to influence ecosystem function. Furthermore, the proximity of residential and other urban land uses to the Pawsey site means that there is a range of simultaneous water demands that must also be supported by any subsurface activity. In this way, the Mullaloo case study acts as a useful analogue for geothermal applications in many shallow aquifer systems within urban environments around the world.

6.4.1 Pawsey Centre site characteristics

A description of the site characteristics and hydrogeology outlined below are principally derived from previous studies (Rockwater, 2011a-c) and references contained therein. The Australian Resources Research Centre (ARRC) precinct is located on the Swan Coastal Plain, about 4.5 km south-east of Perth in Western Australia. The land allocated for the Pawsey Centre covers an area of about 2 ha adjacent to the existing ARRC building.

6.4.1.1 Local geology

The two uppermost aquifers present at the Pawsey site are the unconfined superficial aquifer and the underlying semi-confined Mullaloo Aquifer (Table 6.1). Detailed descriptions of the aquifers are provided by Davidson (1995) and Davidson and Yu (2008). A brief description of the regional setting for the Mullaloo sandstone member (MSM), the target heat rejection zone, based on Davidson and Yu (2008) and previous work undertaken (Rockwater 2011a,b), is given below. The superficial and Mullaloo Aquifers are separated by a confining unit composed of cemented sand

	Age	(10^6 years)	Stratigraphy
Cainozoic	Quaternary - Early Tertiary	Superficial formations	Safety Bay Sand
			Becher Sand
			Tamala Limestone
			Bassendean Sand Gnangara Sand Guilford Clay
		2 2	Yoganup Formation Ascot Formation
		2	Rockingham Sand
	Early Tertiary	54	Kings Park Formation Mullaloo Sandstone Member Como Sandstone Member

Table 6.1: Detailed stratigraphy of the Perth Metropolitan Area from early Tertiary to Quaternary (from Davidson 1995).

and shale. The Mullaloo Aquifer is underlain by confining units in the Kings Park Formation which is principally composed of shale and siltstone. The MSM has been identified within the footprint of the Kings Park Formation but its areal extent has not been accurately defined. Previous studies undertaken by Davidson (1995) and Davidson and Yu (2008) and data from the drilling programme carried out during August and September 2011 at the ARRC (Rockwater 2011b), were also assessed for this study. At the site, the MSM unconformably overlies shale of the Kings Park Formation, and unconsolidated Bassendean Sand unconformably overlies the MSM. The revised interpretation is based on comparison between lithological and geophysical data from Mullaloo production bore MPB 01, Mullaloo monitoring bores MB 04A, AM40B, AM40D and local production bores.

6.4.1.2 Hydrogeology

SUPERFICIAL AQUIFER

The superficial aquifer at the site consists of medium grained leached Bassendean Sand. Aquifer hydraulic conductivity is high, ranging from 10 to 50 m/d^{-1} (Davidson and Yu, 2008). The pumping test results from nearby superficial bores, CSIRO 1 and DEC 1, indicate that the superficial aquifer hydraulic conductivity is likely to be greater than 60 m d^{-1} at the site. Assuming a saturated thickness of about 30 m as inferred from hydrogeological sections, the aquifer transmissivity is calculated to be very high, approximately 1800 m^2 d^{-1} (Rockwater, 2011a).

MULLALOO AQUIFER

The Mullaloo Aquifer is a fluvial paleochannel incised into the Kings Park formation. At the site, it consists of medium to very coarse-grained, slightly glauconitic, clay-bearing sandstone. The MSM can be subdivided into three sub-units: an aquitard composed of shale of few metres of thickness underlain by aquifer units of variable thickness composed of slightly glauconitic, clay-bearing sandstone. The basal unit is coarser-grained with porosities as high as 30% (Rockwater, 2011b). The Mullaloo Aquifer is interpreted to be 85 to 88 m thick at the ARRC (CSIRO 1 bore). Based on the pumping test results (Rockwater, 2011b) estimated aquifer coefficients are: an average transmissivity of about 3675 m^2 d^{-1} , the hydraulic conductivity of approximately 43.5 m d^{-1}, a storativity of 0.0007 to

0.00075 (i.e. specific storage of 0.8-0.85 × 10^{-5} m^{-1}) and the effective porosity of 23-30%. The pumping test results indicate that the Mullaloo Aquifer is semi-confined. The aquitard unit at the top of the MSM, which separates the MSM from the overlying superficial formations is extensive but allows some downward leakage from the superficial aquifer. A constant rate test indicated the average bulk transmissivity of the aquitard to be approximately 2.7 m^2 d^{-1}.

The hydraulic conductivity of the Mullaloo Aquifer from the recent field investigation (August to September 2011) is relatively high when compared to the average regional hydraulic conductivity derived from the previous studies (Davidson and Yu, 2008; Rockwater, 2011a). However, it should be considered in the context of a heterogeneous palaeochannel aquifer, where highly transmissive lenticular sandstone beds occur with less permeable strata. Assumptions associated with the standard analytical methods are therefore not always met and the results should be viewed as indicative and suitable for use as starting parameters for a numerical model. The average regional hydraulic conductivity is likely to be lower with the effective mean dominated by areas of low hydraulic conductivity.

The thermal profile of the uppermost 130 m of sediments at the Pawsey site shows a strong seasonally dominated signal in the top 20 m followed by a rapid decline in the Superficial aquifer and a near-constant signal at approximately 20.5 °C throughout the depth of the Mullaloo Aquifer (see Figure 6.15, sourced from Douglas et al., 2012).

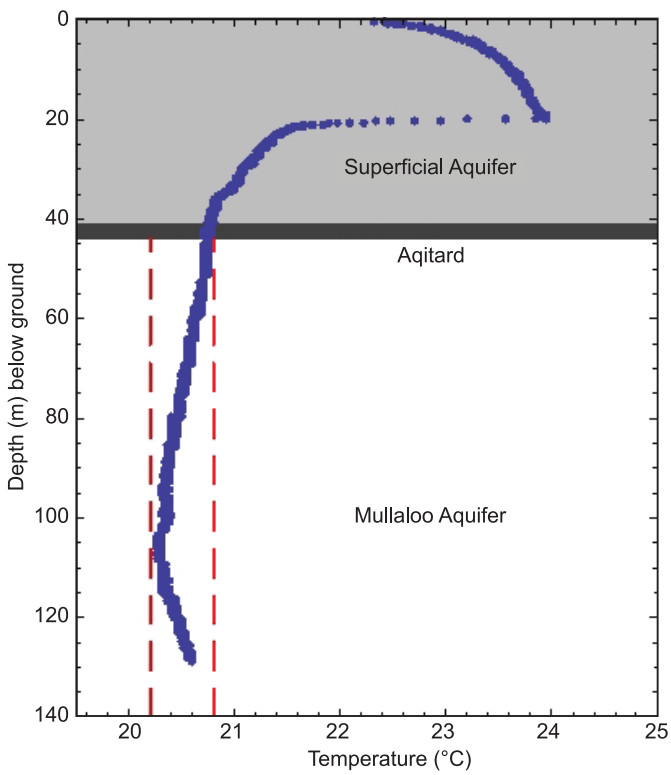

Figure 6.15: Thermal profile measured at borehole MPB01 in November 2011.

6.4.2 Analytical techniques

The following set of analyses was performed on the Mullaloo samples:

1. Petrographic analysis via thin sections and polarised light
2. Sediment analysis including washing and sieving
3. Major and trace element analysis including x-ray fluorescence (fused and pressed)
4. Mineralogy via x-ray diffraction on size fractions
5. Groundwater sampling for major ions, nutrients, organics and physical parameters
6. Microbial sampling including flow cytometry and epifluorescence microscopy

Full details of the methods used are found in Douglas et al. (2012).

6.4.3 Results

6.4.3.1 Mullaloo Aquifer sediment mineralogy

The unfractionated sediment results indicate a predominance of quartz (90->99%) at all depths sampled within the Mullaloo Aquifer. The greatest mineralogical variability occurs within the uppermost sample at 51 m with carbonates, principally calcite and minor dolomite, K-feldspar, rutile, pyrite and kaolinite also present. Within the deepest sample at 120 m, 1% pyrite and minor kaolinite is also present.

A magnetic mineral separate from 51 m depth shows the presence of quartz (suggesting the presence of magnetic inclusions therein), ilmenite, rutile and pseudorutile with minor peaks indicating mica and kaolin. A qualitative XRF scan was performed on this sample and it showed a small Cr peak, and in the absence of a Cr-spinel, indicating possible substitution of Cr for Fe in ilmenite or possibly pseudorutile.

6.4.3.2 Petrographic findings

Petrographic analysis of four Mullaloo Aquifer sediment samples via optical microscopy revealed a general increase in clast grain size with depth with the majority of quartz grains, as the predominant mineralogical component, 0.2-1.0 mm along longest axis in upper samples and 1.0-2.0 mm along longest axis in lower samples and sub- to well-rounded (Figure 6.16). Few, if any groundmass minerals are generally present. The Mullaloo Aquifer sediments are moderately to well sorted. In general, there is also a more even grain size distribution with depth, and absence of smaller, often less rounded quartz grains. Monocrystalline quartz grains predominate, however, polycrystalline quartz grains may be present, particularly at depth (see cross-polarised images, 111 m and 120 m depth, Figure 6.16).

Minor, often irregular, embayments are often present in larger quartz grains at depth that also frequently host the thickest accumulations of armouring minerals, principally Fe-oxyhydroxides. Minor carbonate grains are evident, particularly at 51 m depth. Occasional opaque to semi-opaque, irregularly-shaped organic particles (macerals) are present, particularly in upper samples (Figure 6.16). Similarly, minor blocky opaque minerals, typically 0.1 mm in size are present at most depth. Minor rock fragments are also present, particularly in upper samples; however, there is little evidence of discrete clay minerals.

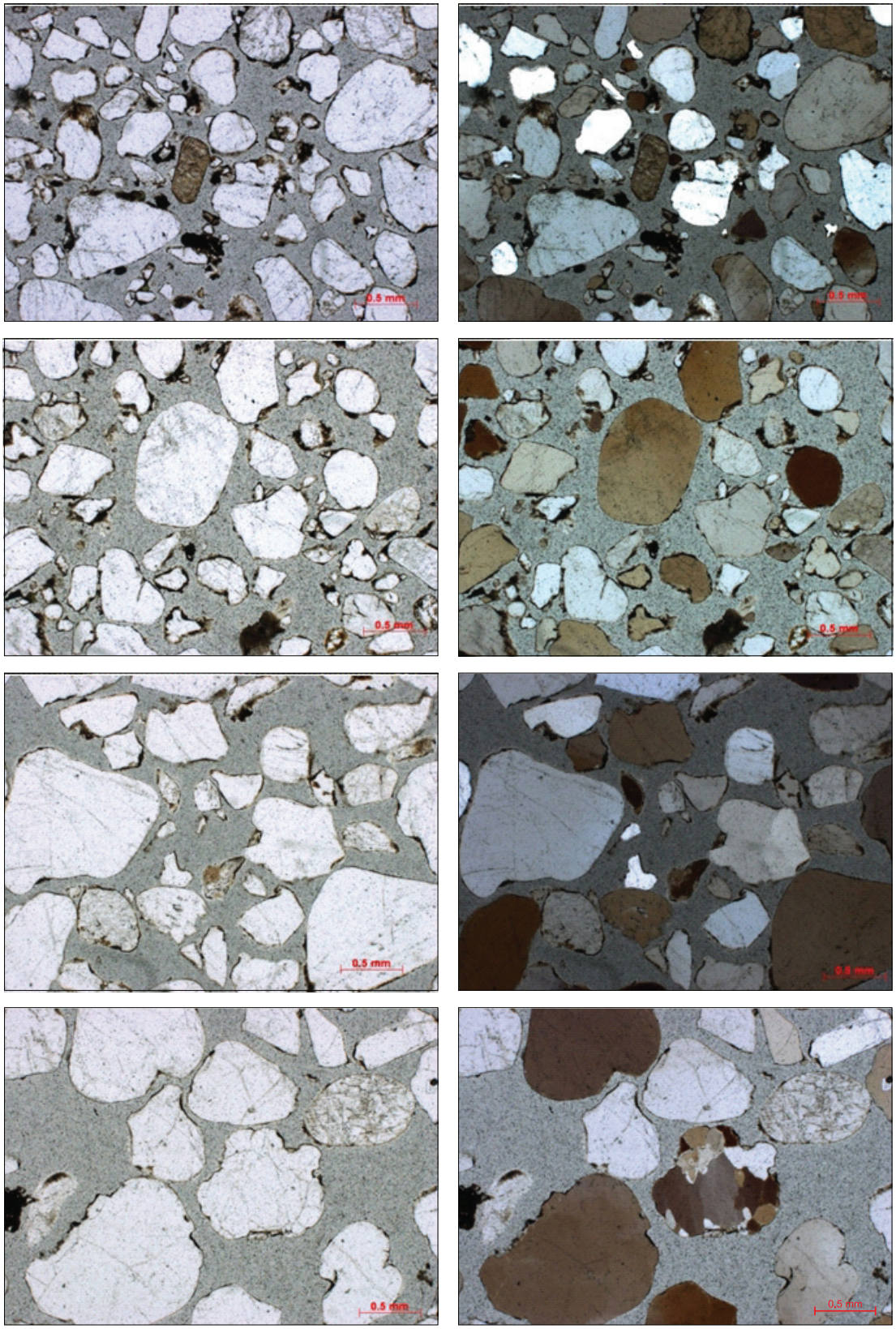

Figure 6.16: Thin section photomicrographs of epoxy grain mounts of Mullaloo Aquifer sediment at 51, 54, 111, and 120 m below ground surface. Images taken in plane-polarized light and crossed-polarized light, respectively.

6.4.3.3 Mullaloo Aquifer sediment geochemistry

Major element geochemical analysis of Mullaloo Aquifer sediments from depths 51, 70, 90, 99, 105, 111, 114, 120 and 126 m below ground level reveal a predominantly siliceous composition (ca. 87-99 wt % SiO_2) in accordance with the high quartz concentration identified in mineralogical analyses (Figure 6.17). Thus, most other major elements (expressed as wt % oxides) are relatively impoverished with only low maximum concentrations of TiO_2 (0.11 wt %), Al_2O_3 (0.84 wt %), Fe_2O_3 (1.24 wt%), MnO (0.015 wt %) MgO (0.13 wt%), Na_2O (0.09 wt %) and K_2O (0.25 wt %) that are associated with heavy minerals and/or clay minerals, predominantly in the uppermost sediment sample (51 m). The only exception is CaO (5.88 wt %), which is associated with the presence of carbonate minerals, principally calcite as indentified in mineralogical analysis, in the uppermost (51 m). Maximum concentrations of both P_2O_5 (0.038 wt %) and SO_3 (0.85 wt %) are low.

Trace element concentrations are in general low within the Mullaloo Aquifer sediments, given the predominance of quartz/SiO_2 (Figure 6.17). Thus a range of elements including Cd, Co, Cu, Ga, Ge, Mo, Nb, Ni, Pb, Sc, Sm, Th, Tl and U are predominantly below or near analytical detection limits for most, if not all, aquifer sediment samples. The highest concentrations of Ba (74 µg/g), and Sr (32 µg/g) are both associated with clay and/or carbonates in the uppermost two sediment samples. Noteworthy, however, are consistently elevated concentrations of Cr (144 - 513 µg/g) and other trace elements including V (9 – 56 µg/g) and Zr (32-53 µg/g).

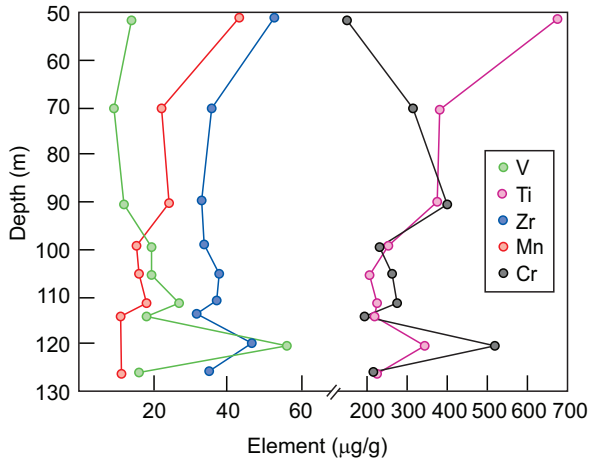

Figure 6.17: Thin section photomicrographs of epoxy grain mounts of Mullaloo Aquifer sediment at 51, 54, 111, and 120 m below ground surface. Images taken in plane-polarized light and crossed-polarized light, respectively.

6.4.3.4 Mullaloo Aquifer water quality

Mullaloo groundwater pH collected in the present study is generally circum-neutral to slightly acidic. The aquifer waters are predominantly of a Na-Cl type with major cations dominated by Na with lower concentrations of Ca and Mg. Major anions are dominated by Cl with lower concentrations of HCO_3^- and SO_4^{2-}. The aquifer waters are of low ionic strength with TDS <400 mg/L^{-1}.

Trace element concentrations are generally low, and depending on the sample, 6-11 of the 25 analytes were below detection limits. No trace elements exceed the ANZECC Water Quality Guidelines (ANZECC, 2000). Nutrient concentrations were mildly elevated, particularly for nitrate (2-9-12 mg/L^{-1}). Filterable P in one sample from 120 m depth was also elevated (1.5 mg/L^{-1}). The nutrients will support microbial growth

6.4.3.5 Organic contaminants and Dissolved Organic Carbon (DOC)

An analysis of the three groundwater samples collected in this present study indicate that all classes of organic contaminants including BTEX and TPH are below detection limits. Dissolved organic carbon, expressed as non-particulate organic carbon showed considerable variability of between 10 and 34 mg/L^{-1} for replicate samples from the deepest sample from 114, 120 and 126 m. An intermediate sample from 97 m and 108 m also varied from <1 to 12 mg/L^{-1}.

6.4.3.6 Microbial biomass

The cell counts obtained by flow cytometry for the deep and intermediate samples were lower than the background values obtained for the filtered control samples. Only the shallow sample gave a cell count $3*10^5$ cells mL^{-1} that was above the background value (2*105 cells mL^{-1}) of that sample.

The cell counts obtained by epifluorescence microscopy for the aquifer samples were 1.4*105 – 5.2*105 cells mL^{-1}. The cell counts were highest in the deepest sample and lowest in the shallowest sample. The cell counts were in the same range as observed by epifluorescence microscopy for the groundwater in the deep geothermal aquifer of the Great Artesian Basin (GAB), in Australia (105 – 106 cells mL^{-1}) (Kimura et al., 2005) and the deep coal seam groundwaters of northern Japan (3.08*105 cells mL^{-1} – 9.88*105 cells mL^{-1}) (Shimizu et al., 2007). Cell counts reported for groundwaters in Virginia have been in the range of 4*104 – 1.2*105 cells mL^{-1} (King and Parker, 1988) and those in the groundwaters of ultraoligotrophic alpine springs in the range of 104 –105 cells mL^{-1} (Farnleitner et al., 2005; Wilhartitz et al., 2007). An example of an epifluorescence microscope image of DAPI stained cells from the intermediate aquifer sample is shown in Figure 6.18.

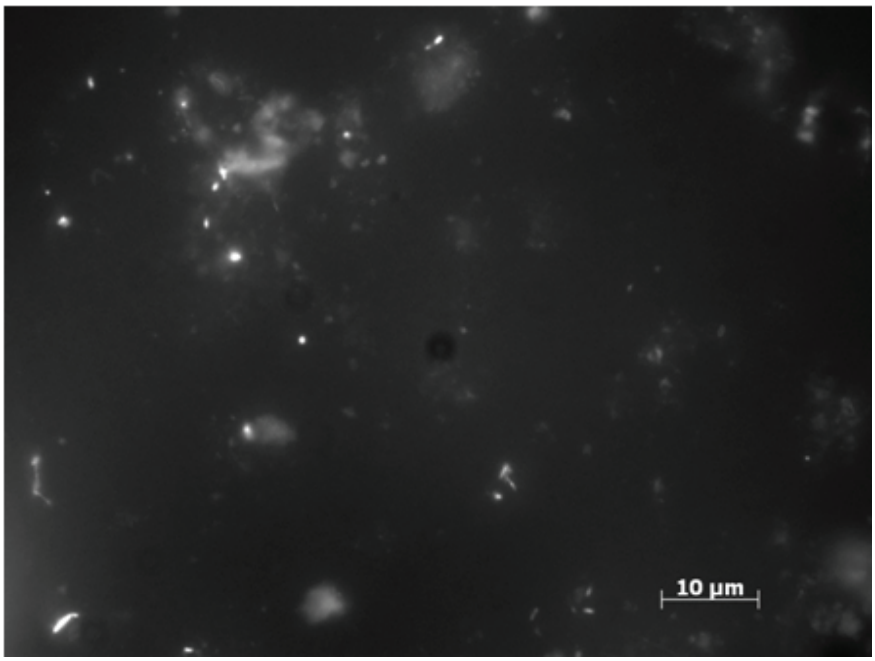

Figure 6.18: Epifluorescence microscope image of DAPI-stained aquifer cells from the intermediate sampling point.

6.4.4 Discussion

6.4.4.1 Stratigraphic variation

The limited down hole major and trace element and mineralogical variation (Figure 6.17) reflects the uniformity of the stratigraphy within the sampled horizons of the Mullaloo Aquifer sediments. It is only within the uppermost two horizons that the presence of calcite and minor dolomite increases the CaO concentration and clay that increases the Al_2O_3 and Fe_2O_3, and to a lesser extent MgO, Na_2O and K_2O concentrations, results in a dilution of quartz abundance, and hence, SiO_2. Similar major element concentration variations also occur due to mineralogical changes, albeit to a lesser extent, further downhole at 120 m, notably due to the presence of minor pyrite contributions. It is noteworthy that no glauconite was identified in the Mullaloo Aquifer samples despite it being noted in a previous study (Davidson, 1995).

Trace element concentrations also occur within the Mullaloo Aquifer with a remarkably consistent pattern of stratigraphic (down hole) variation for V, Ti, Zr, Mn and Cr (Figure 6.17). In the absence of the uppermost, carbonate and most clay-rich sample, similar stratigraphic relationship is present between Cr and Fe ($r^2 = 0.82$), Ti ($r^2 = 0.54$), Zr ($r^2 = 0.55$) and V ($r^2 = 0.43$) attesting to a general relationship between these elements and the intermittent presence of a heavy mineral fraction as identified during heavy mineral separation, notably the likely presence of Cr-bearing ilmenite, and although not identified, possibly chromite, and other heavy minerals such as ilmenite ($FeTiO_3$) and zircon ($ZrSiO_4$), the latter two minerals in particular common in coastal sands of the Swan Coastal Plain (Gozzard, 2007). Interestingly, the abundance of quartz within the magnetic mineral separates suggests that many of the magnetic minerals are present as inclusions within discrete quartz grains.

Extensive, long-term weathering within the Yilgarn Craton, particularly since the Tertiary, has resulted in the concentration of a range of heavy minerals derived predominantly from mafic/ultramafic lithologies (Anand and Paine, 2002, Cornelius et al., 2008). The heavy minerals then accumulated in sandy sediments of the Swan Coastal Plain (Bastian, 1996, Collins and Baxter, 1984). Heavy minerals such as chromite, magnetite and ilmenite, sometimes present as intergrowths (Groves et al., 1977) have long been recognised as abundant in the Western Australian regolith, and in particular mafic/ultramafic regions of the Yilgarn (Simpson, 1912), while chromium-bearing ilmenites in beach sand deposits in south western, Western Australia have also been observed (O'Shaughnessy, 1973).

Within the Mullaloo Aquifer sediments, intermittently enriched Fe in the absence of a significant clay component, and a corresponding enrichment of S indicate the possible presence of pyrite, a common accessory mineral in both superficial (e.g. Bassendean Sand, Yesertener, 2010) and deep (Leederville Formation, Descourvieres et al., 2010) aquifer sediments of the Swan Coastal Plain. The specific presence of pyrite within the deeper portion of the Mullaloo Aquifer has also been confirmed by XRD analysis (Douglas et al., 2012). An analysis of the variation of Fe/S molar ratios with S (wt %) indicates that as the latter increase, Fe/S molar ratio approaches unity in accordance with the presence of pyrite (Figure 6.19). In-situ down hole measurements of Eh with borehole MB04a indicate increasingly reducing conditions with depth (Rockwater, 2011c), again consistent with the presence of pyrite.

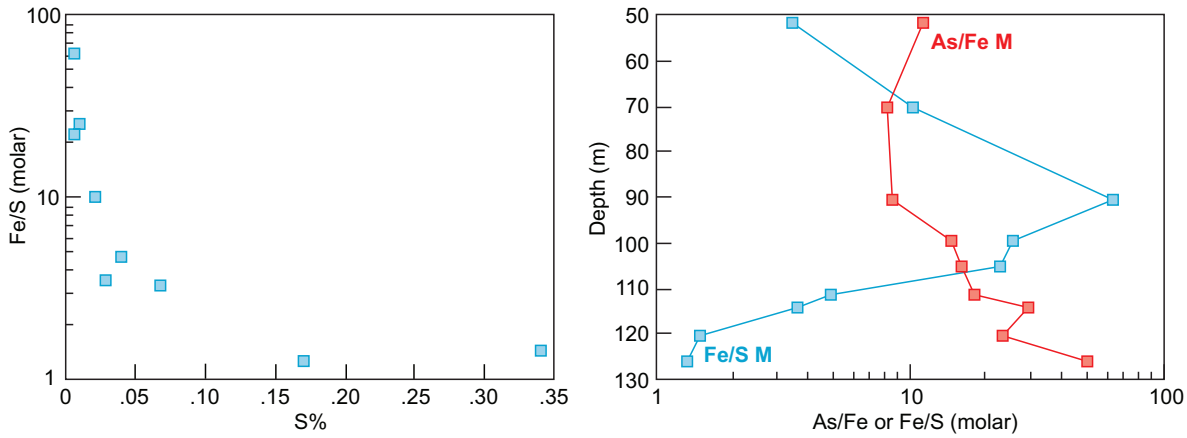

Figure 6.19: Geochemical relationships between Fe/S (molar) and S (wt %), depth and As/Fe (molar) and Fe/S (molar).

The presence of significant pyrite at 120 m depth in the Mullaloo Aquifer also corresponds to an increase in As concentrations (Figure 6.19). The presence of As-bearing pyrite is common across the Swan Coastal Plain (e.g. Appleyard et al., 2006, Yesertener, 2010), particularly within the superficial aquifer dominated by the Bassendean Sands.

In terms of major element geochemistry, the average Mullaloo Aquifer sediment most closely resembles the Bassendean Sand which forms the superficial aquifer at borehole MB04a. Similarly, most trace elements, including average Cr concentrations, are similar between the Mullaloo Aquifer sediments and those of the Bassendean Sand.

By comparison to average Mullaloo Aquifer sediments, regional aquifer sediments from the Osborne and Leederville Formations and South Perth Shale and Baigup soils and Swan River sediment encompass a range of major and trace element concentrations that, due to their relatively low SiO2 concentrations are also substantially enriched. In particular these regional aquifer and riverine soils and sediments are more clay-rich, and hence, also enriched often by one- to two-orders of magnitude in both alkali and alkaline earth element oxides/elements such as CaO, MgO, Na_2O, K_2O, Ba, Rb, Sr, in addition to transition metals (Cd, Cu, Ni, Pb, V, Zn) rare earth elements (e.g. La, Ce and Nd), and actinides (Th, U).

Comparison to the Post-Archean Australian Shale, an estimate of average crustal abundances (Taylor and McLennan, 1985), also suggests that apart from Cr, the average Mullaloo Aquifer sediments are, by virtue of SiO_2 (quartz) enrichment, comparatively impoverished for a range of major and trace elements.

6.4.4.2 Mullaloo Aquifer groundwater composition.

The major composition of the Mullaloo Aquifer groundwater is consistent with derivation from a seawater-Perth rainwater signature with minor modification due to water-rock interaction (e.g. carbonate or clay mineral equilibration) as evidenced by variable concentrations of bicarbonate and

silica respectively. The Mullaloo Aquifer major ion composition is also similar to that of average Perth shallow groundwater (Perth SGW – n=103, after Yesertener, 2010) and that of the superficial aquifer.

Speciation modelling of Fe in the Mullaloo Aquifer samples collected in this study is in general agreement with results of mineral stability modelling (as saturation indices) confirming that the majority of Fe is present as Fe-oxyhydroxide minerals. Groundwater samples previously collected by Rockwater also suggest the possible presence of siderite in more alkaline samples. While pyrite formation is not immediately suggested on the basis of recent Mullaloo Aquifer groundwater sampling and Eh-pH monitoring, only a small decline in Eh/pe is nonetheless required to produce conditions conducive to pyritisation, particularly in the presence of sulfate-reducing bacteria known to occur in Swan Coastal Plain sediments (e.g. Robertson et al., 2000, 2001).

Trace element concentrations are often low and are consistent with the predominantly circum-neutral pH and the present of abundant Fe-oxyhydroxides present as coatings on the majority of quartz grains which would be likely to act as sinks for metals. Nutrient concentrations are within ranges commonly encountered in Perth superficial aquifers (e.g. Bennett et al., 2007; Yesertener, 2010; Sarukkalige, 2011).

6.4.4.3 Microbial substrate and nutrient concentrations

A set of threshold values for biological and chemical clogging are shown in Table 6.2 and Table 6.3 shows guidelines for clogging and redevelopment of aquifers (adapted from Pérez-Paricio, 2000). Apart from the deepest aquifer samples obtained from 114-126 m of the Mullaloo Aquifer, the DOC levels were above the threshold value for bioclogging in deep systems (< 2 mg L^{-1}) (Table 6.2). The TDS was above the threshold limit for chemical clogging in all samples. Ferrous iron concentrations were below the threshold in most samples, except for one sample obtained by Rockwater (2011c). According to the TOC-based guidelines presented in Table 6.3 and the observed DOC results for Mullaloo Aquifer, the water quality in the deepest samples indicate a slight tendency for bioclogging, whereas the shallowest samples indicate a notable or strong tendency for bioclogging. However, it is to be noted that the transformation of natural organic matter (NOM) and microbial growth during artificial groundwater recharge is dependent on a number of site specific and operational factors. Guidelines for the redevelopment of aquifers to prevent clogging are given in Table 6.3.

Concept		Parameter	Limitations	Range in Mullaloo aquifer
Biological clogging	Deep systems	pH DOC Eh	>7.2(iron bacteria) <2 mg L^{-1} >10 mV	6.58-6.99 <1-34 mg L^{-1} 192-392
	Surface systems	TOC	TOC < 10 mg L^{-1}	<1-34 mg L^{-1} (DOC)
Chemical clogging		[Fe^{2+}] pH TDS [Cl^-]	<11.2 mg L^{-1} <7.5 <150 mg L^{-1} <500 mg L^{-1}	0.1-15 mg L^{-1} 6.58-6.99 300-380 78-250

Table 6.2: Recommended values for water quality parameters (adapted from Pérez-Paricio, 2000) and observed range in Mullaloo Aquifer.

	Clogging	Recharge water	Redevelopment
Surface systems	Slight	TOC <10 mg L^{-1}	Natural drying and cracking Once a year mechanical
	Notable	TOC =10-25 mg L^{-1}	Frequent drying and cracking Twice a year mechanical
	Strong	TOC >25 mg L^{-1}	Prefiltration recommended
Deep systems	Slight	TOC <10 mg L^{-1}	Frequent pumping Once a month surging/jetting
	Notable	TOC = 10-25 mg L^{-1}	Pumping once a day Once a week surging/jetting
	Strong	TOC >25 mg L^{-1}	Daily pumping Adapted protocol

Table 6.3: Guidelines for clogging and redevelopment based on TOC (adapted from Pérez-Paricio, 2000).

6.4.4.4 Effect of increased temperature on Mullaloo Aquifer geochemistry

Geochemical modelling of the groundwater geochemistry indicates that subtle changes in mineral solubility occur as a function of increasing temperature (Figure 6.20). Similarly, groundwater pH only marginally declines by ca. 0.1 pH from ca. 6.75 to 6.65 over the 30 °C temperature increment modelled in this study. This potential pH change is likely to be well within the natural pH variation of fluids within the greater Mullaloo Aquifer. Lower temperature changes are predicted to result in even smaller perturbations to the solubilities of dominant mineral phases and the pH (see the shaded zone in Figure 6.20 corresponding to a ΔT of 10 °C).

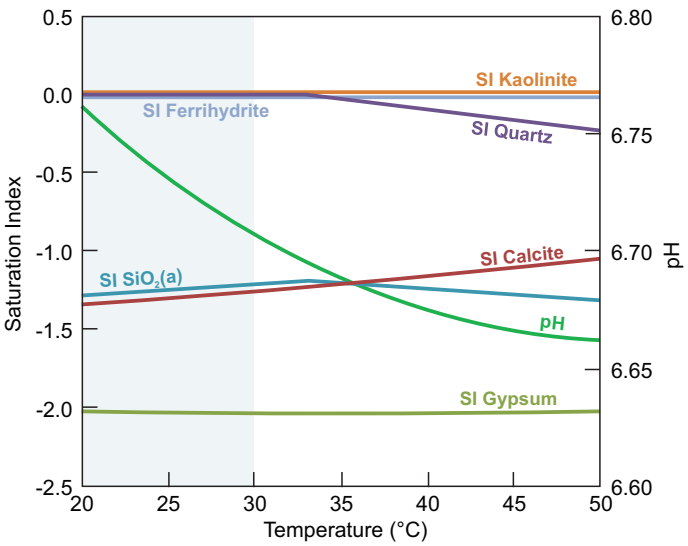

Figure 6.20: Saturation Indices of Mullaloo Aquifer minerals and groundwater pH as a function of temperature from 20 to 50 °C. An average groundwater composition from the three CSIRO samples was used in the model. The forecast range of temperature increase in the Mullaloo Aquifer due to the return of heated groundwater (ΔT = 10 °C) is shaded.

Mineral dissolution rates may be both enhanced and suppressed with changes in ambient temperature (e.g. Aagaard and Helgeson, 1982). Within the Mullaloo Aquifer, modelled mineral solubilities only display small changes in solubility as a function of temperature. In particular, quartz, which is at equilibrium with the prevailing groundwater, and amorphous silica, albeit the latter already undersaturated, display a small increase in predicted solubility (as saturation index), particularly over ca. 35 °C (Figure 6.20). Given that predicted temperatures of returned water are unlikely to exceed 30 °C, it is unlikely that any discernible change would occur in terms of quartz

dissolution or concomitant groundwater composition. Furthermore, the modelling conducted here only considers thermodynamics in terms of the saturation index, and does not include a kinetic term. Many studies conducted on quartz dissolution, however, indicate that rates of crystalline quartz dissolution are exceedingly slow (ca. 10^{-16} mol cm^{-2} s^{-1}, Brady and Walther, 1990), particularly in freshwaters, with minimum dissolution rates at solution pH of ca. 4-6, similar to that of the prevailing Mullaloo Aquifer groundwater. Similarly temperature increase from ca. 20 to 30 °C as envisaged in the Mullaloo Aquifer will be unlikely to significantly enhance dissolution rates of ambient dissolved Si concentrations. Also, mixing with incumbent groundwater upon return to the Mullaloo Aquifer is likely to quickly decrease temperature such that changes to solute composition from mineral dissolution, already small, will be negligible on a more widespread basis. A further barrier to any potential quartz dissolution is the armouring of part of or entire quartz grains by Fe-oxyhydroxides. This armouring is likely to provide an additional physico-chemical barrier to dissolution.

In contrast, calcite, present as a minor mineral, particularly within the upper Mullaloo Aquifer displays a small decrease on solubility similar to that observed in other studies (e.g. Kuhn et al., 2002). Nonetheless, calcite remains over an order of magnitude undersaturated and thus, the groundwater composition will remain essentially unaffected. Gypsum remains strongly undersaturated over the entire temperature range.

Both ferrihydrite (as a proxy for a range of Fe-hydroxides/oxyhydroxides) and kaolinite (partially obscured) both remain in equilibrium (SI = 0) with the prevailing groundwater over the entire temperature range. Thus, it is unlikely that trace elements associated with these contaminants will be mobilised during any increase in groundwater temperature.

6.4.5 Summary

A multi-disciplinary protocol suitable for rapid assessment of the biogeochemical impacts of geothermal operations has been undertaken to assess the potential suitability of the Mullaloo Aquifer to receive heated water generated from the Pawsey Supercomputer (Douglas et al., 2012). The component of the study encompassing a geochemical analysis of the aquifer sediment has yielded the following information:

Sediment mineralogy and petrography - The Mullaloo Aquifer sediments constitute a mature, moderately well sorted, quartz-dominated, possibly shallow marine unit. Minor discrete carbonate and organic matter occurs in the uppermost stratigraphy. In addition, minor heavy minerals dominated by ilmenite occur throughout the stratigraphy, and pyrite is present at depth.

Sediment geochemistry - Aquifer sediments are quartz-dominated, however, significant amounts of calcite and pyrite are present in the shallowest and deepest samples, respectively. Concentrations of trace elements are generally low, however, there are significant enrichments of Cr, that is likely to occur within ilmenite or other heavy minerals present within the aquifer. Significant arsenic is also present, principally associated with pyrite within the deep aquifer.

Groundwater geochemistry - The groundwater geochemistry is of an Na-Cl type with circum-neutral

to moderately alkaline pH, intermediate redox potential (Eh/pe), and low ionic strength with TDS <400 mg/L. Trace element abundances are low and are likely to remain stable under prevailing conditions. Aquifer water quality meets ANZECC drinking water quality guidelines. No BTEX or petroleum hydrocarbons were detected.

Microbiology - Cell counts showed abundances highest in the deepest sample and lowest in the shallowest sample. The cell counts were in the same range as observed by epifluorescence microscopy for the groundwater in a range of local and international locations corresponding to oligotrophic conditions. Dissolved organic carbon, nitrogen and phosphorus are present in the groundwater, which may promote population growth if electron acceptor concentrations increase. According to the TOC-based guidelines and the observed DOC results for Mullaloo Aquifer, the water quality in the deepest samples indicate slight tendency for bioclogging, whereas the shallowest samples indicate notable or strong tendency for bioclogging. As long as electron acceptors are prevented from entering the system, it is likely that microbial population levels will not significantly change, although abundances of the various microbial species comprising the population may vary. Additional sampling and analysis would be required to predict such changes at the species level.

Geochemical modelling - Geochemical modelling indicates there are few, if any adverse implications of increased temperatures on the geochemistry of the Mullaloo Aquifer, assuming the reinjected water does not introduce external reagents (e.g. oxygen). If temperature increases are limited to approximately 10 °C as proposed, it is unlikely that any material change to aquifer geochemistry will occur.

Recommendations - Based on the information obtained in this study a number of operational recommendations can be made for heat rejection operations at the Pawsey site.

- The presence of pyrite within the deeper aquifer in particular signifies the potential for oxidation, acid generation and release of arsenic and potentially other metal/metalloid contaminants. Thus, it is recommended that withdrawal and return of water be confined to a zone sufficiently above pyrite-bearing stratigraphy. In addition, it is recommended that a closed loop configuration be utilised such that anthropogenic oxygen is not introduced into the Mullaloo Aquifer.
- Additional analysis of aquifer sediments be undertaken to confirm the absence of pyrite-bearing stratigraphy prior to operation of any wells.
- Groundwater sampling and analysis should occur monthly during the first year of operation, and at appropriate intervals thereafter, to monitor changes, if any, in groundwater geochemistry and microbiology.

6.5 Conclusions

This section has introduced innovative concepts for characterizing and managing shallow geothermal reservoirs, especially within the hot sedimentary aquifer context. The innovations include stochastic theories useful for estimating moments and integral scales of the reservoir spatial permeability

field, which are crucial in determining the dispersion of heat and solutes within the reservoir. The potential solutes of interest that can be mobilized by thermal perturbations can be identified by application of the rapid biogeochemical assessment protocol discussed in this section. An example application of this protocol to the shallow, cool Mullaloo Aquifer in the context of low grade heat rejection showed that this particular aquifer was likely to accept up to 10 °C or more with minimal biogeochemical disturbance, so long as the rejected heat was delivered via an anoxic flow. Finally, efficient management of the heat exchange process in geothermal production can be boosted by the subsurface stirring technology discussed in this section. Whilst still to be trialled in the field, this technology has shown promising results in 10 cm-scale and metre-scale laboratory experiments.

7. CONCLUDING REMARKS

7.1 Synthesis of research outcomes

This report lays a foundation for Hot Sedimentary Aquifer reservoir engineering in Western Australia. Through a mixture of theoretical, experimental and field reservoir studies, this report provides geothermal specialists with a range of tools, analyses and research innovations for the modern HSA context.

Geothermal reservoir engineering is a truly multidisciplinary field. In this report we have demonstrated the value of combining geology, geophysics, petrophysics, hydrogeology, geochemistry, geomicrobiology and fluid dynamics to elucidate reservoir characteristics and behaviour.

Two integrated modelling studies were carried out in the Canning and the Perth Basins using existing and publicly available data. The Canning Basin study evaluated the geothermal potential for the direct use of geothermal resources by taking into account the local geology, hydrogeology and the thermal characterization of the aquifer.

The Perth Basin study pioneered an innovative, coupled stratigraphic forward modelling and reservoir engineering workflow for exploration of new direct use applications in the Perth Metropolitan Area. This study linked a complex geological description of the Perth Basin to geothermal direct-use requirements to identify target locations for potential geothermal projects. An example application for geothermally powered air conditioning systems in the Perth Metropolitan Area is presented.

WAGCoE developed the GeoTemp™ software to assist temperature data processing, interpretation and modelling for geothermal exploration applications. This software was used extensively for several temperature measurement analyses presented in this report.

The acquisition, processing and interpretation of temperature measurements in artesian monitoring wells was carried out and provided an extensive database of shallow temperature data for the Perth Metropolitan Area. A complementary study confirmed the presence of a low temperature anomaly at the Gnangara Mound which represents an ideal target for heat rejection applications.

Aside from existing temperature measurements, geothermal exploration requires the understanding of the temperature distribution in the subsurface. Regional analysis of deep temperature measurements in the Perth Basin shows that temperatures at 3000 m vary between 80 and 100 °C, representing a good target for direct use geothermal applications. Correction of the temperature data indicates that there are 2 to 5 °C km^{-1} uncertainties on estimates of the thermal gradient, which may impact on geothermal resource evaluations. This study also shows that high temperature gradients are associated with high uncertainties in the North Perth Basin.

Detailed reservoir characteristics of Perth Metropolitan Area geothermal projects have been investigated via the M345 Aquifer Storage and Recovery project being run by Water Corporation of Western Australia. The results concluded that the vertical heterogeneity of the reservoir was playing a large role in the fine-scale thermal equilibration and sustainability of geothermal projects.

The development of geothermal projects involves the anticipation of well and reservoir conditions and the planning of data acquisition. WAGCoE contributed to the development of a large-scale direct-use geothermal application in conjunction with the SESKA project, and the Kensington 1 well.

An innovative approach to optimize the heat storage in the subsurface using stirring protocol was presented as a way to delay the thermal breakthrough but also to contain the thermal storage within a particular zone. This technology is the subject of an international patent application, with a wide range of potential applications, including geothermics, in situ mining, and groundwater remediation.

A rapid biogeochemical assessment protocol was developed and tested for the deployment of thermal energy storage projects. This protocol investigates the suitability and the long-term environmental sustainability of those projects by considering the potential for in situ geochemical disturbances from temperature perturbations, e.g. from waste heat injection. The rapid protocol was tested in the field at the Pawsey Supercomputer Centre site.

The research conducted in the WAGCoE Reservoir productivity and sustainability project was applied to a range of geothermal prospects and existing projects in Western Australia (e,g Canning Basin, Perth Basin, Perth Metropolitan Area, Gnangara Mound, Kensington, M345 ASR project, SESKA Geothermal, etc).

7.2 Future directions

As described in this report, geothermal exploration for direct-use applications in Hot Sedimentary Aquifer requires an accurate resource characterization consistent with desired direct-use applications. Resource evaluation is highly dependent on the temperature estimates for the reservoir and also on the achievable flow rate. While researchers in the oil and gas and groundwater industries have investigated fluid flow in porous media for decades, temperature and heat transfer remains poorly constrained. Accurate temperature predictions require joint-interpretation of geology, hydrogeology and geophysical observations. This not only requires new measurements but also necessitate new data interpretation methods that take into account the various different heat transfer mechanisms. Quantitative understandings of heat flow mechanism are prerequisites to any modelling study.

The exploitation of direct-use HSA reservoirs requires specific field development strategies based on the diverse nature of the direct-use plant requirements. Moreover, with the concept of “geothermal cities” involving multiple cascading thermal technologies gaining ground, the future optimization of energy extraction requires the combination of various applications at the surface with specific, purpose-built designs for the extraction and injection sites. This innovation process will require the development of new tools, and new analytical and numerical methods to achieve success.

The sustainability and optimization objectives of geothermal reservoir management in sedimentary basins require a deeper characterization of the reservoir. The sustainability of HSA geothermal projects has too often been regarded to be determined by simple thermal breakthrough criteria, but the real issues are the thermal power threshold and the required working temperature of the surface infrastructure. The impact of reservoir recharge and discharge has been poorly investigated

and further work must be done to understand biogeochemical impacts on plant, pipework and on the reservoir formation itself.

Exploration and exploitation of geothermal projects requires a risk assessment framework from the definition of a direct-use geothermal risk down to the actual drivers of this risk (e.g. the faulting compartmentalization, the heterogeneity of the reservoir, geochemistry, well location etc) and ways to mitigate the risk (e.g. measurement acquisition, new interpretation of existing datasets, modelling studies) and plan for contingencies.

REFERENCES

Aargard, P. and Helgeson, H.C. (1982). Thermodynamic and kinetic constraints on reaction rates among minerals and aqueous solutions. I. Theoretical considerations. American Journal of Science, 282, 237-285.

Abdulagatova, Z., Abdulagatov, I. and Emirov, V., (2009). Effect of temperature and pressure on the thermal conductivity of sandstone. International Journal of Rock Mechanics and Mining Sciences, 46(6), 1055-1071.

AGRCC. (2010). The Geothermal Reporting Code. Australian Geothermal Energy Group (AGEC) and Australian Geothermal Energy Association (AGEA): Adelaide, SA, Australia:.

Alcolea, A., Renard, P., Mariethoz, G. and Bertone, F. (2009). Reducing the impact of a desalination plant using stochastic modeling and optimization techniques. Journal of Hydrology, 365, 275-288.

Alkan, H. and Satman, A. (1990). A new lumped parameter model for geothermal reservoirs in the presence of carbon dioxide. Geothermics, 19, 469-479.

Anderson, M. P. (2005). Heat as a ground water tracer. Ground Water, 43, 951-968.

Anand, R.R. and Paine, M., (2002). Regolith geology of the Yilgarn Craton, Western Australia: implications for exploration. Australian Journal of Earth Sciences, 49, 3-162.

ANZECC, (2000). Australian and New Zealand Guidelines for Fresh and Marine Water Quality (2000). http://www.mincos.gov.au/publications/australian_and_new_zealand_guidelines_for_fresh_nnd_marine_water_quality

Appleyard, S. J., Angeloni, J. and Watkins, R. (2006). Arsenic-rich groundwater in an urban area experiencing drought and increasing population density, Perth, Australia. Applied Geochemistry, 21, 83-97.

Aref, H. (2002). The development of chaotic advection. Physics of Fluids, 14(4), 1315-1325, (doi:10.1063/1.1458932).

Arnol'd, V. I. (1963). Proof of a theorem of A. N. Kolmogorov on the preservation of conditionally periodic motions under a small perturbation of the Hamiltonian. Uspehi Matematicheskih Nauk 18, 13-40.

Arnol'd, V. (1965). Sur la topologie des ecoulements stationnaires des fluids parfaits. Comptes Rendus Hebdomadaires des Seances de l Academie des Sciences. 261, 17-20.

Banks, D. (2009a). An introduction to 'thermogeology' and the exploitation of ground source heat. Quarterly Journal of Engineering Geology and Hydrogeology, 42, 283-293.

Banks, D. (2009b). Thermogeological assessment of open-loop well-doublet schemes: A review and synthesis of analytical approaches. Hydrogeology Journal, 17, 1149-1155.

Bastian, L. V. (1996). Residual soil mineralogy and dune subdivision, Swan Coastal Plain, Western Australia. Australian Journal of Earth Sciences, 43, 31-44.

Bauer, R. D., Rolle, M., Bauer, S., Eberhardt, C., Grathwohl, P., Kolditz, O., Meckenstock, R. U. and Griebler, C. (2009). Enhanced biodegradation by hydraulic heterogeneities in petroleum hydrocarbon plumes. Journal of Contaminant Hydrology, 105(1-2), 56-68.

Bellin, A. and Rubin, Y. (1996). HYDRO_GEN: A new random field generator for correlated properties. Stochastic Hydrology and Hydraulics, 10(4), 253-278.

Bennett, D., Donnelly, P. and Tille, P. (2007). Assessment of the impact of intensification of grazing agriculture on nitrogen and phosphorus levels in the shallow aquifers of the Southern Perth Basin. Department of Agriculture and Food Resource Management, Technical Report 323.

Bertani, R. (2012). Geothermal power generation in the world 2005–2010 update report. Geothermics, 41, 1-29.

Bestow, T. (1982). The potential for geothermal energy development in Western Australia. Record 1982/6, Geological Survey of Western Australia, x+67pp.

Brady, P. V. and Walther, J. V. (1990). Kinetics of quartz dissolution at low temperatures. Chemical Geology, 82, 253-264.

Brigaud, F., Vasseur, G. and Caillet, G. (1989). Use of well log data for predicting detailed in situ thermal conductivity profiles at well sites and estimation of lateral changes in main sedimentary units at basin scale. Rock at great depth, Eds. Maury and Fourmaintraux, Rotterdam, A.A. Balkema. ISBN 90 6191 975 4, Vol.1, 403-409.

Brinkman, H. C. (1947). A calculation of the viscous force exerted by a flowing fluid on a dense swarm of particles. Journal of Applied Sciences Research, 1, 27-34.

Cacace, M., Kaiser, B. O., Lewerenz, B. and Scheck-Wenderoth, M. (2010). Geothermal energy in sedimentary basins: What we can learn from regional numerical models. Chemie der Erde – Geochemistry, 70, Supplement 3, 33-46.

Cadman, S. J., Pain, L. and Vuckovic, V. (1994). Perth Basin, WA. Australian Petroleum Accumulations Report 10. Canberra: Bureau of Resources Sciences.

Capuani, F., Frenkel, D. and Lowe, C. P. (2003). Velocity fluctuations and dispersion in a simple porous medium. Physical Review E 67, 056306. (doi:10.1103/PhysRevE.67.056306)

Cataldi, R., Hodgson, S. F. and Lund, J. W. (1999). Stories from a heated Earth. Geothermal Resources Council and International Geothermal Association, 569 pp.

Chopra, P. and Holgate, F. (2007). Geothermal Energy Potential in Selected Areas of Western Australia. P.O. Box 3972, Weston ACT 2611 Australia: Earthinsite.com.

Collins, L. B. and Baxter, J. L. (1984). Heavy mineral-bearing strandline deposits associated with high-energy beach environments, southern Perth Basin, Western Australia. Australian. Journal of Earth Sciences, 31, 287-292.

Corbel, S. and Poulet, T. (2010). WAGCoE data catalogue for geothermal exploration. Proceedings of 6th IEEE International Conference on e-Science. Brisbane, Australia, 89-94.

Corbel, S., Griffiths, C., Dyt, C. and Ricard, L. P. (2011). Using stratigraphic forward modelling to characterise and identify geothermal reservoirs. In: Budd, A. R. (ed.) Australian Geothermal Energy Conference. Melbourne: Geoscience Australia.

Corbel, S., Reid, L. B. and Ricard, L. P. (2011). Prefeasibility geothermal exploration workflow applied to the Fitzroy Trough, Western Australia. In: Middleton, M. & Gessner, K. (eds.) Western Australian Geothermal Energy Symposium. Perth, Western Australia, 25.

Corbel, S., Griffiths, C., Dyt, C. and Ricard, L. P. (2012). Hot sedimentary aquifer characterization using stratigraphic forward modelling, Perth Basin, Australia. Proceedings of Thirty-Seventh Workshop on Geothermal Reservoir Engineering. Stanford University, Stanford, California.

Cornelius, M., Robertson, I. D. M., Cornelius, A. J. and Morris, P. A. (2008). Geochemical mapping of the deeply weathered western Yilgarn Craton of Western Australia, using laterite geochemistry. Geochemistry: Exploration, Environment, Analysis, 8, 241-254.

Corry, D. and Brown, C. (1998). Temperature and heat flow in the Celtic Sea basins. Petroleum Geoscience 4, 317-326.

Côté, J. and Konrad, J. (2009). Assessment of structure effects on the thermal conductivity of two-phase porous geomaterials. International Journal of Heat and Mass Transfer 52(3-4), 796-804.

Crostella, A. and Backhouse, J. (2000). Geology and petroleum exploration of the central and southern Perth Basin, Western Australia. Report 57, Geological Survey of Western Australia, vi+87pp.

CSIRO. (2007). PressurePlot. http://www.pressureplot.com

Darcy, H. (1856). Les Fontaines Publiques de la Ville de Dijon. Paris: Dalmont.

Davidson, W. and Yu, X. (2008). Perth regional aquifer modelling system (PRAMS) model development: Hydrogeology and groundwater modelling. Perth, Western Australia: WA Department of Water.

Davidson, W. A. (1995). Hydrogeology and groundwater resources of the Perth Region, Western Australia. Bulletin 142, Geological Survey of Western Australia.

Delle Piane, C., Esteban, L., Timms, N., Israni, S. R., Pimienta, L., Evans, C. and McLarens, S. (2012). Physical properties of Cretaceous and Jurassic units of the Perth Basin, Western Australia. Implications for geothermal exploration, in preparation.

Descourvieres, C., Douglas, G., Leyland, L., Hartog, N. and Prommer, H. (2011). Compositional variation and chemical provenance signature of post-rift passive margin sediments of the early Cretaceous Leederville Formation in the Perth Basin, Western Australia. Sedimentary Geology, 226, 62-76.

DiPippo, R. (2007). Ideal thermal efficiency for geothermal binary plants. Geothermics, 36, 276-285.

Douglas, G. B., Trefry, M. G., Wylie, J., Wilkes, P. G., Puzon, G. J. and Kaksonen, A. H. (2012). Rapid biogeochemical assessment protocol for in situ heat rejection: the Mullaloo Aquifer, Perth, Western Australia, Western Australian Geothermal Centre of Excellence, Report EP12608, 36pp.

Farnleitner, A. H., Wilhartitz, I., Ryzinska, G., Kirschner, A. K. T., Stadler, H., Burtscher, M. M., Hornek, R., Szewzyk, U., Herndl, G. and Mach, R. L. (2005). Bacterial dynamics in spring water of alpine karst aquifers indicates the presence of stable autochthonous microbial endokarst communties. Environmental Microbiology, 7, 1248-1259.

Forster, A. (2001). Analysis of borehole temperature data in the Northeast German Basin: continuous logs versus bottom-hole temperatures. Petroleum Geoscience, 7, 241.

Fortin, J., Guéguen, Y. and Schubnel, A. (2007). Effects of pore collapse and grain crushing on ultrasonic velocities and vp/vs. Journal of Geophysical Research, 112 (B08207).

Freeze, R. A. (1994). Henry Darcy and the Fountains of Dijon. Ground Water, 32, 23–30.

Fridleifsson, I. B. (1998). Direct use of geothermal energy around the world. Geo-Heat Center Quarterly Bulletin, December 1998, 4-9.

Geointrepid. (2011). 3D Geological model building, and 3D temperature and heat flow calculation for the northern Perth Basin. Record 2011/6, Geological Survey of Western Australia. x+64pp.

Geological survey of western Australia and Petroleum Division (2004). Summary of petroleum prospectivity, onshore Western Australia and State waters 2004: Bonaparte, Canning, Officer, Perth, Southern Carnarvon and Northern Carnarvon Basins: Western Australia Geological Survey, 28p.

Giraud, A., Gruescu, C., Do, D., Homand, F. and Kondo, D. (2007). Effective thermal conductivity of transversely isotropic media with arbitrary oriented ellipsoidal inhomogeneities. International Journal of Solids and Structures, 44(9), 2627-2647.

Gomez, C. T., Dvorkin, J. and Vanorio, T. (2010). Laboratory measurements of porosity, permeability, resis- tivity, and velocity on fontainebleau sandstones. Geophysics. 75(6), E191.

Goutorbe, B., Lucazeau, F. and Bonneville, A. (2006). Using neural networks to predict thermal conductivity from geophysical well logs. Geophysical Journal International, 166, 115-125.

Gozzard, J. R. (2007). Geology and Landforms of the Perth Region. Western Australian Geological Survey, 126 pp.

Grant, M. A. and Bixley, P. F. (2011). Geothermal reservoir engineering - second edition. Burlington: Elsevier.

Gringarten, A. C. (1978). Reservoir lifetime and heat recovery factor in geothermal aquifers used for urban heating. Pure and Applied Geophysics 117, 297-308.

Gringarten, A. C. and Sauty, J. P. (1975). A theoretical study of heat extraction from aquifers with uniform regional flow. Journal of Geophysical Research. 80, 4956-4962.

Groves, D. I., Barrett, F. M., Binns, R. A. and McQueen, K. G. (1977). Spinel phases associated with metamorphosed volcanic-type iron-nickel sulfide ores from Western Australia. Economic Geology, 72, 1224-1244.

Gudmundsson, J.-S. (1988). The elements of direct uses. Geothermics, 17, 119-136.

Hamm, V. and Bazargan Sabet, B. (2010). Modelling of fluid flow and heat transfer to assess the geothermal potential of a flooded coal mine in Lorraine, France. Geothermics, 39, 177-186.

Hermanrud, C., Cao, S. and Lerche, I. (1990). Estimates of virgin rock temperature derived from BHT measurements: Bias and error. Geophysics, 55, 924.

Hoefel, D., Grooby, W. L., Monis, P. T., Andrews, S. and Saint, C. P. (2003). Enumeration of water-borne bacteria using viability assays and flow cytometry: a comparison to culture-based techniques. Journal of Microbiological Methods, 55, 585-597.

Holgate, F. and Chopra, P. (2005). Testing models for bottom-of-hole temperature recovery, Cooper Basin, South Australia. Exploration Geophysics 36, 272-280.

Horne, R. N. (1982). Geothermal reinjection experience in Japan. Journal of Petroleum Technology, 34, 495-503.

Hot Dry Rocks Pty Ltd. (2008). Geothermal energy potential in selected areas of Western Australia (Perth Basin). Department of Mines and Petroleum, Western Australia.

Hot Dry Rocks Pty Ltd. (2009). Geothermal energy potential in selected areas of Western Australia (Canning Basin). Department of Mines and Petroleum, Western Australia 83 pp.

Hot Dry Rocks Pty Ltd. (2010a). Geothermal Energy Potential in Selected Areas of Western Australia (Bonaparte Basin). Perth: Geological Survey of Western Australia, 70 pp.

Hot Dry Rocks Pty Ltd. (2010b). Geothermal Energy Potential in Selected Areas of Western Australia (Browse Basin). Perth: Geological Survey of Western Australia, 54 pp.

Hot Dry Rocks Pty Ltd. (2010c). Geothermal Energy Potential in Selected Areas of Western Australia (Carnarvon Basin). Perth: Geological Survey of Western Australia, 24 pp.

Hot Dry Rocks Pty Ltd. (2010d). Geothermal Energy Potential in Selected Areas of Western Australia (Officer Basin). Perth: Geological Survey of Western Australia, 101 pp.

Huenges, E. (Ed.) (2010). Geothermal energy systems - Exploration, development and utilization. Wiley-VCH:Weinheim, 463 pp, ISBN: 978-3-527-40831-3.

iVEC (2010). The Pawsey Centre.

http://www.ivec.org/sites/default/files/PAWSEY%20INFO%20SHEET%20SEPT2010.pdf

Kiryukhin, A. V. (1996). Modeling studies: The Dachny geothermal reservoir, Kamchatka, Russia. Geothermics, 25, 63-90.

Khaled, A.-R.A. and Vafai, K. (2003). The role of porous media in modeling flow and heat transfer in biological tissues. International Journal of Heat and Mass Transfer, 46, 4989-5003.

Kimura, H., Sugihara, M., Yamamoto, H., Patel, B.K.C., Kato, K. and Hanada, S. (2005). Microbial community in a geothermal aquifer associated with the subsurface of the Great Artesian Basin, Australia. Extremophiles, 9, 407-414.

King, L. K. and Parker, B. C. (1988). A simple, rapid method for enumerating total viable and metabolically active bacteria in groundwater. Applied Environmental Microbiology, 54, 1630-1631.

Kitanidis, P. (1994). The concept of a dilution index. Water Resources Research, 30(7), 2011-2026.

Kuhn, M., Bartels, J. and Iffland, J. (2002). Predicting reservoir property trends under heat exploitation: interaction between flow, heat transfer, transport, and chemical reactions in a deep aquifer at Strausland, Germany. Geothermics, 31, 725-749.

Lee, K. S. (2010). A Review on Concepts, Applications, and Models of Aquifer Thermal Energy Storage Systems. Energies, 3, 1320-1334.

Lester, D. R., Metcalfe, G., Trefry, M. G., Ord, A., Hobbs, B. and Rudman, M. (2009). Lagrangian topology of a periodically reoriented potential flow: Symmetry, optimization and mixing. Physical Review E, 80(3), Article 036208, doi:10.1103/PhysRevE.80.036208.

Lester, D. R., Rudman, M., Metcalfe, G., Trefry, M. G., Ord, A. and Hobbs, B. (2010). Scalar dispersion in a periodically reoriented potential flow: Acceleration via Lagrangian chaos. Physical Review E, 81(4), Article 046319, doi:10.1103/PhysRevE.81.046319.

Leyland, L. (2011). Hydrogeology of the Leederville Aquifer, central Perth Basin, Western Australia. University of Western Australia:Perth.

Lindal, B. (1973). Industrial and other applications of geothermal energy. In: Armstead, H. C. H. (ed.) Geothermal energy: review of research and development. Paris: Unesco.

Lund, J. W., Freeston, D. H. and Boyd, T. L. (2011). Direct utilization of geothermal energy 2010 worldwide review. Geothermics, 40, 159-180.

Lund, J. W., Lienau, P. J. and Lunis, B. C. (1998). Geothermal direct-use engineering and design guidebook. Third edition: Geo-Heat Center, Oregon Institute of Technology.

Lund, J. W., Sanner, B., Rybach, L., Curtis, R. and Hellstrom, G. (2004). Geothermal (Ground-source) heat pumps, a world review. Geo-Heat Center Quarterly Bulletin, September 2004, 1-10.

Luo, J., Wu, W.-M., Carley, J., Ruan, C., Gu, B., Jardine, P. M., Criddle, C. S. and Kitanidis, P. K. (2007). Hydraulic performance analysis of a multiple injection-extraction well system. Journal of Hydrology, 336(3-4), 294-302.

Manning, D. A. C., Younger, P. L., Smith, F. W., Jones, J. M., Dufton, D. J. and Diskin, S. (2007). A deep geothermal exploration well at Eastgate, Weardale, UK: a novel exploration concept for low-enthalpy resources. Journal of the Geological Society, 164, 371-382.

Metcalfe, G. (2010). Applied Fluid Chaos: Designing Advection with Periodically Reoriented Flows for Micro to Geophysical Mixing and Transport Enhancement, In Complex Physical, Biophysical, and Econophysical Systems, Robert L. Dewar and Frank Detering Ed.s, Lecture Notes in Complex Systems, World Scientific, vol. 9, pp 189—242.

Metcalfe, G., Rudman, M., Brydon, A., Graham, L. J. W. and Hamilton, R. (2006). Composing chaos: an experimental and numerical study of an open duct mixing flow. American Institute of Chemical Engineers Journal, 52(1), 9-28.

Metcalfe, G., Lester, D., Trefry, M. and Ord, A. (2007). Transport in a partially open porous media flow. Proceedings of SPIE 6802, Article 68020I. doi:10.1117/12.769319.

Metcalfe, G., Lester, D., Ord, A., Kulkarni, P., Trefry, M., Hobbs, B., Regenauer-Lieb, K. and Morris, J. (2010a). A partially open porous media flow towards visualization of coupled velocity, concentration and deformation fields. Philosophical Transactions of the Royal Society A 368, 217-230, doi:10.1098/rsta.2009.0198.

Metcalfe, G., Lester, D. R., Ord, A., Kulkarni, P., Rudman, M., Trefry, M., Hobbs, B., Regenauer-Lieb, K. and Morris, J. (2010b). An experimental and theoretical study of the mixing characteristics of a periodically reoriented irrotational flow. Philosophical Transactions of the Royal Society A 368, 2147-2162, doi:10.1098/rsta.2010.0037.

Mory, A. J. and Iasky R.P. (2005). Geology of the Northern Perth Basin Western Australia: A Field Guide. Western Australia Geological Survey.

Mottaghy, D., Pechnig, R. and Vogt, C. (2011). The geothermal project Den Haag: 3D numerical models for temperature prediction and reservoir simulation. Geothermics, 40, 199-210.

Muffler, P. and Cataldi, R. (1978). Methods for regional assessment of geothermal resources. Geothermics, 7, 53-89.

Norrish, K. and Chappell, B. W. (1977). X-ray fluorescence spectrometry. In Physical Methods in Determinative Mineralogy (Ed. J. Zussman), pp. 201-272 (Academic Press: London).

O'Shaughnessy, P. T. (1973). Determination of trace levels of chromium in ilmenite by atomic absorption spectrometry. Analytical Chemistry, 45, 1946-1947.

O'Sullivan, M. J., Yeh, A. and Mannington, W. I. (2009). A history of numerical modelling of the Wairakei geothermal field. Geothermics, 38, 155-168.

Oldmeadow, E. and Marinova, D. (2011). Into geothermal solutions: The sustainability case for Challenge Stadium in Perth, Western Australia. Environmental Progress & Sustainable Energy 30, 476-485.

Ottino, J. M. (1990). Mixing, chaotic advection, and turbulence. Annual Review of Fluid Mechanics, 22, 207-253.

Ozkahraman, H., Selver, R. and Isik, E. (2004). Determination of the thermal conductivity of rock from P-wave velocity. International Journal of Rock Mechanics and Mining Sciences, 41(4), 703-708.

Paksoy, H. O. (2007). Thermal energy storage for sustainable energy consumption - Fundamentals, case studies and design. Amsterdam: Springer.

Panichi, C. (2004). Geochemical impact of re-injecting geothermal waste waters; example, Larderello, Italy. (in Energy, waste and the environment; a geochemical perspective). Geological Society Special Publications, 236, 337-354.

Pérez-Paricio, A. (2000). Integrated modelling of clogging processes in artificial groundwater recharge. PhD Thesis. Department of Geotechnical Engineering & GeoSciences. Technical University of Catalonia (UCP), Barcelona, Spain.

PESANews (2005). The OZ SEEBASE Project: A new view of Australia's phanerozoic basins. August/ September issue.

Phillips, O. M. (1991). Flow and Reactions in Permeable Rocks. Cambridge University Press. Cambridge, 285 pp.

Pimienta, L., Sarout, J., Esteban, L. and Delle Piane, C. (2011a). Prediction of rock thermal conductivity from mineral composition, elastic wave velocities and microstructure. 9th Euroconference on Rock Physics and Geomechanics, 17-21 October Trondheim, Norway.

Pimienta, L., Sarout, J., Esteban, L. and Ricard, L. (2011b). Microstructure-based modelling of the thermal conductivity of natural and synthetic aggregates. First International Workshop on Rock Physics, August 7-12, Colorado School of Mines, USA.

Pimienta, L., Sarout, J., Esteban, L and Ricard, L., (2012). Thermal conductivity prediction from seismic velocities: a microstructurally-based approach using the effective medium theory. Geophysical Journal International, submitted.

Popov, Y. A., Pribnow, D. F. C., Sass, J. H., Williams, C. F. and Burkhardt, H. (1999). Characterization of rock thermal conductivity by high-resolution optical scanning. Geothermics, 28, 253-276.

Popov Y., Romushkevich R., Bayuk I., Korobkov D., Mayr S., Burkhardt H. and Wilhem H. (2004), Physical properties of rocks from the upper part of the Yaxcopoil-1 drill hole, Chicxulub crater. Meteorics & Planetary Science., 39, 799 - 812.

Post, V. E. A. (2011). PHREEQC for Windows Version 2.18.00. A hydrogeochemical transport model by D.L. Parkhurst and C.A.J. Appelo. Graphical user interface by V.E.A. Post.

http://pfw.antipodes.nl/index.html

Poulet, T. and Corbel, S. (2012). WAGCoE Data Catalogue. Final Report of Project 1, Perth Basin Assessment Program. Western Australian Geothermal Centre of Excellence.

Prensky, S. (1992). Temperature measurements in boreholes: an overview of engineering and scientific applications. The Log Analyst, 33, 313-333.

Pujol, M. (2011). Examples of successful hot Sedimentary Aquifer direct-use projects in Perth, Western Australia. In: Middleton, M. & Gessner, K. (eds.) Western Australian Geothermal Energy Symposium. Perth, Western Australia, 23.

Reid, L. B., Corbel, S., Ricard, L. P., Trefry, M. G. and Wellmann, J. F. (2010). Modelling Hot Sedimentary Geothermal Aquifers: A Groundwater Perspective. Groundwater 2010. Canberra.

Reid, L. B., Bloomfield, G., Botman, C., Ricard, L. and Wilkes, P. (2011). Temperature Regime in the Perth Metropolitan Area: Results of temperature and gamma logging and analysis, June/July 2010. Western Australian Geothermal Centre of Excellence.

Reid, L. B., Corbel, S., Poulet, T., Ricard, L. P., Schilling, O., Sheldon, H. A. and Wellmann, J. F. (2012). Hydrothermal modelling in the Perth Basin, Western Australia - Final report of Project 3, Perth Basin Assessment Program. Kensington: CSIRO.

Revil, A. (2000). Thermal conductivity of unconsolidated sediments with geophysical applications. Journal of Geophysical Research 105 (B7), 16749-16.

Ricard, L. P. and Chanu, J.-B. (2012). GeoTemp 1.0: User Manual. Kensington: CSIRO, in preparation.

Ricard, L. P. and Chanu, J.-B. (2012). GeoTemp 1.0: A MATLAB-based program for the processing, interpretation and modelling of geological formation temperature profiles. Computers & Geosciences, submitted.

Ricard, L. P., Corbel, S., Reid, L. B. and Trefry, M. G. (2010). Assessing sustainability of geothermal resources for Hot Sedimentary Aquifer systems. Groundwater 2010. Canberra.

Ricard, L. P., Chanu, J. and Pons, G. (2011a). Temperature interpretation and modelling for geothermal applications: GeoTemp. Preview (October 2011), 25-30.

Ricard, L. P., Chanu, J.-B. and Esteban, L. (2011b). GeoTemp: A framework for temperature interpretation and modelling. In: Budd, A. R. (ed.) Australian Geothermal Energy Conference. Melbourne: Geoscience Australia, 203-208.

Ricard, L. P., Corbel, S., Reid, L. B., Wilkes, P., Wu, B., Jeffrey, R., Clennell, B., Richard, T. and Trefry, M. G. (2011c). Exploration Well Proposal: Geothermal exploration well Kensington-1, ARRC/ Pawsey Centre Geothermal Project.: CSIRO/ WAGCoE, 50pp.

Ricard L. P., Reid L. B. and Corbel S., (2012a). Deep temperature measurement analysis in the onshore Perth Basin, Western Australia. In: Middleton, M. & Gessner, K. (eds.) Western Australian Geothermal Energy Symposium. Abstracts 2012.

Ricard L. P., Gutbrodt S., Harris B. and Esteban L., (2012b). Time-lapse temperature logging interpretation at the M345 ASR trial site. In: Middleton, M. & Gessner, K. (eds.) Western Australian Geothermal Energy Symposium. Abstracts 2012.

Robertson, W .J., Franzmann, P. D. and Mee, B. J. (2000). Sporeforming, Desulfosporosinus-like sulfate-reducing bacteria from a shallow aquifer contaminated with gasolene. Journal of Applied Microbiology, 88, 248-259.

Robertson, W. J., Franzmann, P. D., Mee, B. J. (2001). Desulfosporosinus meridiei sp. nov., a sporeforming sulfate-reducing bacterium isolated from gasolene-contaminated groundwater. International Journal of Systematic and Evolutionary Microbiology. 51, 133-140.

Rockwater Pty Ltd. (2009). Mirrabooka aquifer storage and recovery trial - Bore completion and hydrogeological evaluation. Rockwater Pty Ltd.

Rockwater Pty Ltd. (2010). Mirrabooka aquifer storage and recovery trial - results of cycle 1: December 2009-April 2010. Jolimont: Rockwater Pty Ltd, 24pp.

Rockwater Pty Ltd. (2011a). Aquifer Heat Rejection for cooling the proposed Pawsey Centre. H2 Level Hydrogeological Assessment. Unpublished report to CSIRO.

Rockwater Pty Ltd. (2011b). Bore Completion and Test Pumping Report. Unpublished report to CSIRO.

Rockwater Pty Ltd. (2011c). Preliminary H3 level hydrogeological assessment for groundwater supply and injection for the proposed Pawsey Supercomputer. Unpublished report to CSIRO.

Rolle, M., Eberhardt, C., Chiogna, G., Cirpka, O.A. and Grathwohl, P. (2009). Enhancement of dilution and transverse reactive mixing in porous media: Experiments and model-based interpretation. Journal of Contaminant Hydrology, 110(3-4), 130-142.

Saar, M. O. (2011). Review: Geothermal heat as a tracer of large-scale groundwater flow and as a means to determine permeability fields. Hydrogeology Journal, 19, 31-52.

Sarak, H., Onur, M. and Satman, A. (2005). Lumped-parameter models for low-temperature geothermal fields and their application. Geothermics, 34, 728-755.

Sarukkalige, P. R. (2011). Assessment of spatial variation of groundwater quality and its relationship with land use in metropolitan Perth. Journal of Water Resource Protection, 3, 311-317.

Shimizu, S., Akiyama, M., Naganuma, T., Fujioka, M., Nako, M. and Ishijima, Y. (2007). Molecular characterization of microbial communities in deep coal seam groundwater of northern Japan. Geobiology, 5, 423-433.

Simpson, E.S. III (1912). Notes on laterite in Western Australia. Geological Magazine (Decade V), 9, 399-406.

Smits, M., Toshihiro, S., Anuchit, L. and Illangasekare, T. H. (2010), Thermal conductivity of sands under varying moisture and porosity in drainage-wetting cycles, Vadose Zone Journal, 9(1), 172-180.

Snap Sampler (2011). ProHydro, Inc., USA, htp:\\www.snapsampler.com

Sposito, G. (1994). Steady groundwater flow as a dynamical system. Water Resources Research 30(8), 2935-2401.

Stopa, J. and Wojnarowski, P. (2006). Analytical model of cold water front movement in a geothermal reservoir. Geothermics, 35, 59-69.

Swift, M. G. (1991). Heat flow modelling: a generalized two-dimensional diffusive and convective numerical model for the Exmouth Plateau, offshore Northwest Australia. Tectonophysics, 194, 409-426.

Taylor, S. R. and McLennan, S. M. (1985). The Continental Crust: its Composition and Evolution. Blackwell, Oxford, 312pp.

Tel, T., de Moura, A., Grebogi, C. and Karolyi, G. (2005). Chemical and biological activity in open flows: A dynamical system approach. Physics Reports, 41(2-3), 91-196.

Timms, N., Corbel, S., Olierook, H., Wilkes, P., Delle Piane, C., Sheldon, H., Alix, R., Horowitz, F., Wilson, M., Evans, K. A., Griffiths, C., Stütenbecker, L., Israni, S., Hamilton, J., Esteban, L., Cope, P., Evans, C., Pimienta, L., Dyt, C., Huang, X., Hopkins, J., and Champion, D. (2012). A new understanding of the Perth Basin for geothermal exploration: WA Geothermal Centre of Excellence.

Trefry, M. G., Lester, D. R., Metcalfe, G., Ord, A. and Regenauer-Lieb, K. (2012). Toward enhanced subsurface intervention methods using chaotic advection. Journal of Contaminant Hydrology, 127(1-4), 15-29, doi:10.1016/j.jconhyd.2011.04.006.

Trefry, M. G., McLaughlin, D., Lester, D. R., Metcalfe, G., Johnston, C. D. and Ord, A. (2011). Stochastic relationships for periodic responses in randomly heterogeneous aquifers. Water Resources Research, 47, W08527, doi:10.1029/2011WR010444.

Trefry, M. G., McLaughlin, D., Metcalfe, G. Lester, D., Ord, A., Regenauer-Lieb, K. and Hobbs, B. (2010). On oscillating flows in randomly heterogeneous porous media. Philosophical Transactions of the Royal Society A 368, 197-216, doi:10.1098/rsta.2009.0186.

Trefry, M. G., Ruan, F. P., McLaughlin, D. (2003). Numerical simulations of pre-asymptotic transport in heterogeneous porous media: Departures from the Gaussian limit. Water Resources Research, 39(3), Article W01063.

Tressler, S. (2011). Temperature and gamma-ray logging in the Perth Metropolitan Area. Honours Thesis. Department of Exploration Geophysics, Curtin University of Technology.

Tureyen, O. I. and Akyapı, E. (2011). A generalized non-isothermal tank model for liquid dominated geothermal reservoirs. Geothermics, 40, 50-57.

Turner, S., Bean, L.B., Dettman, M., McKellar, J.L., McLoughlin, S., & Thulborn, T. 2009. Australian Jurassic sedimentary and fossil successions: current work and future prospects for marine and non-marine correlation, GFF, 131(1), 49—70.Ungemach, P. (2003). Reinjection of cooled geothermal brines into sandstone reservoirs. Geothermics, 32, 743-761.

Waples, D. W. and Ramly, M. (2001). A statistical method for correcting log-derived temperatures. Petroleum Geoscience, 7, 231.

Weatherford Laboratories (Australia) Pty Ltd. (2009). Routine core analysis final report of Mirrabooka-345. Weatherfor Laboratories (Australia) Pty Ltd.

Weeks, S. W. and Sposito, G. (1998). Mixing and stretching efficiency in steady and unsteady groundwater flows. Water Resources Research, 34 (12), 3315-3322.

Wilhartitz, I., Mach, R. L., Teira, E., Reinthaler, T., Herndl, G. J. and Farnleitner, A. H. (2007). Prokaryotic community analysis with CARD-FISH in comparison to FISH in ultra-oligotrophic ground- and drinking water. Journal of Applied Microbiology, 103, 871-881.

Yesertener, C. (2010). Hydrogeochemical assessment of the superficial aquifer. Perth metropolitan area. Department of Water Hydrogeological Record Series. Report No HG37, August 2010, 174 pp.

Zamora, M., Vo-Thanh, D., Bienfait, G. and Poirier, J. (1993). An empirical relationship between thermal conductivity and elastic wave velocities in sandstone. Geophysical Research Letters, 20, 1679-1682.

Zhang, P., Devries, S. L., Dathe, A. D. and Bagtzoglou, A. C. (2009). Enhanced mixing and plume containment under time-dependent oscillatory flow. Environmental Science & Technology. 43, 6283-6288.

APPENDIX A: LISTING OF STUDENTS

Full name	Level	Start	End	Institution	Supervisors Academic/WAGCOE	Topic
Sebastian Gutbrodt	Msc	May-11	Sep-11	ETH Zurich, Switzerland	Wolfgang Kinzelbach / Mike Trefry + Ludovic Ricard	M345 ASR Time-lapse temperature interpretation
Remi Alix	Msc	Mar-11	Jun-11	University of Montpellier, France	Michel Lopez / Ludovic Ricard + Soazig Corbel	Reservoir characterization in the Perth Metropolitan Area
Lisa Miotti	Msc	Apr-11	Sep-11	University of Poitiers, France	Thierry Cabioch / Ludovic Ricard	Geothermal reservoir modelling and engineering in the Perth Metropolitan Area
Lucas Pimienta	Msc	Feb-11	Jun-11	University of Strasbourg , Francel	Yves Geraud / Ludovic Ricard + Lionel Esteban	Thermal conductivity modelling
Jean-baptiste Chanu	Msc	Feb-11	Aug-11	PB Bordeaux, Francel	Iraj Mortazavi / Ludovic Ricard	Temperature interpretation and modelling: GeoTemp
Charlotte Dos Santos	Msc	Jun-10	Sep-10	PB Bordeaux, Francel	Iraj Mortazavi / Ludovic Ricard + Ali Karrech	Effect of pore pressure on geomechanical integrity in reservoir
Guillaume Pons	Msc	Jun-10	Sep-10	PB Bordeaux, Francel	Iraj Mortazavi / Ludovic Ricard + Allison Hortle	Downhole temperature interpretation
Stephane Francois-Lubin	Msc	Jun-10	Sep-10	PB Bordeaux, France	Iraj Mortazavi / Ludovic Ricard + Joel Sarout	Pore pressure diffusion in shales
Stephanie Tressler	Hons	Mar-11	Nov-11	CUT, Perth	Christian Dupuis / Paul Wilkes + Ludovic Ricard	Temperature and gamma logging Perth metro area
Cody Evans	Hons	Mar-11	Nov-11	UWA, Perth	Klaus Gessner / Ludovic Ricard + Lionel Esteban	Thermal conductivity measurements in the Perth Metropolitan Area
Kristina Kazakoff	Hons	Mar-11	Nov-11	UWA, Perth	Hui-Tong Chua + Xiaolin Wang / Ludovic Ricard	Pumping power modelling of geothermal projects in the Perth Metropolitan Area
Gemma Bloomfield	Hons	Jun-10	Nov-10	UWA, Perth	Klaus Gessner / Lynn Reid + Ludovic Ricard	Hydrogeologic study of geothermal logging in the Perth Metropolitan Area
Chris Botman	Hons	Mar-10	Nov-10	CUT, Perth	Christian Dupuis / Paul Wilkes + Frank Horowitz	Determining the geothermal properties of the Perth Basin lithology to aid geothermal energy projects

APPENDIX B: CONFERENCE AND WORKSHOP CONTRIBUTIONS

The developments of WAGCoE Program 1 Project 4 have been presented at many Perth, Australian domestic and overseas conferences, and include as part of course and curriculum development as well as public presentations. Details of conferences/ workshops presentations and publications can be found in Appendix C.

Conferences and workshops

The research has been presented in the following local and international conferences.

Australian Geothermal Energy Conference, Brisbane, Queensland, November 2009.

Direct Heat Use Applications for Hot Sedimentary Aquifers, Mercure Grosvenor Hotel, Adelaide, South Australia, November 2010.

Australian Geothermal Energy Conference 2010, Adelaide Convention Centre, Adelaide, South Australia, November 2010.

GeoNZ 2011, University of Auckland, Auckland, New Zealand, November 2010

West Australian Geothermal Energy Symposium, WAGCoE+GT Power+WA DMP, Perth Conference and Exhibition Centre, March 2011.

Australian Geothermal Energy Conference 2011, AGEA, Sebel Albert Park Hotel, Melbourne, November 2011.

10th Australasian Environmental Isotope Conference & 3rd Australasian Hydrogeology Research Conference, Curtin, Perth, 1-3 December 2009.

Groundwater Quality 2010, 7th International IAHS Conference on Groundwater Quality, ETH, Zürich, June 2010.

6th International Symposium on Environmental Hydraulics, Athens, June 2010.

30 Years of Stochastic Subsurface Hydrology, Centro Stefano Franscini, Monte Verità Ascona, Switzerland, June 2010.

Groundwater 2010, Canberra, Australian Capital Territory, November 2010.

American Geological Union annual fall meeting 2010, San Francisco, California, December 2010.

Sustainable Energy Systems – Finding Solutions through Multi-disciplinary Integration, An IAS Masterclass with Professor Maurice Dusseault, University of Waterloo, and Professor Xiating Feng, President, International Society for Rock Mechanics, UWA Old Senate Room, July 2011.

1st International Workshop on Rock Physics (1IWRP), Colorado School of Mines, USA, August 2011.

9th EuroConference on Rock Physics and Geomechanics, Trondheim, Norway, October 2011.

New technology forum and topical conference: Gas Petrophysics, Perth, Australia, September 2011.

Thirty-Seventh Workshop on Geothermal Reservoir Engineering. Stanford University, Stanford, California, January 2012.

Courses and public outreach

The Reservoir productivity and sustainability project contributes to the WAGCoE Education and public outreach deliverables with several items listed below.

Courses and curriculum

Project 4 has participated in a short course on a Geothermal Energy Resources course. This week-long Honours course was organized and taught at the University of Western Australia in March 2011 by the School of Earth Environment as unit EART4423. This unit was open to UWA and Curtin University of Technology geoscience students enrolled in BSc. The unit was structured with the following topics:

Direct heat use in Perth

Tectonic Perspective on Geothermal systems

Thermal Geology properties and concepts

Basic hydrogeology concepts

Engineering perspectives on direct use geothermal

Geothermal geophysics

Geothermal reservoir engineering

Geothermal chemistry.

The contribution of Project 4 was on the geothermal reservoir engineering course.

The University of Western Australia with support of the Western Australian Department of Education has created a series of secondary science teacher enrichment courses with the SPICE program. SPICE develops teaching and learning resources for classroom, provides professional development for teachers and facilitate interaction with scientists. Project 4 staff acted as technical experts to the SPICE team and provided technical support regarding the understanding of geothermal systems and the development of the supporting material.

Project 4 contributed significantly to the training of students with research projects. Three Honours students from The University of Western Australia and two Honours students from Curtin University of Technology have accomplished research projects directly related to Project 4. About eight international students from six different European universities contributed to the research effort of Project 4. Details of the student contribution are given in Appendix A.

Local and national outreach

Project 4 is representing WAGCoE within the Australian Geothermal Energy Group by participating in Technical Interest Group 9 on reservoir characterization and modelling.

A public presentation about Western Australia geothermal opportunities was delivered to the Oil and Gas Facility group of the Society of Petroleum Engineer and Engineers Australia on December 6th 2011.

Kensington 1 workshops

As part of the CSIRO ARRC/Pawsey Centre Geothermal Project, member of project 4 has run a series of external and internal workshops with several state stakeholders (WA Department of Mines and Petroleum, WA Department of Water, Water Corporation, Schlumberger, The University of Western Australia, Curtin University of Petroleum). Those workshops aimed to present the technical aspects of the geothermal project and to raise the research interests of the different parties. A synthesis of the outcomes of those workshops can be found in section 4.

APPENDIX C: SCIENTIFIC PUBLICATIONS

In this appendix, publications from WAGCoE authors involved in Project 4 are listed. Some of these publications may appear in the reference section of this report or in other Program 1 reports.

Student theses

Alix, R. (2011). Reservoir characterization of the Yarragadee formation for geothermal exploration in the Perth Metropolitan area (Perth Basin, Western Australia). Masters Thesis, University of Montpellier 2, France.

Bloomfield, G. (2010). Hydrogeologic study of geothermal logging in the Perth Metropolitan Area, Western Australia. Honours Thesis, School of Earth and Environmental Science, University of Western Australia.

Botman, C. (2010). Determining the geothermal properties of the Perth Basin lithology to aid geothermal energy projects. Honours Thesis. Department of Exploration Geophysics, Curtin University of Technology.

Chanu J-B. (2011). Temperature interpretation and modelling for geothermal applications. Masters Thesis. University of Bordeaux 1, France.

Evans, C. (2011). Thermal conductivity measurements in the Perth basin, Western Australia and implications for geothermal resource exploration. Honours Thesis. Faculty of Natural and Agricultural Sciences, University of Western Australia.

Kazakoff, K. (2011). Pumping power modelling of geothermal projects in the Perth Metropolitan Area. Honours Thesis. School of Mechanical and Chemical Engineering, University of Western Australia.

Miotti, L. (2011). Modelling study of St Hilda's geothermal heating project. Masters Thesis. University of Poitiers, France.

Pimienta, L. (2011). Thermal conduction modelling. Masters Thesis. University of Strasbourg, France.

Tressler, S. (2011). Temperature and gamma-ray logging in the Perth Metropolitan Area. Honours Thesis. Department of Exploration Geophysics, Curtin University of Technology.

Peer-reviewed journal articles

Lester, D. R., Metcalfe, G., Trefry, M. G., Ord, A., Hobbs, B. and Rudman, M. (2009). Lagrangian topology of a periodically reoriented potential flow: Symmetry, optimization and mixing. Physical Review E 80(3), Article 036208, doi:10.1103/PhysRevE.80.036208.

Lester, D. R., Rudman, M., Metcalfe, G., Trefry, M. G., Ord, A. and Hobbs, B. (2010). Scalar dispersion in a periodically reoriented potential flow: Acceleration via Lagrangian chaos. Physical Review E 81(4), Article 046319, doi:10.1103/PhysRevE.81.046319.

Li, J., Liu, J., Trefry, M. G., Park, J., Liu, K., Haq, B., Johnston, C. D., Volk, H. (2011). Interactions of microbial-enhanced oil recovery processes. Transport in Porous Media, 87(1), 77-104, doi:10.1007/s11242-010-9669-6, 2011.

Li, J., Liu, J., Trefry, M. G., Liu, K., Park, J., Haq, B., Johnston, C. D., Clennell, B. and Volk, H. (2012). Impact of rock heterogeneity on interactions of microbial enhanced oil recovery processes. Transport in Porous Media, 92(5), 373-396, doi: 10.1007/s11242-011-9908-5.

Metcalfe, G. (2010). Applied Fluid Chaos: Designing Advection with Periodically Reoriented Flows for Micro to Geophysical Mixing and Transport Enhancement, In Complex Physical, Biophysical, and Econophysical Systems, Robert L. Dewar and Frank Detering Ed.s, Lecture Notes in Complex Systems, World Scientific, vol. 9, pp 189-242.

Metcalfe, G., Lester, D., Ord, A., Kulkarni, P., Trefry, M., Hobbs, B., Regenauer-Lieb, K. and Morris, J. (2010a). A partially open porous media flow towards visualization of coupled velocity, concentration and deformation fields. Philosophical Transactions of the Royal Society A 368, 217-230, doi:10.1098/rsta.2009.0198.

Metcalfe, G., Lester, D.R., Ord, A., Kulkarni, P., Rudman, M., Trefry, M., Hobbs, B., Regenauer-Lieb, K. and Morris, J., 2010b. An experimental and theoretical study of the mixing characteristics of a periodically reoriented irrotational flow. Philosophical Transactions of the Royal Society A 368, 2147-2162, doi:10.1098/rsta.2010.0037.

Ricard L. P., Godel B. and Chanu J-B. (2012). CSDToolbox 1.0: A MATLAB-based program for crystal-size distribution analysis of large datasets. Computers & Geosciences, in press.

Ricard, L. P., Chanu, J.-B. (2012). GeoTemp 1.0: A MATLAB-based program for the processing, interpretation and modelling of geological formation temperature profiles. Computers & Geosciences, submitted

Roberts, M. E., Trefry, M. G., Fowkes, N., Bassom, A. P. and Abbott, P. C. (2011). Water table response to tidal forcing at sloping beaches. Journal of Engineering Mathematics, 69(4), 291-311, doi:10.1007/s10665-010-9407-7, 2011.

Trefry, M. G., Lester, D. R., Metcalfe, G., Ord, A. and Regenauer-Lieb, K. (2012). Toward enhanced subsurface intervention methods using chaotic advection. Journal of Contaminant Hydrology, 127(1-4), 15-29, doi:10.1016/j.jconhyd.2011.04.006.

Trefry, M. G., McLaughlin, D., Lester, D. R., Metcalfe, G., Johnston, C. D. and Ord, A. (2011). Stochastic relationships for periodic responses in randomly heterogeneous aquifers. Water Resources Research, 47, W08527, doi:10.1029/2011WR010444.

Trefry, M. G., McLaughlin, D., Metcalfe, G. Lester, D., Ord, A., Regenauer-Lieb, K. and Hobbs, B. (2010). On oscillating flows in randomly heterogeneous porous media. Philosophical Transactions of the Royal Society A 368, 197-216, doi:10.1098/rsta.2009.0186.

Conference abstracts

Clennell, B., Esteban, L., Ricard, L. P., Josh, M., Liu, J. and Regenauer-Lieb, K. (2010). Petrophysical Methods for Characterization of Geothermal Reservoirs. Australian Geothermal Energy Conference. Adelaide, November 2010.

Corbel, S., Griffiths, C., Dyt, C. and Ricard, L. P. (2011). Using stratigraphic forward modelling to characterise and identify geothermal reservoirs. In: Budd, A. R. (ed.) Australian Geothermal Energy Conference 2011. Melbourne: Geoscience Australia.

Corbel, S., Griffiths, C., Dyt, C. and Ricard, L. P. (2012). Hot sedimentary aquifer characterization using stratigraphic forward modelling, Perth Basin, Australia. Thirty-Seventh Workshop on Geothermal Reservoir Engineering. Stanford University, Stanford, California, January 2012.

Corbel, S., Reid, L. B. and Ricard, L. P. (2011). Prefeasibility geothermal exploration workflow applied to the Fitzroy Trough, Western Australia. In: Middleton, M. & Gessner, K. (eds.) Western Australian Geothermal Energy Symposium. Perth, Western Australia, March 2011, 25.

Descourvieres, C., Prommer, H. and Trefry M. (2009). Numerical modelling as a tool for anticipating water quality changes during aquifer storage and recovery. MODELCARE 2009, 7th International Conference on Calibration and Reliability in Groundwater Modeling, Wuhan, China, September 20-23, 2009.

Hortle, A., de Caritat, P. and Trefry, M. (2010). Water level monitoring: Why is it necessary? 2010 CO2CRC Research Symposium 2010, Melbourne, 1-3 December 2010.

Li, J., Liu, J., Trefry, M. G., Park, J., Liu, K., Haq, B., Johnston, C. D., Clennell, B., Volk, H. (2010). Numerical simulation of two-phase flow and solute transport during microbial enhanced oil recovery. 17th Australasian Fluid Mechanics Conference, Auckland, New Zealand, 5-9 December 2010.

Metcalfe, G., Lester, D. R., Trefry, M. G., Ord, A. and Regenauer-Lieb, K. (2010). How is fluid mixing important to high enthalpy extraction and geothermal energy? American Institute of Chemical Engineering Spring Conference, San Antonio, TX, USA, March 21-25 2010.

Ord, A., Metcalfe, G., Trefry, M., Lester, D., Kulkarni, P., Kesari, S., Hobbs, B., Rudman, M. and Hornby, P. (2009). Chemical and Biological Transport in Deforming Porous Media. Geofluids VI, Adelaide, April 15-18, 2009. Journal of Geochemical Exploration, 101, 77, 2009.

Pimienta, L., Sarout, J., Esteban, L. and Ricard, L. P. (2011). Microstructure-based modelling of the thermal conductivity of natural and synthetic aggregates. 1st International Workshop on Rock Physics (1IWRP). Colorado School of Mines, USA, August 2011.

Pimienta, L., Sarout, J., Esteban, L., Delle Piane, C. and Ricard, L. P. (2011). Thermal conductivity prediction from elastic wave velocity. In: New technology forum and topical conference: gas petrophysics, Formation Evaluation Society of Australia, Perth, Australia.

Pimienta, L., Sarout, J., Esteban, L. and Delle Piane, C. (2011). Prediction of rock thermal conductivity from mineral composition, elastic wave velocities and microstructure. 9th EuroConference on Rock Physics and Geomechanics. Trondheim, Norway.

Prommer, H., Davis, G. B. and Trefry M. (2009). Model-based identification and quantification of contaminant attenuation processes in hydrogeologically and geochemically complex settings. MODELCARE 2009, 7th International Conference on Calibration and Reliability in Groundwater Modeling, Wuhan, China, September 20-23, 2009.

Reid, L. B., Corbel, S., Ricard, L. P., Trefry, M. G. and Wellmann, J. F. (2010). Modelling Hot Sedimentary Geothermal Aquifers: A Groundwater Perspective. Groundwater 2010. Canberra.

Reid, L. B., Bloomfield, G., Botman, C., Ricard, L. P.. and Wilkes, P. (2011). A temperature investigation in Perth, Western Australia. In: Middleton, M. & Gessner, K. (eds.) Western Australian Geothermal Energy Symposium. Perth, Western Australia, 25.

Reid, L. B., Bloomfield, G., Ricard, L. P., Wilkes, P. and Botman, C. (2011). Geothermal Logging in Perth, Western Australia. In: Budd, A. R. (ed.) Australian Geothermal Energy Conference. Melbourne: Geoscience Australia.

Ricard, L. P., Bolton, G., Reid, L. B. and Trefry, M. G. (2010). Sustainability and management of HSA geothermal systems in Perth Metropolitan Area. Groundwater 2010. Canberra, Australia.

Ricard, L. P., Corbel, S., Reid, L. B. and Trefry, M. G. (2010). Assessing sustainability of geothermal resources for Hot Sedimentary Aquifer systems. Groundwater 2010. Canberra.

Ricard, L. P. and Pujol, M. (2010). Hot Sedimentary Aquifer geothermal engineering frameworks in the Perth Metropolitan Area. GeoNZ2010. Auckland, New Zealand.

Ricard, L. P., Chanu, J.-B. and Pons, G. (2011). Temperature interpretation and modelling for geothermal applications: GeoTemp. In: Middleton, M. & Gessner, K. (eds.) Western Australian Geothermal Energy Symposium. Perth, Western Australia.

Ricard, L. P., Chanu, J.-B. and Esteban, L. (2011). GeoTemp: A framework for temperature interpretation and modelling. In: Budd, A. R. (ed.) Australian Geothermal Energy Conference. Melbourne: Geoscience Australia.

Ricard, L. P., Esteban, L., Pimienta, L., Delle Piane, C., Evans, C., Chanu, J.-B. and Sarout, J. (2011). Temperature Estimates for Geothermal Application: Cockburn 1, Perth Basin, Australia. In: Budd, A. R. (ed.) Australian Geothermal Energy Conference. Melbourne: Geoscience Australia.

Trefry, M. G., Lester, D. R., Metcalfe, G, Chua, H.-T., Regenauer-Lieb, K. (2011). Opportunities for Shallow Heat Management via Subsurface Stirring. In Budd, A.R. (editor), 2011, Proceedings of the 20101 Australian Geothermal Energy Conference (AGEC2011), 16-18 November, Melbourne, Geoscience Australia, Record 2010/35, 263-266.

Trefry, M. G., McLaughlin, D., Lester, D. R., Metcalfe, G., Johnston, C. D. and Ord, A. (2010). A stochastic framework for the analysis of tidal effects in heterogeneous coastal aquifers. In Environmental Hydraulics (G. C. Christodoulou & A. I. Stamou, Eds), Proceedings of 6th International Symposium on Environmental Hydraulics, Athens, Greece, 23-25 June 2010, Volume 2, Taylor & Francis:London, ISBN 978-0-415-58475-3, pp. 655-660.

Trefry, M. G., Metcalfe, G., Lester, D. R., Ord, A., Regenauer-Lieb, K. (2010). Toward enhanced subsurface mixing methods using chaotic advection. 7th International IAHS Groundwater Quality Conference, Zurich, Switzerland, June 2010.

Trefry, M. G., Metcalfe, G., Lester, D. R., Ord, A., Regenauer-Lieb, K. (2010). Stochastic influences of Lagrangian chaos. “Thirty years of stochastic subsurface hydrology: where do we stand and what are the emerging challenges?”, ETH Conference, Centro Stefano Franscini, Monte Verita, Ascona, 27 June - 2 July 2010.

Wellmann, J. F., Ricard, L. P., Horowitz, F. and Regenauer-Lieb, K. (2010). Guided Geothermal Exploration in Hot Sedimentary Aquifers. AGU Fall Meeting 2010. San Francisco, USA.

Wellmann, J. F., Horowitz, F., Ricard, L. P. and Regenauer-Lieb, K. (2010). Estimates of sustainable pumping in Hot Sedimentary Aquifers: Theoretical considerations, numerical simulations and their application to resource mapping. Australian Geothermal Energy Conference. Adelaide.

WAGCOE TECHNICAL REPORTS

Bloomfield G., Ricard L. P.. and Reid L. B. (2011). Temperature logging and analysis protocol. WAGCoE Report, February 2011, EP112037, 38 pp.

Douglas, G. B., Trefry, M. G., Wylie, J., Wilkes, P. G., Puzon, G. J. and Kaksonen, A. H. (2012). Rapid biogeochemical assessment protocol for in situ heat rejection: the Mullaloo Aquifer, Perth, Western Australia, Western Australian Geothermal Centre of Excellence, Report EP12608, 36pp.

Reid, L. B., Trefry, M., Regenauer-Lieb, K. (2011). Heat Rejection to the Mullaloo Aquifer: Technical Review of the Rockwater Hydrogeology and H3 Assessment Reports to CSIRO. WAGCoE Report, 12 December 2011, 20+v pp.

Reid, L. B., Bloomfield, G., Botman, C., Ricard, L. and Wilkes, P. (2011). Temperature Regime in the Perth Metropolitan Area: Results of temperature and gamma logging and analysis, June/July 2010. WAGCoE Report, June 2011, EP111422, 197 pp.

Ricard, L., Corbel, S., Reid, L., Wilkes, P., Wu, B., Jeffrey, R., Clennell, B., Richard, T., Trefry, M. and Regenauer-Lieb, K. (2011). Exploration Well Proposal: Geothermal exploration well Kensington-1, ARRC/Pawsey Centre Geothermal Project. WAGCoE Report to ARRC/Pawsey Project, May 2011, EP113898, 50pp.

Ricard L. P., Godel B. and Chanu J.-B. (2011), CSDToolbox 1.0: User Manual, CSIRO report, January 2012, EP114448, 50 pp.

Trefry, M. G., Ricard, L., Wilkes, P., Reid, L., Wang, X., Corbel, S., Horowitz, F. G., Webb, S. and Regenauer-Lieb, K. (2010). Preliminary prefeasibility desktop study of geothermal potential for the Telfer Province. Western Australian Geothermal Centre of Excellence Report to Newcrest Mining Limited, May 2010.

Patents

Metcalfe, G. P., Lester, D. R., Trefry, M. G. and Regenauer-Lieb, K. (2010). Method, system and apparatus for subsurface flow manipulation. Australian Provisional Patent Specification No. 2009903821, 14 August 2009; PCT International Application PCT/tba, 13 August 2010. Patent Number WO2011017771-A1, 17 February 2011.

Additional publications

Ricard, L. P., Chanu, J. and Pons, G. (2011). Temperature interpretation and modelling for geothermal applications: GeoTemp. Preview (October 2011), 25-30.